INFORMATION TO USERS

This manuscript has been reproduced from the microfilm master. UMI films the text directly from the original or copy submitted. Thus, some thesis and dissertation copies are in typewriter face, while others may be from any type of computer printer.

The quality of this reproduction is dependent upon the quality of the copy submitted. Broken or indistinct print, colored or poor quality illustrations and photographs, print bleedthrough, substandard margins, and improper alignment can adversely affect reproduction.

In the unlikely event that the author did not send UMI a complete manuscript and there are missing pages, these will be noted. Also, if unauthorized copyright material had to be removed, a note will indicate the deletion.

Oversize materials (e.g., maps, drawings, charts) are reproduced by sectioning the original, beginning at the upper left-hand corner and continuing from left to right in equal sections with small overlaps.

ProQuest Information and Learning
300 North Zeeb Road, Ann Arbor, MI 48106-1346 USA
800-521-0600

INTER-ANNUAL VARIABILITY OF NET ECOSYSTEM CO_2 EXCHANGE AT A SUBARCTIC FEN

By

TIMOTHY JOHN GRIFFIS, B.Sc.

A Thesis

Submitted to the School of Graduate Studies

in Partial Fulfilment of the Requirements

for the Degree

Doctor of Philosophy

McMaster University

NET ECOSYSTEM CO_2 EXCHANGE AT A SUBARCTIC FEN

DOCTOR OF PHILOSOPHY (2000) McMASTER UNIVERSITY
(School of Geography and Geology) Hamilton, Ontario

TITLE: Inter-annual variability of net ecosystem CO_2 exchange at a subarctic fen

AUTHOR: Timothy John Griffis, B.Sc. (Brock University)

SUPERVISOR Professor W. R. Rouse

NUMBER OF PAGES: xvii, 204

ABSTRACT

This thesis examines the inter-annual variability in growing season net ecosystem CO_2 exchange (NEE) at a subarctic sedge fen located near Churchill, Manitoba, Canada. Landscape-scale NEE and the energy and water balance of the fen were studied during five growing seasons between the years 1994 and 1999. Inter-annual variability in NEE was large and ranged from a net source to the atmosphere and a net sink to the ecosystem. Estimates of landscape-scale gross ecosystem production (GEP) and ecosystem respiration (ER) indicate that GEP is largely responsible for the inter-annual variability in NEE. Annual estimates of NEE indicate that, during the present period, the fen is losing carbon nearly three times faster than its long-term historical accumulation rate of approximately -11 g CO_2 m^{-2} y^{-1}.

The position of the polar jet stream and synoptic scale weather patterns has an important control on the timing of snowmelt, leaf emergence, and development of the vegetation during early spring. The 1997-1998 El Niño phenomenon caused a warm and wet spring that lengthened the growing season and increased carbon acquisition at the fen. Spring season hydroclimatological conditions play a key role in determining the source and sink strength of the wetland.

Community-scale NEE measurements revealed that sedge-moss communities account for the majority of the CO_2 exchange at the fen. Community relationships of GEP and ER indicate that changes in community spatial distribution within the fen could nearly triple the net carbon acquisition of this wetland.

Model simulations show that the sensitivity of NEE to changing environmental conditions varies inter-annually depending on the initial conditions of the wetland. Simulations using climatic change scenarios indicate that warmer air temperatures will increase carbon acquisition during wet years but may act to reduce wetland carbon storage in years that experience a large water deficit.

ACKNOWLEDGEMENTS

I am extremely grateful for having had the opportunity to study at McMaster University in the School of Geography and Geology. There are many people I wish to thank for helping me through my studies and making the past five years a special time in my life.

First and foremost, I would like to thank my supervisor, Dr. Wayne Rouse, for his endless support both academically and personally. His experience, vision, and enthusiasm have been a tremendous resource to this research. His dedication to science and northern research has made working with him especially rewarding.

I am indebted to Dr. John Davies who introduced to me climate models, biosphere feedback, homeostasis, and "Daisy World". Thank you for all of the enlightening discussions we have had regarding climatology, Fortran and Cichlids.

Dr. Susan Dudley has worked hard to displace some of my ignorance surrounding the Plant Kingdom. I thank her for taking the time to deal with my many questions and for offering a much-needed reading course in plant biology.

I am grateful to Dr. Mike Waddington for the numerous conversations we have had with respect to wetland biogeochemistry and his integral role in the chamber flux experiments we conducted at Churchill.

I would especially like to recognize a number of friendships that have developed and added to this experience along the way from Ridgeway to Hamilton, Churchill, and Inuvik. Sean Carey, Rich Petrone, Mark Stradiotto, and StinkCharmer have made this a most memorable and irreplaceable five years. The band sessions were "instrumental" in dealing with the "blues" of graduate school. Thank you for all the memories.

I give a special thank you to Peter Lafleur, Dale Boudreau, Jackeline Binyamin, Peter Blanken, Nigel Roulet, Kim Gravelle, Cheryl Schreader, Rich Petrone, Sandra Rolph, Peter Brown, Claire Oswald, Kirsten Weisz, and Andrea Eaton for all of their support while in the field and at McMaster. I would also like to thank the anonymous reviewers who have helped improve the quality of this thesis.

Finally, I would like to thank friends and family behind the scenes who have made this pursuit possible: Joe and Virginia Mymryk and Tony Shaw for all of their advice; my parents, Jim and Sharon Griffis, for providing the opportunity and encouragement; Les and Glenn Griffis, the Storm Chasers; Sandra Rolph, editor, and formatting disaster aide; Scott Darragh and Mark Lindsay, for tolerating the "Harsh Climate".

Funding for this research was generously provided by the National Science and Engineering Research Council of Canada, the Department of Indian and Northern Development, an Ontario Graduate Scholarship, the Meteorological Service of Canada, and McMaster University.

TABLE OF CONTENTS

LIST OF FIGURES

FIGURE

LIST OF TABLES

TABLE

PREFACE

This thesis consists of published journal articles and prepared manuscripts submitted for peer-reviewed publication. The ideas expressed here are my own and have been written by me. Any errors occurring in this thesis are my responsibility.

Chapter Two, "Inter-annual variability of net ecosystem CO_2 exchange at a subarctic fen", authored by T.J. Griffis, W.R. Rouse, and J.M. Waddington, was accepted for publication in *Global Biogeochemical Cycles* on February 21, 2000. W.R. Rouse provided the financial support for this research and selected the research site. Both W.R. Rouse and J.M. Waddington assisted in the field and provided editorial comments on the original manuscript.

Chapter Three, "A synoptic climatological investigation of net ecosystem CO_2 exchange at a subarctic wetland", authored by T.J. Griffis, R. Petrone, and W.R. Rouse, is submitted to *Arctic, Antarctic, and Alpine Research*. R. Petrone developed the Matlab program for analyzing the synoptic surface pressure data. W.R. Rouse provided the financial support for this research and critiqued the original manuscript.

Chapter Four, "Scaling net ecosystem CO_2 exchange from the community to landscape-level at a subarctic fen", authored by T.J. Griffis, W.R. Rouse, and J.M. Waddington, was accepted for publication in *Global Change Biology* on November 12, 1999. W.R. Rouse and J.M. Waddington provided the financial support for this research. J.M. Waddington helped with the development and use of the CO_2 chamber system in the field. W.R. Rouse and J.M. Waddington provided a critique of the original manuscript.

Chapter Five, "Modelling the inter-annual variability in net ecosystem CO_2 exchange at a subarctic fen", authored by T.J. Griffis and W.R. Rouse, was accepted for publication in *Global Change Biology* on June 1, 2000. W.R. Rouse provided the financial support for the development of this model and critically reviewed the original manuscript.

CHAPTER ONE

INTRODUCTION

1.1. INTRODUCTION

Over the past decade greenhouse gases have received unparalleled attention from scientists and policy makers owing to their rapidly increasing atmospheric concentrations (Barnola *et al.*, 1987; IPCC, 1990) and their potential to alter global climate (Cess *et al.*, 1993; IPCC, 1996). Concerns over the threat of global warming and its implications for severe weather phenomena and climate change have provided the impetus for studying the links between global energy, water and carbon cycling. This thesis examines the feedback between climate variability and net ecosystem CO_2 exchange (NEE) at a subarctic sedge fen in Churchill, Manitoba, Canada.

1.2. VARIABILITY IN ATMOSPHERIC CO_2 CONCENTRATION

Near the earth's surface heat and mass are exchanged vigorously between the oceanic and terrestrial surface and the atmosphere. The concentration of CO_2 near the surface exhibits a strong spatial and temporal pattern due to biological and physical processes acting in the biosphere. During the growing season, ambient CO_2 shows a strong circadian signal. It decreases during the day, as light-driven photosynthesis acquires CO_2 from the lower atmosphere and increases at night as photosynthetic

processes cease while plant growth and maintenance continue to use photosynthetic products in respiration. Plant respiration continues day and night providing the necessary energy to sustain survival.

As plant structures expire, organic carbon is added to the earth's surface through leaf, stem, wood litter fall and root accumulation. Heterotrophic bacteria consume these dead tissues as a source of energy and release CO_2 to the atmosphere during aerobic respiration. This microbial activity persists day and night, thereby, contributing to the temporal and spatial variability observed in ambient CO_2 concentrations.

The net exchange of CO_2 (NEE) occurring between the land surface and atmosphere defines the balance between carbon acquisition through gross ecosystem production (GEP) and carbon loss resulting from ecosystem respiration (ER). Photosynthesis, plant respiration, and soil respiration are sensitive to variations in radiation, temperature, and water (Billings, 1982; Oechel *et al.*, 1993; Frolking *et al.*, 1997; Moore *et al.*, 1998). Climatic variability is, therefore, expected to have a significant effect on terrestrial carbon exchange and the global carbon budget.

The National Oceanic and Atmosphere Administration (NOAA) and the Climate Diagnostics Center (CDC) monitoring network show that there is a large amount of seasonal and inter-annual variability in CO_2 concentrations (Keeling, 1986). Three trends have emerged from the network data and these provide considerable insight into the global carbon cycle. First, the record from the Mauna Loa observatory indicates that the annual variation in atmospheric CO_2 concentration has increased by about 0.4% y^{-1} since

1960. The rate of increase supports the claim that pre-industrial atmospheric CO_2 concentrations will double by the year 2100. Second, the seasonal amplitude in CO_2 concentration reveals the importance of land vegetation on the global carbon budget especially in the Northern Hemisphere (D'Arrigo *et al.*, 1987). This seasonal variability is most pronounced in the northern hemisphere due to a larger area of land surface (Schlesinger, 1991). Third, there is considerable evidence that large-scale weather phenomena such as El Niño have important implications for the annual variation in the global carbon budget (Keeling *et al.*, 1989). This suggests that climatic change will also have a pronounced impact on the global carbon cycle.

1.3. CARBON STORAGE

Carbon reservoirs represent large stores of carbon that have accumulated through the earth's history and are often referred to as "pools" or "stores" in the global carbon budget. Storage of carbon in each of the earth's reservoirs has been estimated from a number of approaches combining mass balance sampling and extrapolation employing satellite imagery and modelling. The global soil carbon pool (1500 Pg) represents the largest pool in the biosphere. Terrestrial plants store 560 Pg of carbon and the upper mixed layer of the ocean represents a pool of approximately 620 Pg of carbon. The amount of carbon stored in the atmosphere is relatively large at 720 Pg (Schlesinger, 1991).

1.4. CARBON FLUXES

The atmosphere is unique as it links together the global carbon reservoirs. A change in the rate of carbon exchange over time (flux) between any one of these pools will result in a carbon perturbation in the atmosphere.

In the biosphere, the annual flux of carbon between reservoirs is relatively large compared to the carbon stored in each reservoir. As a result, the average CO_2 molecule has an atmospheric residence time of about three years (Olson *et al.*, 1985). Typical exchange rates of carbon between the reservoirs and the atmosphere are not well known. A large reason for this uncertainty is the lack of temporal and spatial sampling of the major ecosystem types. The best-known flux in the global carbon budget is the anthropogenic emission of carbon (5-7 Pg C y^{-1}) resulting from fossil fuel burning (Rotty and Masters, 1985). Based on the annual anthropogenic flux and the current understanding of the global carbon cycle, the atmospheric content of carbon is predicted to increase by about 0.7% y^{-1}.

1.5. THE MISSING CARBON SINK

The expected increase in atmospheric carbon is substantially larger than the observed trend at the Mauna Loa Observatory. Disparity between estimated and observed changes in the atmospheric carbon content defines the so-called "missing carbon sink", equivalent to 2.2 Pg of carbon (Schlesinger, 1991). Assuming the average car has a mass of 1200 kg the missing carbon sink represents the mass of approximately 2 billion cars that disappear from the global carbon budget each year.

The implications of this missing carbon are important for climate modelling and prediction, as climate models require an accurate description of greenhouse gas concentrations to adequately model radiative transfer. If the missing carbon sink or carbon reservoirs reach saturation, then atmospheric concentrations of CO_2 could increase at rates far greater than anticipated, thereby, accelerating the doubling time of a $2xCO_2$ atmosphere. Furthermore, a better understanding of the global carbon budget will be necessary in the immediate future for addressing CO_2 reduction strategies as outline in the 1997, Kyoto Protocol.

1.6. SEARCH FOR THE MISSING CARBON

Scientists first hypothesized that the missing carbon sink was due to an incorrect assessment of the carbon balance for the world's oceans. Recent studies, however, have revealed that oceanic carbon acquisition can only account for 0.5 Pg (25%) of the carbon needed to restore the global carbon budget (Tans *et al.*, 1990). The time series of CO_2 concentrations recorded at northern observatories caused scientists (Keeling *et al.*, 1995; Ciais *et al.*, 1995) to speculate on a missing carbon sink in the Northern Hemisphere. The increasing amplitude in Northern Hemisphere CO_2 concentration suggested amplification in summer season carbon acquisition. Studies conducted by Kindermann *et al.*, (1996) and Myneni *et al.*, (1997) hypothesize that the amplification of carbon acquisition is related to an increase in growing season duration at northern latitudes.

Investigation of a northern carbon sink has concentrated on temperate and boreal forests, northern peatlands, and arctic tundra. Townsend *et al.*, (1996) report that

stimulated productivity resulting from increased anthropogenic nitrogen deposition on northern temperate forests could account for up to 60% of the missing carbon based on an analysis of 1990 data. However, nitrogen-label experiments by Nadelhoffer *et al.*, (1999) concluded that enhanced carbon acquisition through nitrogen fertilization would only account for 10% of the missing carbon.

To date, the largest concentrated research effort attempting to understand the missing global carbon sink and biosphere feedback is the Boreal Ecosystem Atmosphere Experiment (BOREAS) spearheaded by the National Aeronautics and Space Administration (NASA) between the years 1994 and 1996. Research sites were concentrated in Prince Albert National Park, Saskatchewan, and near Thompson, Manitoba, Canada.

Plant physiological measurements and fluxes of carbon, water, and heat were made at the leaf, community, landscape, and regional scale from a number of methodological approaches. Analyses of the large data sets acquired during BOREAS are still being carried out. Preliminary evidence, however, suggests that boreal fluxes of carbon were in near balance over the measurement period. While some experiments within BOREAS, such as an aspen forest site (Black *et al.*, 1996) and a southern fen site (Suyker *et al.*, 1997) at Prince Albert National Park exhibited a net carbon acquisition, other boreal sites, such as beaver ponds (Roulet *et al.*, 1997), a black spruce forest (Goulden *et al.*, 1997), and a northern fen (Lafleur *et al.*, 1997) near Thompson experienced a net loss of carbon to the atmosphere.

The investigation of missing carbon has also extended beyond the boreal treeline. Carbon accumulation in arctic tundra has been estimated at 55 Pg, amounting to an historical accumulation rate of 0.1 to 0.3 Pg of carbon y^{-1} (Kling *et al.*, 1991). Although early investigations reported net carbon losses from arctic Alaskan tundra during the growing season (Oechel *et al.*, 1993) more recent studies (Vourlitis and Oechel, 1997) have shown that these sites are in near balance.

1.7. RESEARCH NEEDS

There is an increasing need to improve the understanding of land surface CO_2 exchange in order to resolve the missing carbon sink problem and forecast the effect of global warming on the global carbon budget. Previous studies (Black *et al.*, 1996; Shurpali *et al.*, 1995; Vourlitis and Oechel, 1997) have demonstrated the importance of inter-annual variability in climate and its impact on NEE. Improvements in temporal and spatial sampling are needed for development and validation of carbon exchange models and to gain a greater understanding of feedback between climate and carbon cycling processes in the biosphere.

1.8. THESIS OBJECTIVES

This thesis advances the understanding of the global carbon budget and biosphere feedback in the earth-atmosphere system by examining NEE at a subarctic sedge fen wetland in Churchill, Manitoba. The general objectives of this thesis are:

1) to quantify the amount of inter-annual variability in growing season NEE;

2) to account for the processes driving the inter-annual variability in NEE; and

3) to simulate the potential impact of climate change on NEE.

These objectives are addressed by studying the temporal variability in CO_2 exchange at the landscape and plant community scale. A biometeorological approach is used to bridge the gap between biological and atmospheric processes acting near the earth's surface.

1.9. RESEARCH SITE

The experimental area is located on the southwestern shore of Hudson Bay, within the Hudson Bay Lowland (Figure 1.1). Patches of open woodland near the experimental area mark the edge of the northern boreal tree line and the transition to large expanses of open tundra. The region is underlain by continuous permafrost. Hudson Bay has a strong influence on the regional climate and energy balance during the growing season through the advection of cold moist air (Rouse, 1991).

The research site is an extensive fen and is located 20 km east of the town of Churchill, Manitoba (58° 45'N, 94° 04'W), and 12.5 km south of the Hudson Bay shoreline. This fen is characterized by non-patterned, hummock-hollow terrain. Detailed surveying within a 150 m radius of the main micrometeorological measurement tower indicates that small hummocks comprise 47%, hollows 48% and large hummocks 5% of the landscape with respect to the water table position. At this fen, brown moss (*Scorpidium turgescens*) is the dominant vegetation found in the wet hollows. Small hummocks exhibit a limited moss cover (*Tomenthypnum nitens*) but are dominated by the vascular species *Carex aquatilis, C. limosa, C. saxatilis and C. gynocrates*. Larger

hummocks support vascular species (*Betula glandulosa, Ledum decumbens Salix arctophila or Carex* spp.) and non-vascular species of lichen (*Cladina stellaris, C. rangiferina*) and moss (*Dicranum undulatum*).

The fen has a mean peat depth of 0.25 m and is underlain by glaciomarine till, consisting of fine silts and clays with interspersed layers of carbonate shingles. The regional landscape continues to respond to isostatic rebound following the last glaciation. Elevation increase at the research site is about 0.01 m y^{-1}. At present, the fen is approximately 22 meters above sea level, and therefore, it is estimated that vegetation and peat development was initiated about 2200 years before present.

1.10. Historical Carbon Balance

The Hudson Bay Lowland represents the second largest contiguous wetland globally and has accumulated significant amounts of atmospheric carbon since the retreat of glacial ice and the isostatic emergence of the tundra wetlands from Hudson Bay. Gorham (1991) suggests that northern peatlands have historically accumulated -29 g C m^{-2} y^{-1}. The carbon balance, as determined from peat cores, accounts for NEE, net methane exchange, and transport of dissolved inorganic (DIC) and organic (DOC) carbon from runoff processes. In northern wetlands NEE accounts for approximately 90% of the carbon exchange (Gorham, 1995).

Examination of peat cores from the Churchill fen indicate that carbon has accumulated at an average rate of -7 g C m^{-2} y^{-1} over its 2200 year history. This rate of accumulation is directly related to the hydroclimatological and ecological conditions that

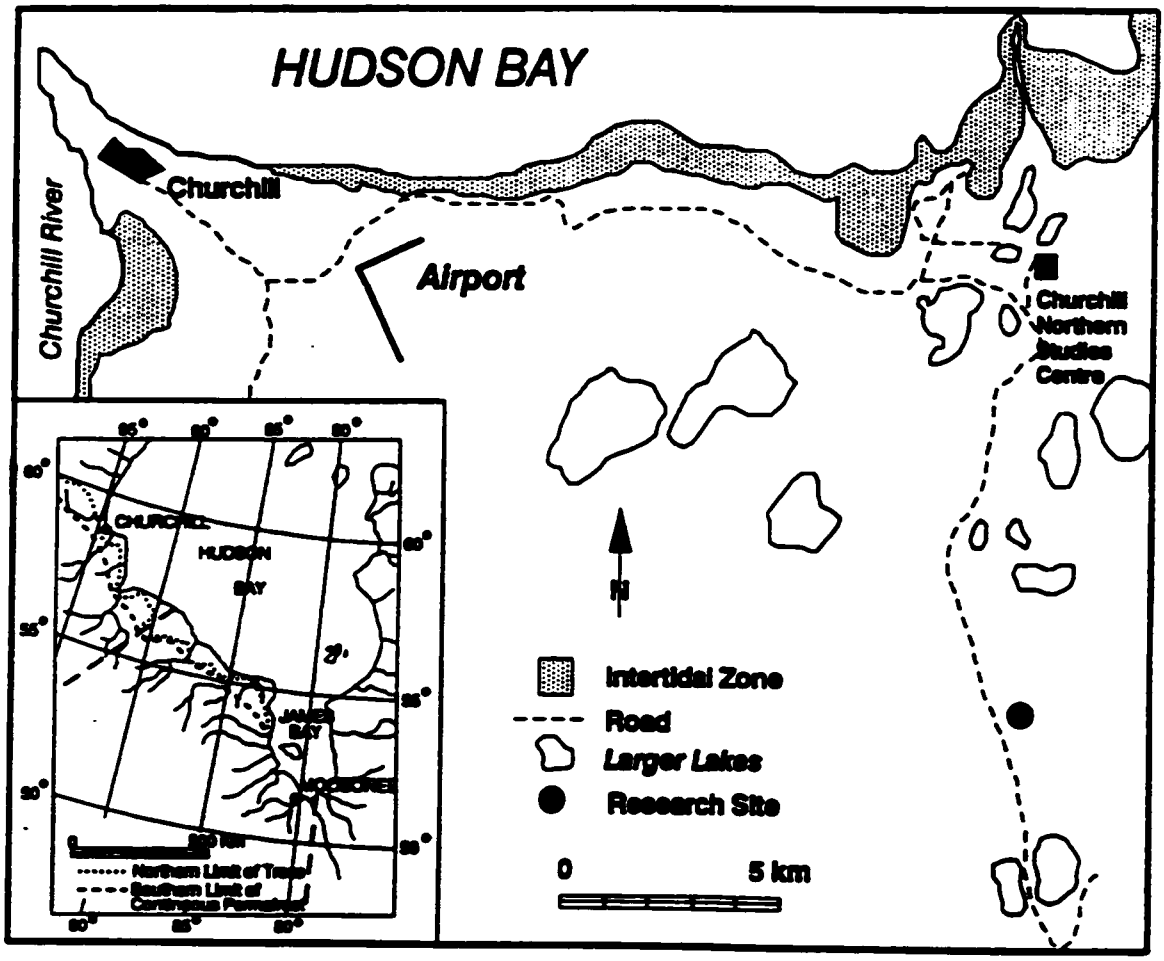

Figure 1.1: Research area and study site.

have persisted over this period. Macrofossil evidence indicates that the fen vegetation has consisted of varying amounts of sedges and mosses throughout its developmental history (Coristine, 1998). On shorter time scales (days to years) the variability in NEE is related to changes in radiation, energy, water balance, and phenology.

1.11. THESIS OUTLINE

The following chapters present papers that have been accepted or are currently submitted for peer-reviewed publication:

Chapter 2 examines the inter-annual variability in landscape scale NEE. Micrometeorological gradient techniques are used to estimate the CO_2 budget of the fen during five growing seasons. This paper currently represents the longest time series study of NEE for any subarctic environment globally. It is the first paper to examine the inter-annual variation in NEE by isolating the components of GEP and ER. This research is accepted for publication in *Global Biogeochemical Cycles*.

Chapter 3 examines the inter-annual variability in large-scale weather patterns and their influence on the timing of snowmelt, phenology, and day-to-day variability in NEE. Large-scale atmospheric phenomenon such as the position of the polar jet stream, and El Niño, is shown to have a significant impact on NEE at this northern wetland. This paper has been submitted to *Arctic, Antarctic, and Alpine Research*.

Chapter 4 considers the role of individual plant communities and their influence on NEE at the landscape-level. This paper speculates on the possibility of homeostatic

adjustment of NEE to future hydroclimatological conditions through a biological feedback mechanism. This study will be published in *Global Change Biology*.

Chapter 5 presents a model for the simulation of the inter-annual variability in NEE. Empirical algorithms describing CO_2 exchange processes are coupled to a water model developed by Rouse (1998) to help explain the inter-annual variation in CO_2 exchange and explore the sensitivity of NEE to changes in air temperature, precipitation, net radiation, and above ground biomass. The potential response of NEE at this northern fen is examined in the context of future climatic change. This work is accepted for publication in *Global Change Biology*.

Chapter 6 concludes with a summary of the significant findings arising from this study and future research needs are addressed.

CHAPTER TWO

INTER-ANNUAL VARIABILITY OF NET ECOSYSTEM CO_2 EXCHANGE AT A SUBARCTIC FEN [1]

2.1. INTRODUCTION

Northern wetlands are an important sink of atmospheric CO_2. They contain approximately one third of the total global soil carbon pool (Gorham, 1991) and represent 60% of the carbon currently stored in the atmosphere (Sundquist, 1993). Stored carbon in northern wetlands is vulnerable to climatic change (Oechel *et al.*, 1993). General circulation models (GCMs) forecast warming and decreased soil moisture at higher latitudes (IPCC, 1996), which will accelerate the decomposition of organic material and the efflux of CO_2 to the atmosphere (Billings *et al.*, 1987a; Moore *et al.*, 1998). However, increased carbon acquisition resulting from a longer growing season, warmer air temperatures and increased nutrient turnover, could offset this initial increase in decomposition (Oechel and Billings, 1992). Northern wetlands, therefore, represent an important biosphere feedback to global climate through the CO_2 -greenhouse effect.

The Hudson Bay Lowland is the second largest contiguous wetland in the world, yet few studies (Neumann *et al.*, 1994; Burton *et al.*, 1996; Schreader *et al.*, 1998 and Lafleur, 1999) have examined the CO_2 sink/source magnitudes in this environment.

[1] A modified version of this chapter, authored by T. J. Griffis, W. R. Rouse, and J. M. Waddington, will be published in *Global Biogeochemical Cycles*.

A few studies (Coyne and Kelley, 1975; Fan *et al.*, 1992; Vourlitis and Oechel, 1997 and McFadden *et al.*, 1998) have investigated landscape-scale net ecosystem CO_2 exchange (NEE) at other high latitude wetlands. Coyne and Kelley, (1975), Fan *et al.*, (1992) and Vourlitis and Oechel, (1997) working in Alaskan arctic tundra observed a small net acquisition of CO_2 over the growing season, while Burton *et al.*, (1996) and Schreader *et al.*, (1998) reported significant growing-season losses of CO_2 from a fen site located within the Hudson Bay Lowland (Table 2.1).

The biophysical processes regulating CO_2 exchange in these ecosystems are complex and identifying the causal mechanism(s) of inter-annual variability in CO_2 flux is difficult to assess. Net ecosystem CO_2 exchange (NEE) is the difference between the efflux of CO_2 (ecosystem respiration, ER) and carbon acquisition (gross ecosystem production, GEP). ER is comprised of both heterotrophic soil respiration and autotrophic dark respiration resulting from plant growth and tissue maintenance (Oechel and Billings, 1992; Oberbauer *et al.*, 1992; Moore *et al.*, 1998). Experimental evidence and field observations indicate that lower water table position and drier soil conditions enhance organic decomposition and increase the rate of ER to the atmosphere (Billings *et al.*, 1983; Peterson *et al.*, 1984; Oechel *et al.*, 1995). Plant and root respiration, which may account for 30 to 70% of ER in arctic ecosystems (Semikhatova *et al.*, 1992; Silvola *et al.*, 1996; Bhardwaj, 1997), is affected by environmental factors such as temperature but is more strongly related to the growth stage of the plant (Semikhatova *et al.*, 1992). Bubier *et al.*, (1998) have shown that ER accounts for approximately 33% of GEP under high light conditions and that this relationship varies seasonally as soil

TABLE 2.1: Landscape-Scale Estimates of ΣNEE (g CO_2 m^{-2}) and Daily NEE (g CO_2 m^{-2} d^{-1}) for Northern, Subarctic and Arctic Wetlands

Study	Site	Duration	ΣNEE	Daily
Burton *et al.*, (1996)	Churchill Manitoba. Fen (58° N, 94° W)	July to August 1993 (27 days)	+30	+1.1
Schreader *et al.*, (1998)	Churchill Manitoba. Fen (58° N, 94° W)	June to August 1994 (75 days)	+76	+1.0
This study	Churchill Manitoba. Fen (58° N, 94° W)	June to August 1996 (75 days)	-235	-3.1
	Churchill Manitoba. Fen (58° N, 94° W)	June to August 1997 (75 days)	-49	-0.7
	Churchill Manitoba. Fen (58° N, 94° W)	June to August 1998 (75 days)	-229	-3.1
	Churchill Manitoba. Fen (58° N, 94° W)	June to August 1999 (72 days)	-34	-0.5
Joiner et al., (1999)	Thompson Manitoba. Fen (56° N, 98° W)	May to Sept. 1996 (124)	-120	-1.0
Lafleur *et al.*, (1997)	Thompson Manitoba. Fen (56° N, 98° W)	May to Sept. 1994 (124 days)	+40	+0.3
Suyker *et al.*, (1997)	Prince Albert Saskatchewan. Fen (53° N, 105° W)	May to Oct. 1994 (136 days)	-366	-2.7
Vourlitis and Oechel (1997)	Alaska U-Pad. Sedge Tundra (70° N, 148° W)	June to August 1994 (90 days)	-66	-0.7
	Alaska U-Pad. Sedge Tundra (70° N, 148° W)	May to Sept. 1995 (90 days)	-48	-0.5
	Alaska 24-Mile. Sedge Tundra (70° N, 148° W)	June to August 1995 (77 days)	-101	-1.3
Coyne and Kelley (1975)	Barrow Alaska Wet Tundra (71° N 160° W)	June to July 1971 (20 days)	-69	-3.5
Neumann *et al.*, (1994)	Lake Kinosheo, Ontario Bog (51° N, 81° W)	June to July 1990 (33 days)	-56	-1.7
Shurpali *et al.*, (1995)	Northern Minnesota. Bog (47° N 93° W)	May to October 1991 (145 days)	+123	+0.9
	Northern Minnesota. Bog (47° N 93° W)	May to October 1992 (145 days)	-55	-0.4
Fan *et al.*, (1992)	Bethel Alaska Mixed Tundra (61° N, 162° W)	July to August 1988 (30 days)	+9	+0.3

moisture, surface temperature, and plant phenology change. Furthermore, ER is affected by the nutrient status of the substrate. Organic material with higher nutrient levels is decomposed and consumed more rapidly than substrates of poor nutrient quality (Moore *et al.*, 1998).

Photosynthesis in arctic plants has been found to range between 10 and 20 g CO_2 m^{-2} d^{-1} (Semikhatova *et al.*, 1992). The spatial and temporal variability observed in GEP is attributed to plant type, growth stage, nutrient conditions, and variations in soil moisture, photosynthetically active radiation (PAR), and temperature (Green and Lange, 1994; Bubier *et al.*, 1998; Waddington *et al.*, 1998; Griffis *et al.*, 2000a). Oechel and Vourlitis (1997) have shown that the dependence of GEP and NEE on PAR and temperature is strongly correlated to the seasonal development of these ecosystems. The timing of leafout is a major event in the CO_2 balance and is often correlated with a change from a net loss to a net gain of CO_2 in fens (Schreader *et al.*, 1998). This is especially important in arctic ecosystems where the growing season is typically less than four months in duration (Burton *et al.*, 1996; Lafleur *et al.*, 1997 and Schreader *et al.*, 1998). Growing season GEP may also be limited by a large soil moisture deficit (Green and Lange, 1994) and low air temperatures (Semikhatova *et al.*, 1992).

Daily variability in the overlying meteorological conditions can also have a strong influence on GEP. Griffis *et al.*, (2000b) have shown that GEP at a subarctic fen near Churchill Manitoba is most efficient when anticyclones are positioned to the east of the study site. These synoptic conditions are associated with clear skies and the advection of warm southerly air into the region providing near optimal temperatures for

photosynthesis. Furthermore, Froking (1997) using a boreal forest model showed that NEE is strongly sensitive to the pattern and timing of weather events. The link between climate and the biophysical processes operating in these ecosystems indicate that climatic variability should be the key factor in determining the CO_2 sink and source strength of these ecosystems.

At present, the amount of inter-annual variability in growing-season NEE and its cause is speculative for these ecosystems (Vourlitis and Oechel, 1997) due to a scarcity in landscape-scale observations. As a result, our understanding of the sensitivity of CO_2 exchange to climatic variability for these landscapes is limited. There are two main problems that arise from this limitation. First, estimates of CO_2 exchange between northern wetlands and the atmosphere under future climate change scenarios are difficult to quantify and second, the development and validation of carbon exchange models for these environments is lacking.

This paper examines the sensitivity of landscape-scale NEE at a subarctic fen to climatic variability during five growing seasons. The variability in NEE is investigated by quantifying the changes in GEP and ER through each of the five seasons and by qualitatively relating these changes to key environmental factors of temperature, precipitation, radiation, water deficit and soil moisture content.

2.2. Site and Methods

2.2.1. Research Site

The experimental area is located on the southwestern shore of Hudson Bay, within the Hudson Bay Lowland (Figure 2.1). Patches of open woodland near the

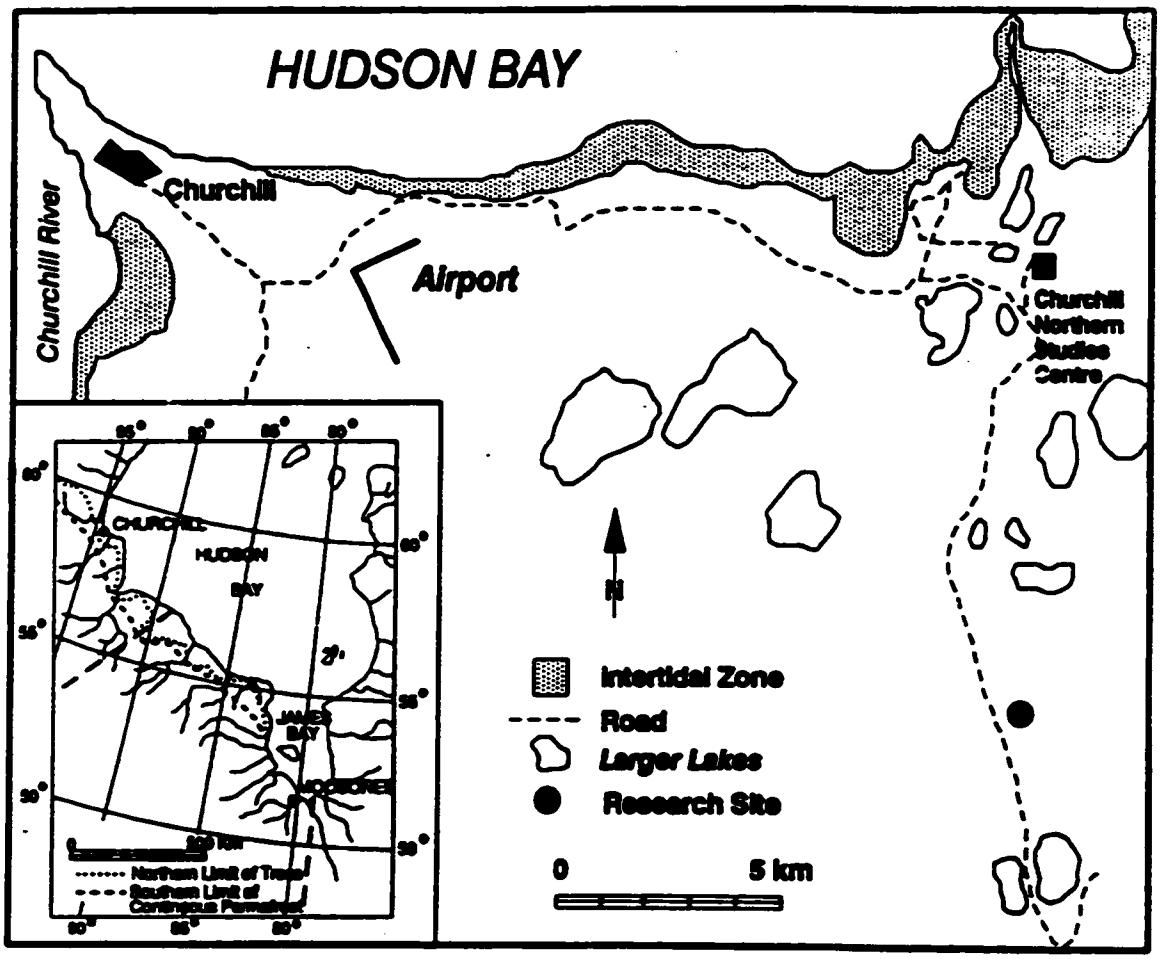

Figure 2.1: Location of research area and study site

experimental area mark the edge of the northern boreal tree line and the transition to large expanses of open tundra. The region is underlain by continuous permafrost. Hudson Bay has a strong influence on the regional climate and energy balance during the growing season through the advection of cold moist air (Rouse, 1991).

The research site is an extensive fen and is located 20 km east of the town of Churchill Manitoba (58° 45'N, 94° 04'W), and 12.5 km south of the Hudson Bay shoreline. This fen is characterized by non-patterned, hummock-hollow terrain. Detailed surveying within a 150 m radius of the main micrometeorological measurement tower indicates that small hummocks comprise 47%, hollows 48% and large hummocks 5% of the landscape with respect to the water table position. The maximum difference in vertical height between large hummocks and hollows is approximately 0.75 m. The configuration and height of the hummocks and hollows determines the depression storage of surface water. A maximum amount of water storage occurs at a mean height of 0.08 m above the base of the hollows (depression storage surface) (Rouse, 1998). As the water table rises above this equilibrium level, lateral drainage of water begins. The water table disappears below the hollow surfaces at a height of -0.08 m relative to the equilibrium storage level.

Average water table height relative to the hummocks and hollows has an important influence on the distribution of vegetation (Billings, 1987b; Bubier *et al.*, 1995). At this fen, brown moss (*Scorpidium turgescens*) is the dominant vegetation found in the wet hollows. Small hummocks exhibit a limited moss cover (*Tomenthypnum nitens*) but are dominated by the vascular species *Carex aquatilis, C. limosa, C. saxatilis*

and C. gynocrates. Larger hummocks support vascular species *(Betula glandulosa, Ledum decumbens Salix arctophila or* Carex spp.) and non-vascular species of lichen (*Cladina stellaris, C. rangiferina*) and moss (*Dicranum undulatum*).

The fen has a mean peat depth of 0.25 m and is underlain by glaciomarine till, consisting of fine silts and clays with interspersed layers of carbonate shingles. The regional landscape continues to respond to isostatic rebound following the last glaciation. Elevation increase at the research site is about 0.01 m y^{-1}. At present, the fen is approximately 22 meters above sea level, and therefore, it is estimated that vegetation and peat development was initiated about 2200 years ago. The historical rate of carbon accumulation for the fen is estimated at 11 g CO_2 m^{-2} y^{-1}.

2.2.2. Measurement

Measurements in all seasons are similar to those described in Schreader *et al.*, (1998). The Bowen ratio energy balance approach (BREB) was used to calculate the energy balance over the fen. Temperature and vapor pressure profiles were measured with wet and dry-bulb psychrometers. The sensors were mounted at heights of 0.35, 0.70, 1.10, 1.60, 2.30 and 3.20 m. A wind speed profile was measured using cup anemometers mounted at the same heights. Wind direction was measured at a height of 3.5 m. Data logger sampling was every 2 s, and the averaging period was 0.5 hour. Precipitation was recorded daily using a standard rain gauge, and half-hourly with a tipping bucket rain gauge. Water table position was measured relative to the equilibrium water storage level at a manual well and recorded continuously with a float-potentiometer system. Volumetric soil moisture was measured using a water content reflectrometer (CS615,

Campbell Scientific) during 1997, 1998 and 1999. Volumetric soil moisture was measured gravimetrically in 1994 and 1996 and also modeled as an exponential function of water table position ($R^2 = 0.88$)

$$\theta_v = 0.60 + 0.28e^{4.4WT}, \qquad (2.1)$$

where θ_v is the volumetric soil moisture content, and WT is the water table position in meters. Net radiation Q^* was measured at a height of 3 m above ground using a Middleton net pyrradiometer. Ground heat flux was measured with 4 Middleton heat flux plates, which were arranged to give a spatially representative flux. The calorimetric ground heat flux calculation was used to correct the heat flux plate measurements following Halliwell and Rouse (1987) to correct for inconsistencies in thermal conductivity and poor thermal contact between the heat flux plates and the organic soil.

2.2.3. Net CO_2 Flux Calculation

The theory and methodology for calculating the net CO_2 flux F_c using gradient techniques has been described previously in Burton *et al.*, (1996) and Schreader *et al.*, (1998). F_c is derived from the following expression

$$F_C = -K_C \frac{\partial \rho_C}{\partial z}, \qquad (2.2)$$

where K_c is the turbulent transfer coefficient for CO_2 and $\partial \rho_c / \partial z$ is the time averaged vertical gradient of CO_2 concentration. K_c is assumed identical to the turbulent heat transfer coefficient K_h and is derived from the basic energy balance equations,

$$K_C = K_h = \frac{-Q_h}{\left(\frac{\partial T}{\partial z}\right) C_p \cdot \rho_a}, \qquad (2.3)$$

where Q_h is the sensible heat flux, $\partial T/\partial z$ is the vertical temperature gradient, C_p is the atmospheric heat capacity and ρ_a is the air density. Q_h is calculated from the Bowen ratio energy balance expression:

$$Qe = \frac{Q^* - Qg}{1 + \beta} \tag{2.4}$$

where Q_e is the latent heat flux, and $\beta = Q_h/Q_e = \gamma \Delta T/\Delta e$ is the Bowen ratio, γ is the psychrometric constant and ΔT and Δe are obtained from the finite differences of temperature and vapor pressure between levels respectively. Q_h can be calculated as a residual of the energy balance equation

$$Qh = Q^* - Qe - Qg\,. \tag{2.5}$$

CO_2 concentrations were measured at the same height intervals as for temperature, vapor pressure and wind speed. Air from the six levels was drawn through equal length tubing into 1-L buffer sample volumes. Buffer volume air was continuously replenished by the pumping system. Sequential sampling from the six buffer volumes was controlled with a solenoid-actuated valve manifold system. Samples were analyzed on an infrared gas analyzer (LI-COR 6262). A time interval of 1 minute was used to determine the CO_2 concentration from the six buffer volumes. The net CO_2 flux was calculated from 0.5 hr time averaging and corrected for density variations resulting from the latent heat flux (Webb *et al.*, 1980). A correction for sensible heat flux was omitted since the samples from each level were analyzed at the same constant temperature (Burton *et al.*, 1996). Due to the remote location of the research site, all instrumentation was powered by 12-V storage batteries and charged with a wind generator and solar panels.

2.2.4. Measurement Accuracy

CO_2 flux measurements derived from the gradient approach are prone to substantial errors resulting from fetch limitations, determination of the turbulent transfer coefficient, K_c, and systematic bias in one or more of the measuring sensors. Schreader *et al.*, (1998) give a detailed discussion of these errors, which is summarized as follows.

The measurements were made over a large homogeneous fen with a minimum fetch of 2500 m in the southerly direction. Analysis indicates that 80% of the flux footprint lies within 238 m of the tower and that the most sensitive distance is at 26.5 m from the tower (Schreader *et al.*, 1998). Calculating the turbulent transfer coefficients K_h and K_c from BREB-Q_h can be problematic when Q^* is small such as at night or during sunrise or sunset. At these times, temperature and humidity gradients tend to be small and β is often unreliable. Under these conditions K_h has been derived from either the aerodynamic or eddy covariance calculation of Q_h. These data have been provided from micrometeorological stations located at the same site. This approach has been successful due to the relatively vigorous nocturnal wind speeds typically experienced at Churchill. Systematic bias in the sensors has been remedied by using a multiple level flux calculation scheme and a software package originally described by Halliwell and Rouse (1989) to test for measurement error and boundary layer problems. However, under calm conditions K_h is unreliable and the fluxes must be interpolated. Data interpolation used in this study was based on half-hour ensemble averages computed from measured data during the early, mid and late growing season periods.

The magnitude of the error in F_c resulting from the propagation of errors in the calculation of the energy balance and turbulent transfer coefficient K_h can be estimated using the root mean squared error method (RMSE) outlined by Bevington (1969). This approach estimates the error in F_c by examining the partial derivatives of F_c (proportionality constants) with respect to each of its dependent variables

$$\Delta F_c = \Delta\left(\frac{d\rho c}{dz}\right)\frac{\partial F_c}{\partial\left(\frac{d\rho_c}{dz}\right)_{K_h}} + \Delta K_h\left(\frac{\partial F_c}{\partial K_h}\right)_{\frac{d\rho c}{dz}} . \qquad (2.6)$$

The error propagating through the calculation of F_c can therefore be estimated as

$$\delta F_C = \sqrt{\left[\left(\frac{d\rho_C}{dz}\delta K_h\right)^2 + \left(K_h\frac{d\rho_C}{dz}\frac{\partial G}{\partial C}\right)^2\right]} , \qquad (2.7)$$

where δK_h is the 19% error calculated for K_h and $\partial G/\partial C$ is the 0.3% error in measuring the CO_2 concentration gradient at 350 μmol/mol. The second term in equation 2.7 can be neglected since the random error in measuring CO_2 cancels with time and the systematic bias between levels is offsetting when calculating the finite difference in CO_2 concentration. We estimate a relative maximum probable error of 24% for the measurement of F_c.

2.2.5. Estimating Ecosystem Respiration and Gross Ecosystem Production

Soil and plant root respiration has been shown to correlate with near-surface temperature (Waddington *et al.*, 1998). As well, ER increases linearly with lower water table position, which has a direct effect on Redox potential (Moore *et al.*, 1998). The amount of plant respiration is proportional to the amount of biomass present and also

varies with maturity and growth stage (Semikhatova *et al.*, 1992). Despite these complexities, some success has been achieved in estimating total respiration fluxes from tower and chamber data as functions of temperature and or water table position (Oberbauer *et al.*, 1991; Kim and Verma, 1992; Shurpali *et al.*, 1995; Waddington *et al.*, 1998). We used nighttime (solar radiation = 0 W m^{-2}) NEE tower data from four growing seasons to estimate ER as a linear function of surface temperature

$$ER = \alpha Ts + R_{\max} + R_p \qquad (2.8)$$

where α (0.15 g CO_2 m^{-2} d^{-1} $°C^{-1}$) is the slope of the *ER* vs surface temperature relationship describing microbial and plant response to surface temperature change, R_{max}, is the maximum ER rate (4.9 g CO_2 m^{-2} d^{-1}) at a surface temperature of 0 °C. R_{max} can be viewed as a relative measure of microbial activity and is also dependent on plant biomass and growth stage. R_p, is a correction factor used to adjust the ER estimate to match the observed mean nighttime measured NEE during each growing period of each year. The adjustment was used to account for changes in ER caused by variation in water table, amount of biomass, and phenology within and between the growing seasons. Since these factors cannot be modeled adequately at the present time, the use of R_p in equation 2.8 introduces less bias to the daytime ER estimate. Four years of data were used to construct the model in order to reduce the bias resulting from a relatively small data set, and as well, to facilitate a direct comparison of the daytime ecosystem respiration estimate with chamber measurements made during the 1997 growing season. Figure 2.2 shows the relationship between the estimated ER and the measured chamber ER for the 1997 growing season. Further details regarding the chamber measurements and the

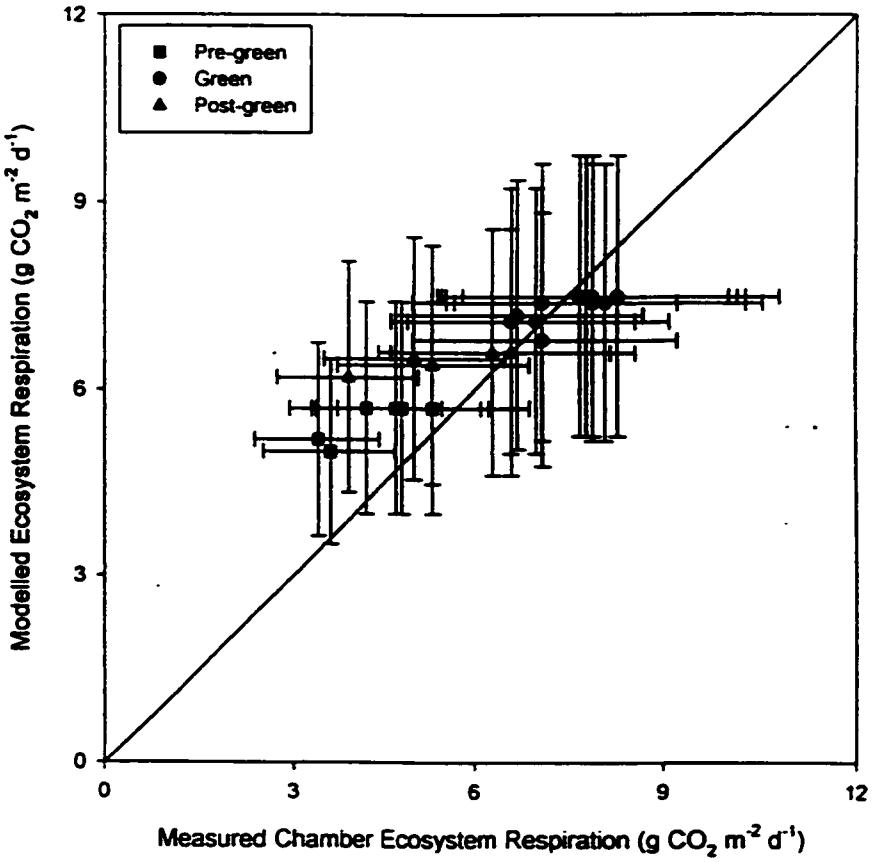

Figure 2.2: Comparison of modeled ecosystem respiration versus daytime measured ecosystem respiration. Results are averaged for individual half-hour periods during pre-green, green, and post-green periods of the 1997 growing season. Error bars represent the maximum probable error.

comparison of community-scaled chamber fluxes of ER and GEP are discussed in (Griffis *et al.* 2000a). Although our estimates of GEP and ER do not always give a balance to the observed NEE, our approach permits us to gain some insight into the variability of NEE by studying the climatic effects on GEP and ER.

2.2.6. Study Years and Growth Periods

The study years include 1994, 1996, 1997, 1998 and 1999. CO_2 fluxes and energy balance data are compared over the measurement period DOY 164 (June 13) to DOY 238 (August 26). Due to equipment failure the 1999 measurement period ends on DOY 235 (August 23). This includes the majority of the growing season at this tundra location. For comparative purposes each growing season has been divided into three periods following Schreader *et al.*, (1998). Period one (normal pre-green) extends from DOY 164 to DOY 172 (June 21). At this time the vascular species emerge but are immature. Period two (normal green) includes DOY 173 to DOY 220 (August 8). In this period vascular species reach maturity and leaf area index (LAI) reaches a maximum. Period three (normal post-green) extends from DOY 221 to DOY 238. The normal post-green period generally coincides with the onset of dormancy.

2.3. RESULTS

2.3.1. General Climatic Conditions

Growing season climatic differences between each of the years were relatively small in terms of air temperature and precipitation. However, stronger differences were evident for the pre-green, green and post-green periods. Each season was warmer than the Churchill 30-year (1965-1994) normal (Table 2.2a). During the 1994 pre-green

TABLE 2.2: Growing Season Climatological Characteristics.

(a) Mean Daily Air Temperature by Growing Period and Season (°C).

Year	Pre-green	Green	Post-green	Season
1994	12.5 (+5.7)	12.3 (+1.0)	11.1 (-0.4)	12.0 (+1.2)
1996	7.0 (+0.2)	13.0 (+1.7)	11.5 (0.0)	11.9 (+1.1)
1997	6.1 (-0.7)	13.8 (+2.5)	13.0 (+1.5)	12.7 (+1.9)
1998	5.5 (-1.3)	14.1 (+2.8)	12.9 (+1.4)	12.8 (+2.0)
1999	13.0 (+6.2)	12.6 (+1.3)	12.1 (+0.6)	12.5 (+1.7)
Normal	6.8	11.3	11.5	10.8

(b) Total Precipitation by Growing Period and Season (mm).

Year	Pre-green	Green	Post-green	Season
1994	4 (-9)	32 (-47)	37 (0)	73 (-56)
1996	35 (+22)	70 (-9)	41 (+4)	145 (+16)
1997	8 (-5)	109 (+30)	7 (-30)	125 (-4)
1998	23 (+10)	58 (-21)	35 (-2)	118 (-11)
1999	0 (-13)	72 (-7)	45 (+8)	118 (-11)
Normal	13	79	37	129

*bracketed term indicates the departure from normal.

period air temperature was nearly 6 °C above normal. Precipitation in 1994 was also below normal, providing a strong contrast to the other years (Table 2.2b). The 1996 season had above normal precipitation with an especially wet pre-green period. Air temperature and precipitation differences between 1997 and 1998 were small over the entire measurement period (Figure 2.3a). Each season was about 2 °C warmer than normal with slightly below normal precipitation. The 1998 season, however, received above normal precipitation during the pre-green period while 1997 had above normal precipitation during the green period (Figure 2.3b). In 1999, net radiation and evaporation were 20% greater than the other seasons (Figure 2.3c and 2.3d). Air temperature was 1.7 °C warmer than normal. Precipitation was slightly below normal for the growing season but especially dry during the pre-green and early green period. The approximate timing of snowmelt, based on personal observations and albedo measurements for the 1994, 1996, 1997, 1998, and 1999 seasons, was May 10, May 30, May 31, May 9, and April 22 respectively.

2.3.2. Cumulative Net Ecosystem CO_2 Exchange

During the 1994 season cumulative NEE (Figure 2.4) showed a net loss of +76 g CO_2 m^{-2} (Schreader *et al.*, 1998). Losses increased rapidly to +55 g CO_2 m^{-2} in the pre-green period where approximately 63% of the CO_2 loss occurred within this 9-day period (Table 2.3). GEP balanced ER through the green period. ER exceeded GEP in the post-green period and accounted for 37% of the total seasonal CO_2 loss.

In 1996 the wetland gained -235 g CO_2 m^{-2}. GEP exceeded ER losses by day four of the pre-green period (Figure 2.4). The rate of change in cumulative NEE was

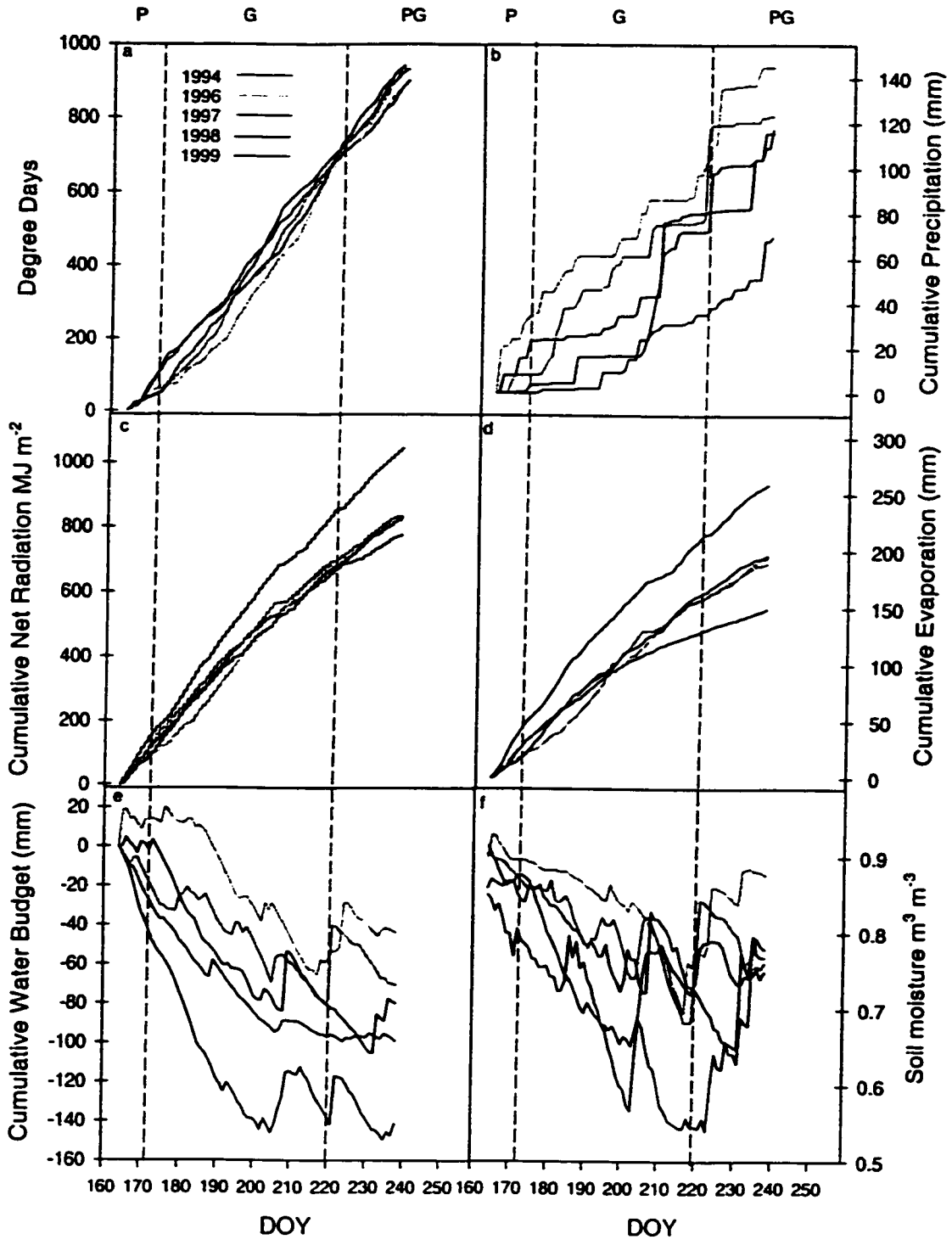

Figure 2.3: Comparison of hydroclimatological conditions during five seasons of NEE measurements at the Churchill fen. a) number of degree days, b) cumulative precipitation, c) cumulative net radiation, d) cumulative evaporation, e) cumulative water budget Σ(P-E), f) volumetric soil moisture. Years include 1994, 1996, 1997, 1998, and 1999. Periods include pre-green (P), green (G), and post-green (PG).

TABLE 2.3: Cumulative Net Ecosystem CO_2 Exchange and Estimate of Maximum Probable Error (g CO_2 m^{-2}).

Year	Pre-green	Green	Post-green	Season
1994	+55 (± 14)	-12 (± 3)	+33 (± 8)	+76 (± 19)
1996	-20 (± 5)	-135 (± 34)	-80 (± 20)	-235 (± 59)
1997	+12 (± 3)	-61 (± 15)	0 (± 0)	-49 (± 12)
1998	-22 (± 6)	-189 (± 47)	-17 (± 4)	-228 (± 57)
1999	-0.6 (± 0.2)	-41 (± 10)	+8 (± 2)	-34 (± 9)
Days	9	48	18	75

relatively constant through the green period and GEP remained larger than ER through to the end of the measurement period (August 26). The percentage of total cumulative acquisition during the pre-green, green, and post-green periods was 8, 59, and 32% respectively.

The wetland gained -49 g CO_2 m^{-2} over the 1997 growing season. During the pre-green period, cumulative NEE was positive and did not switch to a net gain until DOY 181 (June 30). NEE oscillated through the green and post-green period but remained a net CO_2 sink (Figure 2.4). Post-green period ER was larger than GEP. Nearly 85% of the net CO_2 loss occurred during the pre-green period and 15% in the post-green period.

Cumulative net exchange of CO_2 during 1998 showed strong similarity to the 1996 season (Figure 2.4). The wetland gained -230 g CO_2 m^{-2}. GEP was larger than ER at the beginning of the measurement period. The rate of cumulative gain was faster through the pre-green and early green period compared to 1996 but attained a similar rate midway through the season. A sharp reduction in cumulative NEE in the post-green period correlated with the maximum draw down of the water table that followed the very dry green period. The percentage of total cumulative NEE for the pre-green, green, and post-green period was 10, 84 and 6% respectively.

The 1999 season shows some similarity to 1997 (Figure 2.4), gaining approximately -34 g CO_2 m^{-2} by the end of the measurement period. Cumulative NEE was near zero at the end of the pre-green period. The gain of CO_2 during the early green period progressed at a rate near the 1996, 1997 and 1998 seasons. However, on DOY 188 (July 7), the net gain of CO_2 diminished considerably and GEP and ER were

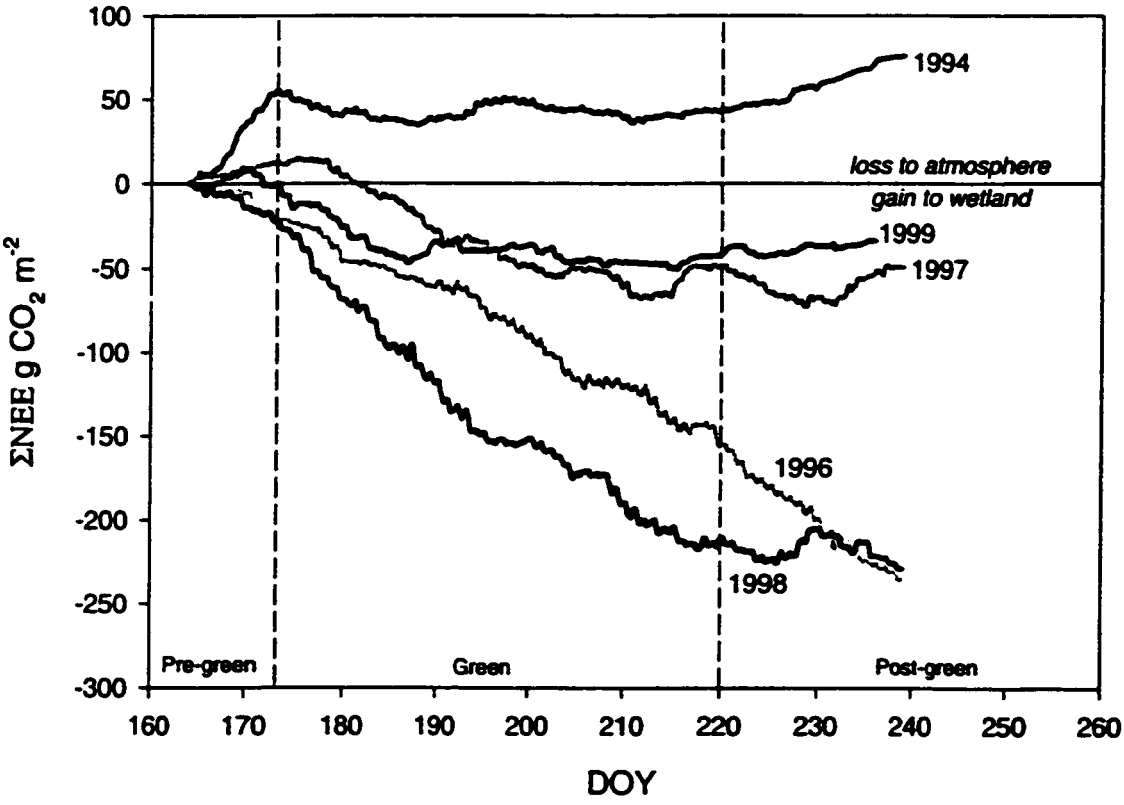

Figure 2.4: Growing season cumulative net ecosystem CO_2 exchange during five seasons of measurement at a subarctic fen near Churchill, Manitoba. Years include 1994, 1996, 1997, 1998, and 1999.

approximately balanced. During the post-green period ER was larger than GEP causing a net loss of CO_2 to the atmosphere. Approximately 99% of the net CO_2 gain occurred during the green period while all of the net loss of CO_2 occurred during the post-green period.

2.3.3. Seasonal CO_2 Exchange Patterns and Environmental Characteristics

2.3.3.1. Pre-green Period

Strong differences in diurnal NEE, GEP and ER are observed between each of the years during the pre-green period (Figure 2.5). In 1994, NEE was positive to the atmosphere for each half-hour period, averaging a net loss of +6.1 g CO_2 m^{-2} d^{-1} (Figure 5a). Pre-green GEP is dominated by bryophytes (*Scorpidium turgescens* and *Tomenthypnum nitens*) prior to vascular leaf emergence. In 1994, GEP averaged -2.6 g CO_2 m^{-2} d^{-1} while ER averaged +8.5 g CO_2 m^{-2} d^{-1}. The large net loss of CO_2 from the wetland is attributed to the hot and dry surface conditions. Air temperature was 6 °C above normal and cumulative precipitation was less than 5 mm (Figure 2.3b). The cumulative water budget, Σ(P-E), was negative (Figure 2.3e) as a result of little precipitation and strong surface evaporation (Figure 2.3d) and there was a small reduction of soil moisture by the end of pre-green the period (Figure 2.3f).

During 1996, NEE averaged -2.2 g CO_2 m^{-2} d^{-1} and exhibited a strong diurnal fluctuation (Figure 2.5b). Estimates of GEP and ER averaged -4.4 and +2.5 g CO_2 m^{-2} d^{-1} respectively. The surface conditions during this period were considerably cooler and wetter than the 1994 year. Cumulative water budget showed a net gain through the pre-

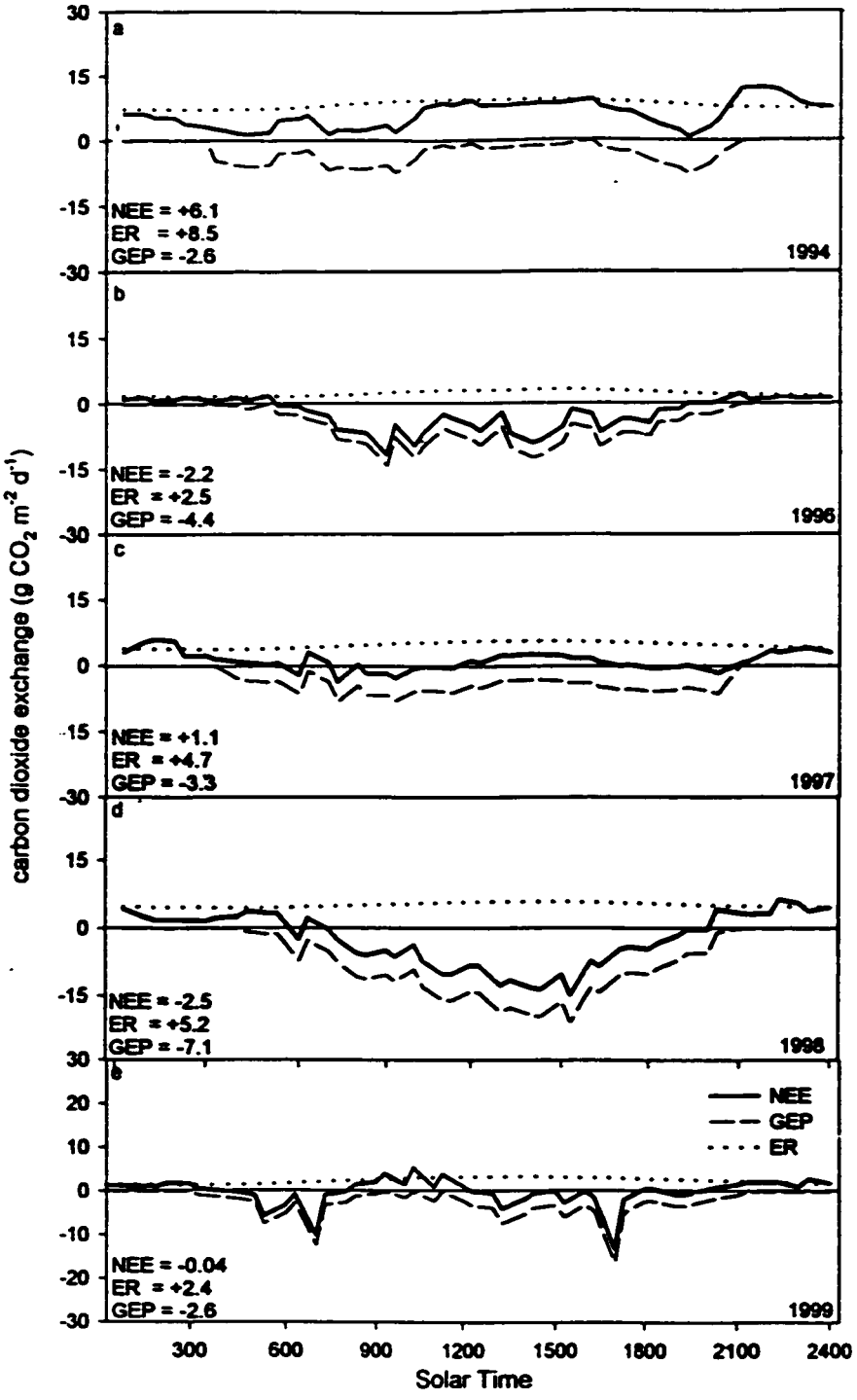

Figure 2.5: Diurnal patterns of measured NEE (solid line), estimated GEP (dashed line), and estimated ER (dotted line) during the pre-green period (DOY 164 -172).

green period and maintained soil moisture values near their maximum water holding capacity (Figure 2.3f).

The 1997 patterns of CO_2 exchange were similar to 1994 (Figure 2.5c). However, ER was approximately 45% smaller and two brief episodes of net CO_2 acquisition were observed in the early morning and late afternoon. NEE decreased substantially through the late morning hours and became positive by solar noon, averaging a loss of +1.1 g CO_2 m^{-2} d^{-1}. GEP and ER averaged -3.3 and +4.7 g CO_2 m^{-2} d^{-1} respectively. Temperatures were relatively cool compared to 1994 and 1996. The cumulative water budget was negative during the pre-green period due to low rainfall and large evaporation. However, volumetric soil moisture was near saturation at the end of the period due to a relatively late snowmelt and high initial water table position.

NEE during the 1998 pre-green period was similar to 1996, averaging -2.5 g CO_2 m^{-2} d^{-1} (Figure 2.5d). GEP averaged -7.1 g CO_2 m^{-2} d^{-1}, which was significantly larger than any other pre-green period in this study. However, ER was also relatively large and averaged +5.2 g CO_2 m^{-2} d^{-1}. Air temperature in 1998 was about 1 °C below normal. As in 1996, the cumulative water budget was positive through the pre-green period due to above normal precipitation. Consequently, soil moisture content was maintained near its maximum capacity (Figure 2.3f).

The 1999 patterns of pre-green CO_2 exchange (Figure 2.5e) is comparable to 1994 and 1997. Only brief periods of net CO_2 gain are observed during the early morning and late afternoon hours and substantial losses of CO_2 occurred prior to solar noon. Measured NEE showed a net balance. Estimates of ER and GEP averaged +2.4 and -2.6 g

CO_2 m^{-2} d^{-1}. The 1999 pre-green period was approximately 6 °C warmer than normal and did not record a single precipitation event. The cumulative water budget was -43 mm, exceeding all other years in this study. However, the volumetric soil moisture remained relatively large at 0.85 due to the initial high water table position. Personal field observations showed that the bryophytes on the larger hummocks were desiccated.

2.3.3.2. Green Period

The diurnal patterns of CO_2 exchange during the green period (Figure 2.6) differ substantially from pre-green exchange. In general, the shapes of the curves show stronger similarity between the years, which can be attributed to the emergence, and maturing of the vascular species.

In 1994, NEE was negative during most of the daytime period (Figure 2.6a) and averaged -0.2 g CO_2 m^{-2} d^{-1}. GEP averaged -6.6 g CO_2 m^{-2} d^{-1} and showed a strong decline through midday. The mean daily estimate of ER was +6.5 g CO_2 m^{-2} d^{-1}. Cumulative water budget reached -97 mm, reducing the soil water content to below 0.55. Blanken and Rouse (1996) and Schreader *et al.*, (1998) demonstrated evidence of water conservation via a decrease in stomatal conductance for *Carex* spp. at this site and other wetlands near Churchill. We hypothesize that plant moisture stress was the cause of the observed midday reduction in GEP and NEE. Given the drier and warmer temperature conditions and the increase in biomass, it is surprising that ER decreased from the pre-green period. However, Lafleur *et al.*, (1997) reported similar findings for a northern boreal fen in the same year. The reduction may be related to rapid consumption of fresh litter at the surface in the pre-green period (Schreader *et al.*, 1998) and also a depletion of

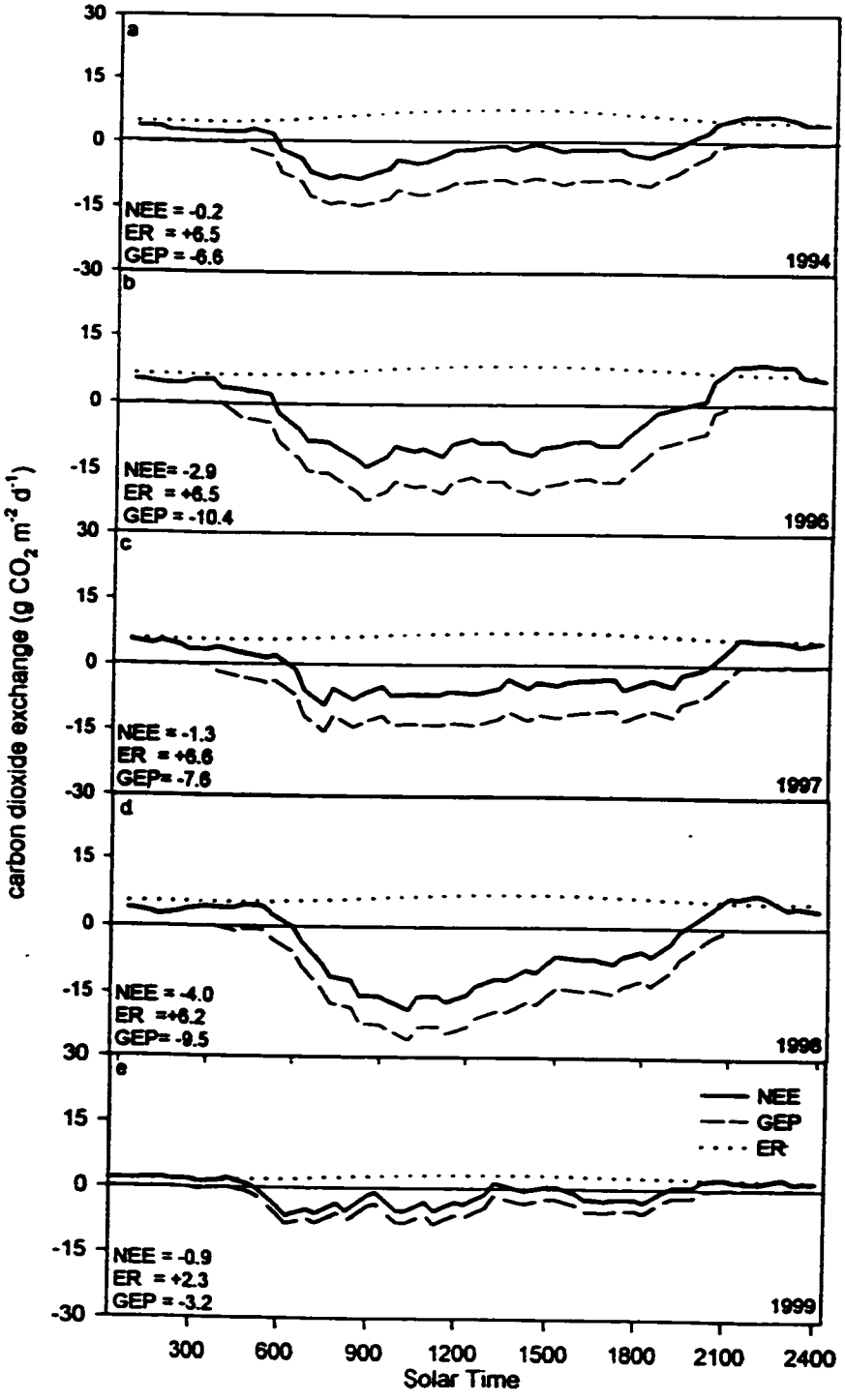

Figure 2.6: Diurnal patterns of measured NEE (solid line), estimated GEP (dashed line), and estimated ER (dotted line) during the green period (DOY 173-219).

CO_2 supplied from the melting of ice in peat soils of the active layer. Furthermore, it may reflect changes in plant growth or a relaxation in energy supply for tissue maintenance.

Mean NEE was -2.9 g CO_2 m^{-2} d^{-1} in 1996 (Figure 2.6b). GEP and ER averaged -10.4 and +6.5 g CO_2 m^{-2} d^{-1} respectively. A reduction in NEE and GEP during midday is apparent but less pronounced than in the 1994 season. Air temperature was above normal during this period and the cumulative evaporative flux exceeded precipitation. Soil moisture decreased through the green period (Figure 2.3f) and reached a season minimum of 0.64 on DOY 218 (August 6).

Patterns of CO_2 exchange in 1997 are similar to 1994 (Figure 2.6c). NEE averaged -1.3 g CO_2 m^{-2} d^{-1} and estimates of GEP and ER averaged -7.6 and +6.6 g CO_2 m^{-2} d^{-1}. The diurnal pattern of NEE and GEP exhibit a steady reduction through the late morning and afternoon hours. Air temperature was above normal during this period. Despite the large increase in precipitation, large evaporative fluxes caused the cumulative water budget to become more negative. As a result, the volumetric soil moisture decreased (Figure 2.3f) and reached a season minimum on DOY 219 (August 7). We hypothesize that the observed increase in ER from the pre-green period is due to the warmer temperatures, lower soil moisture content, and increased plant biomass.

The 1998 green period (Figure 2.6d) was similar to the 1996 period. NEE, GEP, and ER averaged -4.0, -9.5, and +6.2 g CO_2 m^{-2} d^{-1} respectively. The main distinction between the two years is greater net CO_2 gain during the early morning and stronger midday reduction in GEP during 1998. Air temperature was approximately 3 °C warmer

than normal and precipitation was near normal for the period. The cumulative water budget decreased substantially during the 1998 period causing a soil moisture deficit, which was on average, larger than the 1997 period (Figure 2.3f). Despite the warm temperatures and reduction in soil moisture, the net acquisition of CO_2 remained relatively large compared to 1997 and 1996.

During the 1999 green period NEE averaged -0.9 g CO_2 m^{-2} d^{-1}. The pattern is similar to the 1994 season, exhibiting a strong reduction in net CO_2 gain through the midday period. Both GEP and ER are small compared to the other seasons (-3.2 and +2.3 g CO_2 m^{-2} d^{-1}) and suggest that the canopy did not develop to its normal potential or that it experienced high mortality rates due to the drier conditions. Precipitation during this period was slightly below normal. Evaporation exceeded precipitation resulting in a large negative cumulative water budget of -134 mm. Volumetric soil moisture was reduced to a minimum of 0.72 (Figure 2.3f).

2.3.3.3. Post-green Period

In general, the post-green patterns of CO_2 exchange (Figure 2.7) indicate a reduction in GEP and the relatively quick transition to dormancy which is most pronounced in the years that experienced dry pre-green conditions.

In 1994, the wetland showed a net gain of CO_2 for two short intervals during the early morning and late afternoon (Figure 2.7a). NEE averaged +1.8 g CO_2 m^{-2} d^{-1}. GEP and ER decreased substantially from the green period rates to -2.5 and +4.3 g CO_2 m^{-2} d^{-1}. The post-green period was cooler than normal but had near normal rainfall. The cumulative water budget was positive and raised the volumetric soil water content to 0.80

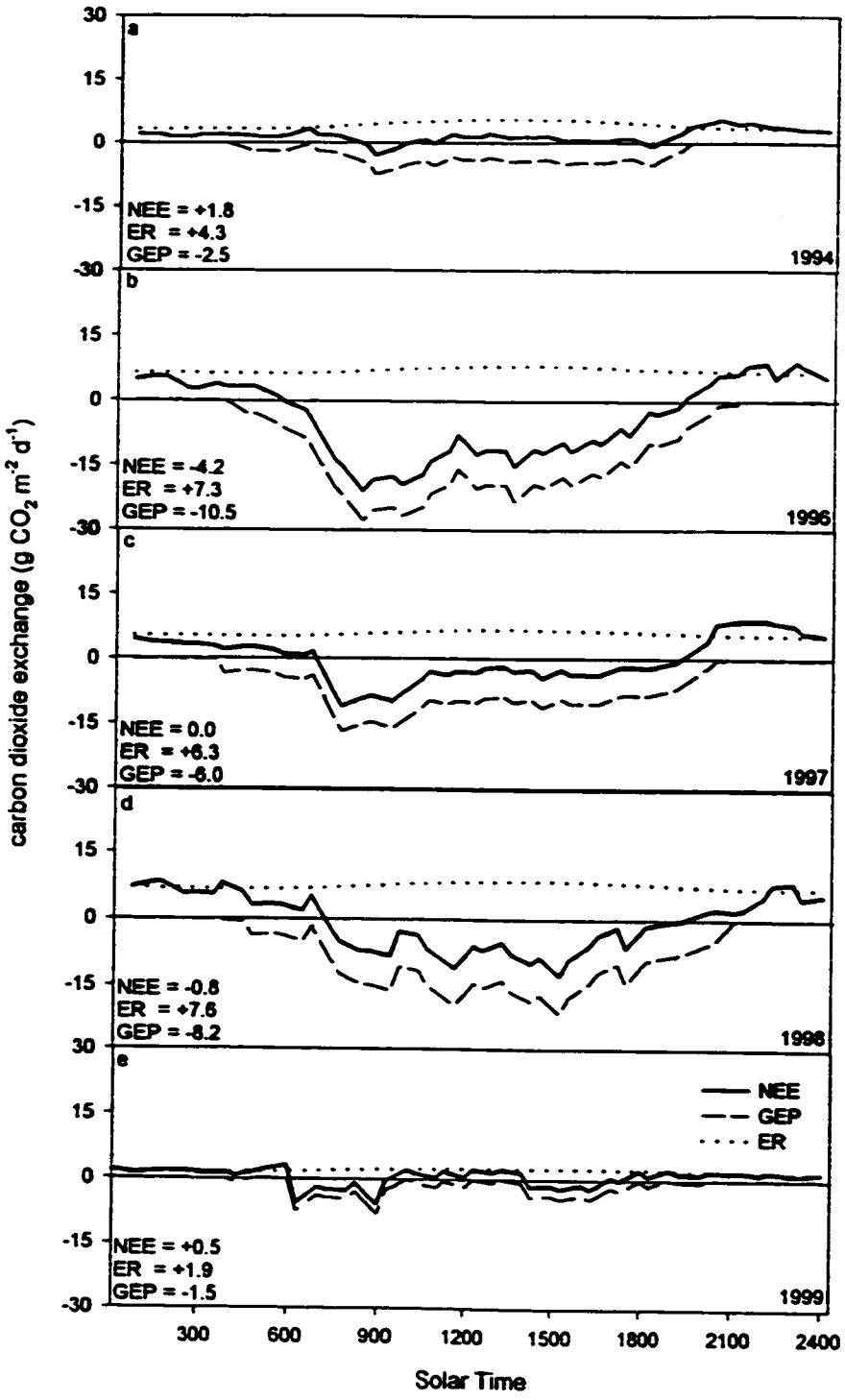

Figure 2.7: Diurnal patterns of measured NEE (solid line), estimated GEP (dashed line), and estimated ER (dotted line) during the post-green period (DOY 220-238).

by the end of the period (Figure 2.3f). The estimated reduction in GEP indicates that the vascular vegetation was beginning to senesce. LAI and shoot density of *Carex* spp. had started to decrease by DOY 201 (July 20) (Schreader *et al.*, 1998). The transition to dormancy of the vascular species appears to have been initiated relatively early due to the persistent drought conditions. Field observations by Schreader *et al.*, (1998) found that the effects of the dry summer on the vegetation caused a marked reduction in the "greenness" of the canopy. The mosses in the hollows and sedges on the small hummocks were desiccated. We hypothesize that the reduction in ER from the green period is related to the wetter soil conditions, cooler temperatures, and reduction in living plant tissue.

The 1996 post-green period gained CO_2 at a faster rate than the green period (Figure 2.7b). NEE, GEP and ER averaged -4.2, -10.5, and +7.3 g CO_2 m^{-2} d^{-1} respectively. The increased acquisition of CO_2 resulted from a reduction in ER. The post-green period was both warmer and wetter than normal. The delayed senescence of the fen vegetation due to the wet seasonal conditions may explain the sustained rate of GEP. Personal field observations found that the fen vegetation remained "green" until the end of the measurement period.

The 1997 post-green period yielded a net efflux of +0.1 g CO_2 m^{-2} d^{-1} (Figure 2.7c). The net loss of CO_2 can be attributed to a reduction in GEP relative to ER. The respective fluxes were -6.0 and +6.3 g CO_2 m^{-2} d^{-1}. Temperature was above normal and precipitation below normal. Soil moisture decreased rapidly over the final 15 days of the measurement period.

Patterns of CO_2 exchange in 1998 showed strong diurnal variability (Figure 2.7d). GEP decreased to -8.2 g CO_2 m^{-2} d^{-1} while ER increased to +7.6 g CO_2 m^{-2} d^{-1}. NEE averaged -0.8 g CO_2 m^{-2} d^{-1}. The net gain of CO_2 decreased substantially in 1998 due to a near equal increase in ER and reduction in GEP. This reduction in net CO_2 acquisition on the seasonal cumulative exchange is apparent in Figure 2.4. Air temperature was warmer than normal and precipitation near normal during this period. However, soil moisture content reached a minimum on DOY 231 (August 19). This minimum occurred about 12 days later than the other experimental years.

There is strong similarity between 1999 (Figure 2.7e) and the 1994 post-green period. We hypothesize that this similarity stems from advanced dormancy caused by drought conditions experienced through the majority of each growing season. NEE averaged a net loss of + 0.5 g CO_2 m^{-2} d^{-1}. GEP and ER decreased on average to -1.5 and +1.9 g CO_2 m^{-2} d^{-1} respectively. Even though the post-green period received more precipitation than normal, this failed to rejuvenate the GEP of the canopy.

2.4. DISCUSSION AND CONCLUSIONS

2.4.1. Inter-annual Variability in NEE

The five-year experiment captured a wide range of climatic conditions and included the strong El Niño phenomenon of spring-1998. Large inter-annual variability is observed in the net ecosystem CO_2 exchange ranging from a net source to a net sink over the five-year study. The cause of inter-annual variability in NEE is complex, driven by change in the net photosynthetic rate of moss and sedges and, as well, variation in heterotrophic and autotrophic respiration. GEP rates were generally more variable than

measured nighttime and estimated daytime ER rates on a diurnal and seasonal basis. Soil moisture, air temperature and stomatal conductance are important variables in causing the observed diurnal patterns of NEE. The growth stage and phenology of the wetland vegetation are especially important during the pre-green and post-green periods. Inter-annual variability in NEE is most pronounced during these shoulder periods. Consequently, it is necessary for climate models to describe phenology and growth cycles properly. Phenology has also been identified as a key variable driving the inter-annual variability in the global carbon budget. Kindermann *et al.*, (1996) using the Frankfurt Biosphere Model to reconstruct annual changes in atmospheric CO_2 concentrations suggest that anomalous sink years might result from early leafing. Furthermore, modeling efforts by Frolking (1997) found that the timing of weather patterning had a strong influence on CO_2 exchange for a boreal forest. The link between climate and phenology is emerging as a key determinant in the observed variability in global atmospheric CO_2 concentrations.

Large losses of CO_2 experienced during 1994 are related to the dry and hot surface characteristics of the fen. The climatic conditions during the early spring and pre-green period (when the wetland vegetation is developing) appear from this evidence to have a profound impact on NEE. This impact persists through the remainder of the season. Dry conditions at the beginning of 1997 and 1999 cause a similar diurnal pattern in NEE during the pre-green period as in 1994. Both 1997 and 1994 experienced large losses of CO_2 during this period. Increased precipitation during the green period of 1997, 1999 and the post-green period of 1994 did not cause a substantial increase in GEP. In

contrast, above normal precipitation during the pre-green period of 1996 and 1998 resulted in a net gain of CO_2. The gain in 1996 was largely due to the high soil moisture content and associated low ER, whereas the gain in 1998 was caused by a large increase in GEP. In 1998, early snowmelt, and above normal precipitation and temperature (Griffis *et al.*, 2000b) caused an earlier greening of the fen. Wet and warm conditions sustained through the 1996 growing season resulted in a large GEP rate during the green and post-green periods. There was no sign of the onset of dormancy at the end of the measurement period. The green and post-green periods in 1998 were drier than the 1996 and 1997 periods. However, GEP remained large and cumulative NEE was comparable to 1996. Climatic differences between 1998 and 1997 are small over the entire measurement season. The disparity in cumulative NEE between the two years is therefore somewhat surprising. However, Lafleur *et al.*, (2000) have found similar observations for an open subarctic forest site located adjacent to the Churchill fen. This evidence further supports the hypothesis that NEE is strongly influenced by the early spring climatic conditions. Wet and warm conditions during the early growing period increase the photosynthetic capacity and fitness of the vegetation and largely determine the CO_2 sink/source magnitude of this wetland environment.

2.4.2. Comparison with other Landscape Scale Studies

Table 2.1 provides a summary of the major studies examining landscape-scale NEE measurements over northern wetlands using eddy covariance or gradient micrometeorological techniques. Twelve of the seventeen field studies show ecosystems that were net sinks of CO_2 over the growing-season, however, the majority of these

indicated only weak net sinks of less than -2.0 g CO_2 m^{-2} d^{-1}. Given the errors involved in measurement and the lack of complete CO_2 flux information for the non-growing season (Zimov *et al.*, 1993; Fahnestock *et al.*, 1999), it is reasonable to conclude that most of these landscapes, on an annual basis, experienced a net loss of CO_2 to the atmosphere. Only three of the studies suggest a net annual CO_2 sink including Suyker *et al.*, (1997) and the 1996 and 1998 seasons in Churchill. The CO_2 sink strength for Churchill is speculative given the lack of spring, fall and wintertime NEE measurements. The three net sink studies indicate that northern wetlands have the potential to sequester significant amounts of CO_2 when climatic conditions are favorable. These favorable conditions for CO_2 sequestration include frequent rain events combined with high water table position and warm temperatures at least during the beginning of the growing-season.

Shurpali *et al.*, (1995), Vourlitis and Oechel (1997), Schreader *et al.*, (1998) and our results confirm that water balance (soil moisture) is critical to the sink/source strength of these wetlands. The limited number of studies conducted over the past three decades suggest that northern wetlands have experienced a reduction in their average sink strength of approximately -40 g CO_2 m^{-2} y^{-1} (Gorham, 1991) and in most cases have switched to a net source of atmospheric CO_2. Zimov *et al.*, (1993), Vourlitis and Oechel (1997), Oechel *et al.*, (1997) and Fahnestock *et al.*, (1999) support that wintertime respiration rates have the potential of offsetting summertime CO_2 gains despite the cold conditions in these arctic environments. If we take the average CO_2 exchange for the Churchill fen over the five growing seasons and assume a non-growing season of 240 days with a soil respiration rate of +0.5 g CO_2 m^{-2} d^{-1} (Zimov *et al.*, 1993) we find that the fen is losing

approximately +30 g CO_2 m^{-2} y^{-1}. The 5-year NEE budget of the Churchill fen suggests a contemporary loss of CO_2 that is proceeding at about 3 times the rate of its long-term historical gain.

2.4.3. Implications for Climate Change

Atmospheric general circulation models predict warmer temperatures and increased precipitation over subarctic and arctic regions given a doubling of atmospheric CO_2 (IPCC, 1996). Projected temperatures for the summer range from 1 to 4 °C, while winter temperatures are predicted to increase 2 to 5 °C. Coupled GCMs forecast an increase in precipitation. Simulations from a number of models predict an increase of 0 to 2 mm d^{-1} during the summer months and 0 to 0.5 mm d^{-1} during the winter. At the present it is difficult to conclude with confidence how these climatic changes will immediately affect the net ecosystem exchange of CO_2 at high latitudes. This is due to uncertainty surrounding the changes in 1) evaporation rates 2) active layer deepening 3) water balance and water table position and 4) soil moisture content.

Rouse (1998) developed a model to explore the potential impact of a $2xCO_2$ warming on the water balance of the Churchill fen. The model was run with changes in air temperature and precipitation forecast for the Churchill region by a number of GCMs. The scenario employed was an increase in the annual air temperature by 4 °C (Mitchell, 1990) and an increase in precipitation of 20% (Maxwell, 1992). The water balance calculations show that evaporation increases would exceed precipitation increases and cause water deficits to be greater than the recent 30-year normal. The Churchill fen would experience a lower water table position and decreased soil moisture. These results,

coupled to our present study, indicate that ER will increase relative to GEP. Reductions in CO_2 acquisition will be most severe if future spring conditions become drier than present. The transient response of carbon storage at the Churchill fen, therefore, is likely to be a greater net loss under a $2xCO_2$ climate change scenario. However, over longer time scales the wetland may experience greater CO_2 sequestration due to changes in nutrient cycling and plant response (Waddington *et al.*, 1998; Griffis *et al.*, 2000a).

2.5. CONCLUSIONS

Growing season net ecosystem CO_2 exchange shows large inter-annual variability, ranging from a net source to a net sink over the five years of measurement. Variability results from daily and seasonal changes in the GEP of the mosses and sedges and from changes in soil and plant respiration rates. We hypothesize that GEP is more variable than ER on a daily and seasonal basis. Our evidence suggests that climate conditions during the pre-growth and pre-green period are critical to the sink/source strength of the wetland over the growing season. The linkage between phenological stage and climatic conditions is important in determining the CO_2 sink/source strength, especially during the shoulder seasons. It is, therefore, imperative that climate models describe phenological stage accurately for this type of landscape. Years which experience a drier than normal spring experience either a loss or near balance exchange of CO_2 between the wetland and atmosphere. A comparison of landscape-scale NEE studies from northern latitudes over the last three decades suggests that most wetlands are sequestering considerably less CO_2 from the atmosphere when compared to their historical rates and appear to be net sources of CO_2 to the atmosphere rather than sinks. Future research

efforts need to combine process based chamber studies with landscape scale measurements in order to determine and model the contributions of GEP and ER at the community level. The measurement and modelling of non-growing season respiration is needed in order to improve our understanding of the annual CO_2 budget of northern wetlands.

CHAPTER THREE

A SYNOPTIC CLIMATOLOGICAL ANALYSIS OF NET ECOSYSTEM CO_2 EXCHANGE AT A SUBARCTIC WETLAND [1]

3.1. INTRODUCTION

Few studies have examined the impact of synoptic scale weather systems on boundary layer processes such as surface energy partitioning (Petrone and Rouse, 2000) or net ecosystem CO_2 exchange (NEE). NEE is the balance between gross ecosystem production (GEP) and ecosystem respiration (ER). To our knowledge the link between synoptic scale systems and NEE has not been explored using field based observations. Synoptic systems affect radiative exchange at the surface and have an important influence on boundary layer processes through long-range advection and the development of mesoscale circulation (Petrone and Rouse, 2000; Rouse, 1991; Rouse and Bello, 1985). In turn, surface exchange processes modulate synoptic air parcels so that the trajectory of the air mass (source region) becomes an important forcing parameter downstream. Petrone and Rouse (2000) show that the source region of an air mass can have a strong impact on the downstream surface energy balance in subarctic environments. Synoptic weather patterns should also have a strong influence on the behavior of NEE, since GEP ER are sensitive to variations in radiation, air temperature and water exchange (Vourlitis

[1] A modified version of this chapter, authored by T. J. Griffis, R. Petrone, and W. R. Rouse, has been submitted to *Arctic, Antarctic, and Alpine Research*.

and Oechel, 1997; McFadden *et al.*, 1998; Griffis *et al.*, 2000a). Perhaps of greater importance, synoptic activity and the general circulation of the atmosphere may have a profound influence on the timing of snowmelt and freeze-back, thereby, affecting the length of the growing season. Generalizing the behavior of surface exchange processes with synoptic scale activity and the general circulation of the atmosphere is valuable for understanding the feedbacks operating within the system and as well, to help better parameterize surface processes in General Circulation Models (GCMs).

The climate of mid and high latitude regions can be viewed as a composite of the daily synoptic weather types experienced over time. Recent El Niño events suggest that future climate warming will be accompanied by significant changes in the general circulation of the atmosphere. Thus, the pattern, frequency, and source regions of synoptic types will likely vary with climate change. This would give rise to important changes in the energy, water and carbon cycle of the affected underlying surfaces.

Annual variation in the seasonal amplitude of atmospheric CO_2 implies that global terrestrial primary production decreases during El Niño years (Keeling *et al.*, 1989). The El Niño events of 1973 and 1983 were each characterized by a large anomalous input (5 Pg or 5 x 10^{15} g) of CO_2 into the atmosphere (Kindermann *et al.*, 1996). Investigations using the Frankfurt Biosphere Model (FBM) provide strong evidence that the increase of atmospheric CO_2 during El Niño years resulted from a reduction in net photosynthesis due to increased photorespiration over tropical rain forests (Kindermann *et al.*, 1996). Their study also found an increase in net photosynthetic rates at northern boreal regions due to the warmer temperature conditions

and earlier leaf development. Photosynthesis in arctic ecosystems is constrained by cold temperatures (Tieszen, 1973; Zalensky, 1977; Semikhatova *et al.*, 1992) and therefore, warming of the arctic should enhance gross ecosystem productivity. However, the impact of synoptic systems on the net exchange of carbon will be more difficult to assess given the interactive effects of temperature, moisture and nutrient availability on photosynthesis, respiration and plant growth. Plant acclimation to increasing air temperature, changes in available nutrients, and as well, changes in carbon allocation within plants need to be considered for assessing the long-term effect of climatic change on NEE (Oechel and Billings, 1992).

This paper investigates the impact of synoptic scale weather patterns, using the Bergereon mid-latitude cyclone model, on the carbon dioxide budget of a subarctic sedge fen near Churchill, Manitoba during three different growing seasons. Of particular interest, the 1997/1998 winter-spring season experienced strong El Niño conditions and may serve as a simple analog for climatic change and may also provide empirical support for the simulation experiments conducted by Kindermann *et al.*, (1996).

Three hypotheses are tested in this paper: 1) synoptic types and their source regions influence NEE through their affect on the timing of snowmelt and length of the growing season; 2) photosynthetic efficiencies vary according to synoptic type. 3) climate change predicted for the Churchill region using typical GCM $2xCO_2$ simulations conforms to the conditions experienced during El Niño events and provides evidence that phenology is a key parameter affecting the CO_2 budget during the growing season.

3.2. METHODS AND INSTRUMENTATION

3.2.1. Study Area

The experimental area is located on the southwestern shore of Hudson Bay, within the Hudson Bay Lowland (Figure 3.1). Patches of open woodland near the experimental area mark the edge of the northern boreal tree line and the transition to large expanses of open tundra underlain by continuous permafrost, which begins to the immediate south of the region. The region is dominated by wetlands.

The research site is an extensive fen, located 20 km east of the town of Churchill Manitoba (58° 45 ' N, 94° 04 ' W), and 12.5 km south of the Hudson Bay coast. This fen is characterized by non-patterned, hummock-hollow terrain with hummocks comprising 47%, hollows 48% and large hummocks 5% of the landscape (Griffis *et al.*, 2000a). Brown moss (*Scorpidium turgescens*) is the dominant vegetation found in the wet hollows. The moss (*Tomenthypnum nitens*) and vascular species (*Carex aquatilis, C. limosa, C. saxatilis and C. gynocrates*) cover the small hummock sites. Larger hummocks support vascular species (*Betula glandulosa, Ledum decumbens Salix arctophila or Carex* spp.) and non-vascular species of lichen (*Cladina stellaris, C. rangiferina*) and moss (*Dicranum undulatum*). The fen has a mean peat depth of 0.25 m and is underlain by glaciomarine till, consisting of fine silts and clays with interspersed layers of carbonate shingles.

3.2.2 Energy and CO_2 Flux Measurements

The Bowen ratio energy balance approach (BREB) was used to calculate the energy balance over the fen. Temperature and vapor pressure profiles were measured

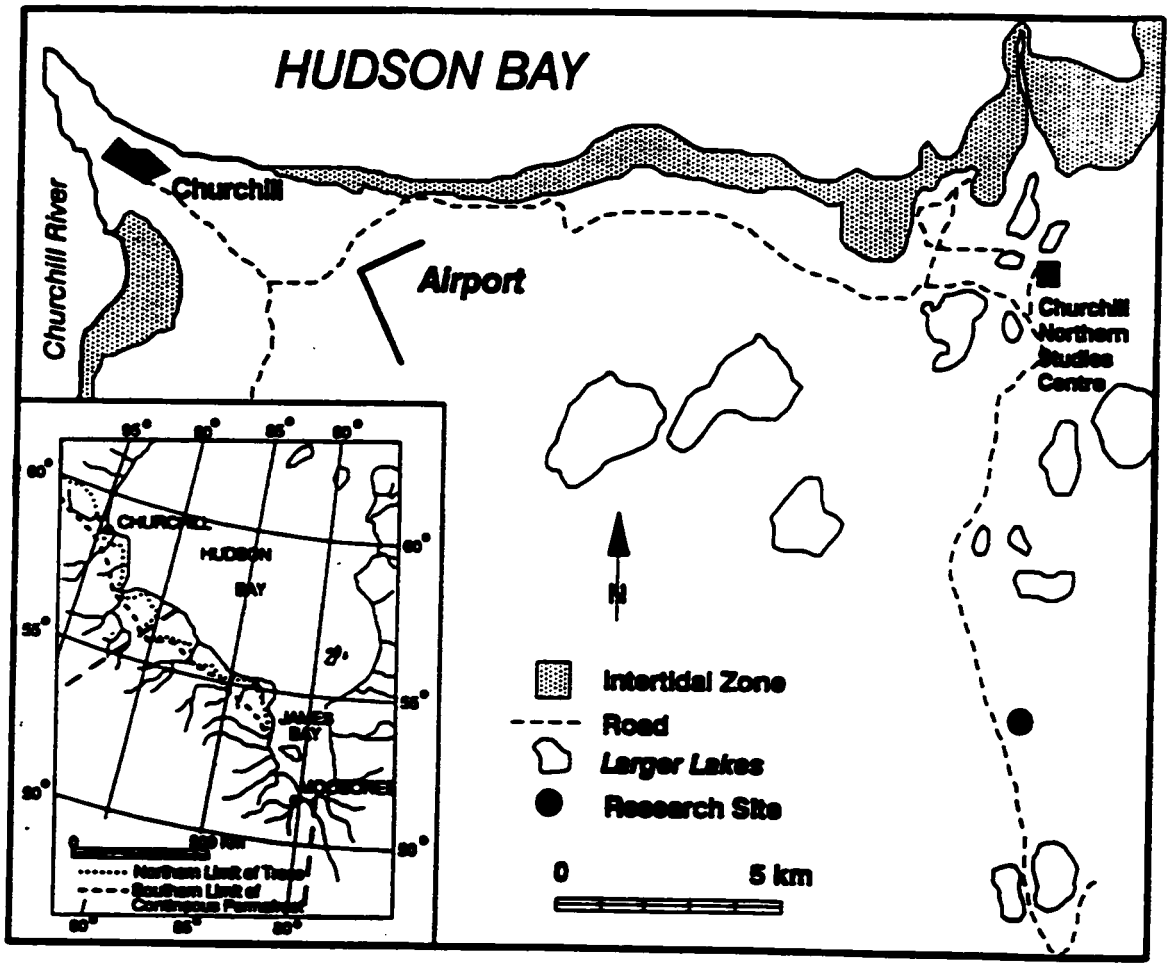

Figure 3.1: Research area and study site.

with wet and dry-bulb psychrometers. The sensors were mounted at heights of 0.35, 0.70, 1.10, 1.60, 2.30 and 3.20 m. A wind speed profile was measured using cup anemometers mounted at the same heights. Wind direction was measured at a height of 3.5 m. Data logger sampling was every 2 s, and the averaging period was 0.5 hour. Precipitation was recorded daily using a standard rain gauge, and half-hourly with a tipping bucket rain gauge. Water table position was measured relative to the equilibrium water storage level at a manual well and recorded continuously with a float-potentiometer system. Net radiation Q* was measured at a height of 3 m above ground using a Middleton net pyrradiometer. Incoming, $K\downarrow$, and reflected, $K\uparrow$, solar radiation were measured with Eppley pyranometers. Surface temperature was monitored using a series of thermocouple arrays. Ground heat flux was measured with 4 Middleton heat flux plates, which were arranged to give a spatially representative flux. The calorimetric ground heat flux calculation was used to correct the heat flux plate measurements following Halliwell and Rouse (1987) to correct for differences in thermal conductivity between the plate and organic substrate.

The theory and methodology for calculating the net CO_2 flux F_c using gradient techniques has been described previously in Burton *et al.*, (1996), Schreader *et al.*, (1998) and Griffis *et al.*, (2000b). F_c is derived from the following expression

$$F_C = -K_C \frac{\partial \rho_C}{\partial z} \qquad (3.1)$$

where K_c is the turbulent transfer coefficient for CO_2 and $\partial\rho_c/\partial z$ is the time averaged vertical gradient of CO_2 concentration. K_c is assumed identical to the turbulent transfer coefficient K_h and is derived from the basic energy balance equations where

$$K_C = K_h = \frac{-Q_h}{\left(\frac{\partial T}{\partial z}\right) C_p \cdot \rho_a} \quad , \qquad (3.2)$$

Q_h is the sensible heat flux, $\partial T/\partial z$ is the vertical temperature gradient, C_p is the atmospheric heat capacity and ρ_a is the air density. Q_h is calculated from the Bowen ratio energy balance expression

$$Qe = \frac{Q^* - Qg}{1+\beta} \quad , \qquad (3.3)$$

where Q_e is the latent heat flux, and $\beta = Q_h/Q_e = \gamma\Delta T/\Delta e$ is the Bowen ratio, γ is the psychrometric constant and ΔT and Δe are the finite differences in temperature and vapor pressure respectively. Q_h can be calculated as a residual of the energy balance equation

$$Q_h = Q^* - Q_e - Q_g \, . \qquad (3.4)$$

CO_2 concentrations were measured at the same height intervals as for temperature, vapor pressure and wind speed. Due to the remote location of the research site, all instrumentation was powered by 12-V storage batteries, which were charged with a wind generator and solar panels. Air from the six levels was drawn through equal length tubing into 1-L buffer sample volumes. Buffer volume air was continuously replenished by the pumping system. Sequential sampling from the six buffer volumes was controlled with a solenoid-actuated valve manifold system. Samples were analyzed on an infrared gas

analyzer (LI-COR 6262). A time interval of 1 minute was used to determine the CO_2 concentration from the six buffer volumes. The net CO_2 flux was calculated from 0.5 hr time averaging and corrected for density variations resulting from the latent heat flux (Webb *et al.*, 1980).

3.2.3. Synoptic Classification

Daily surface weather maps (1200 UTC) were obtained from the Arctic Weather Service, Atmospheric Environment Service for the periods April to September, 1996 to 1998. A "Hybrid Classification" developed by Frakes and Yarnal (1997), which combines a manual classification scheme (Bergen School mid-latitude cyclone model) and the Kirchhofer correlation-based map-pattern classification scheme, was applied to the synoptic data set to produce a synoptic catalogue for the Churchill region (Kirchhofer, 1973; Bradley and England, 1979; Yarnal, 1984; Yarnal, 1993; Frakes and Yarnal, 1997; Yarnal and Frakes, 1997; Petrone and Rouse, 2000).

3.3. RESULTS

3.3.1. Growing-Season Climatic Conditions

Each of the growing seasons was warmer than the Churchill 30-year normal (Table 3.1a). The 1996 season was wetter than normal while the 1997 and 1998 seasons were both slightly drier than average (Table 3.1b). Although the El Niño growing season (1998) was similar to the 1997 season in terms of solar radiation, air temperature, energy balance, and total precipitation, its main distinction was an abnormally warm-wet spring and early snowmelt which was completed by mid-May (Griffis *et al.*, 2000b). The timing

Table 3.1: Seasonal precipitation and temperature at the Churchill fen

(a) Total precipitation (mm) by period and season. Bracketed term indicates the departure from the Churchill Airport 30-year normal (1965 to 1994).

Year	DOY 164 to 172	DOY 173 to 219	DOY 220 to 238	Season
1996	35 (+22)	70 (-9)	41 (+4)	145 (+16)
1997	8 (-5)	109 (+30)	7 (-30)	125 (-4)
1998	23 (+10)	58 (-21)	35 (-2)	118 (-11)
Normal	13	79	37	129

(b) Mean daily air temperature (°C) by period and season. Bracketed term indicates the departure from the Churchill Airport 30-year normal (1965 to 1994).

Year	DOY 164 to 172	DOY 173 to 219	DOY 220 to 238	Season
1996	7.0 (+0.2)	13.0 (+1.7)	11.5 (0.0)	11.9 (+1.1)
1997	6.1 (-0.7)	13.8 (+2.5)	13.0 (+1.5)	12.7 (+1.9)
1998	5.5 (-1.3)	14.1 (+2.8)	12.9 (+1.4)	12.8 (+2.0)
Normal	6.8	11.3	11.5	10.8

of snowmelt during the El Niño year was approximately three weeks earlier than normal (Lafleur *et al.*, 2000).

3.3.2. Net Ecosystem CO_2 Exchange

Each year experienced a net gain of CO_2 during the growing season. The 1996 and 1998 El Niño season were similar, sequestering about -3.1 g CO_2 m^{-2} d^{-1}. In 1997, NEE was significantly lower at -0.7 g CO_2 m^{-2} d^{-1}. Dividing NEE into its components of GEP and ER indicates that photosynthesis experiences greater seasonal and inter-annual variability than ecosystem respiration (Griffis *et al.*, 2000a; Griffis *et al.*, 2000b). Table 3.2 indicates that GEP fluxes were larger in 1996 and 1998 compared to the 1997 growing season (Griffis *et al.*, 2000b). Representative values of LAI were not available for each of the years of study at similar time periods. However, based on the changes observed in the daily GEP rate, we estimate that full canopy development was attained at different times during each study year. The estimate of full canopy development was obtained by taking the derivative of the changing photosynthetic rate in each of the years. Maximum photosynthetic rates were established on DOY 215, 201, and 187 in 1996, 1997 and 1998 respectively. At this site, the inter-annual variability in NEE is primarily related to changes in photosynthetic activity. Our analysis, therefore, examines the synoptic influence on GEP.

3.3.3. Synoptic Pattern Identification and Circulation Traits

Nine synoptic types were identified using the hybrid classification scheme for the three years (Figure 3.2) for the period of April 15 to September 15 (Petrone and Rouse,

Table 3.2: Estimated gross ecosystem production (GEP) and ecosystem respiration (ER) for each period, and measured net ecosystem exchange (NEE) during the season.

Year	Pre-green GEP/ER	Green GEP/ER	Post-green GEP/ER	Season NEE
1996	-4.4, +2.5	-10.4, +6.5	-10.5, +7.3	-3.1
1997	-3.3, +4.7	-7.6, +6.6	-6.0, +6.3	-0.7
1998	-7.1, +5.2	-9.5, +6.2	-8.2, +7.6	-3.1

* all units are g CO_2 m^{-2} d^{-1}

2000; Petrone *et al.*, 2000). There were a few days from each year that were not classified (N.C.) by the hybrid system. The important synoptic types are briefly defined below and the frequency of occurrence is given. The total frequency of occurrence for all synoptic types combined is less than 100% due to unclassified cases.

3.3.3.1 Type 1: Warm Frontal Passage

Synoptic Type 1 is a cyclonic system that moves into the Hudson Bay region from the northwest or west-northwest. Churchill is located within the warm sector of the system. The trajectory can be tracked back to the Gulf of Alaska. The air mass traverses east to northeast out of the Hudson Bay region. Type 1 frequency for 1998 was 13% and did not occur in either 1996 or 1997. Type 1 produced relatively warm and cloudy conditions with an average precipitation rate of 0.7 mm per event (Table 3.3).

3.3.3.2 Type 3: Pre-High to the Northwest

Synoptic Type 3 is defined as a pre-high pressure condition with a trajectory approaching from the northwest of Churchill. Northerly to northeasterly flow are characteristic of this system. Advection of air across Hudson Bay brings cold temperatures and frequent fog into the Churchill region. This acts to enhance the sensible heat flux and suppresses the evaporative flux causing larger than normal Bowen ratios for the study area (Rouse and Bello 1985; Petrone and Rouse 2000). The frequency of synoptic Type 3 was largest in 1996 and 1997 at about 20%. During the 1998 El Niño year the frequency was lower at 15%. These systems account for approximately 2 mm of precipitation per event and are characterized by near freezing air temperatures over the study period (Table 3.3).

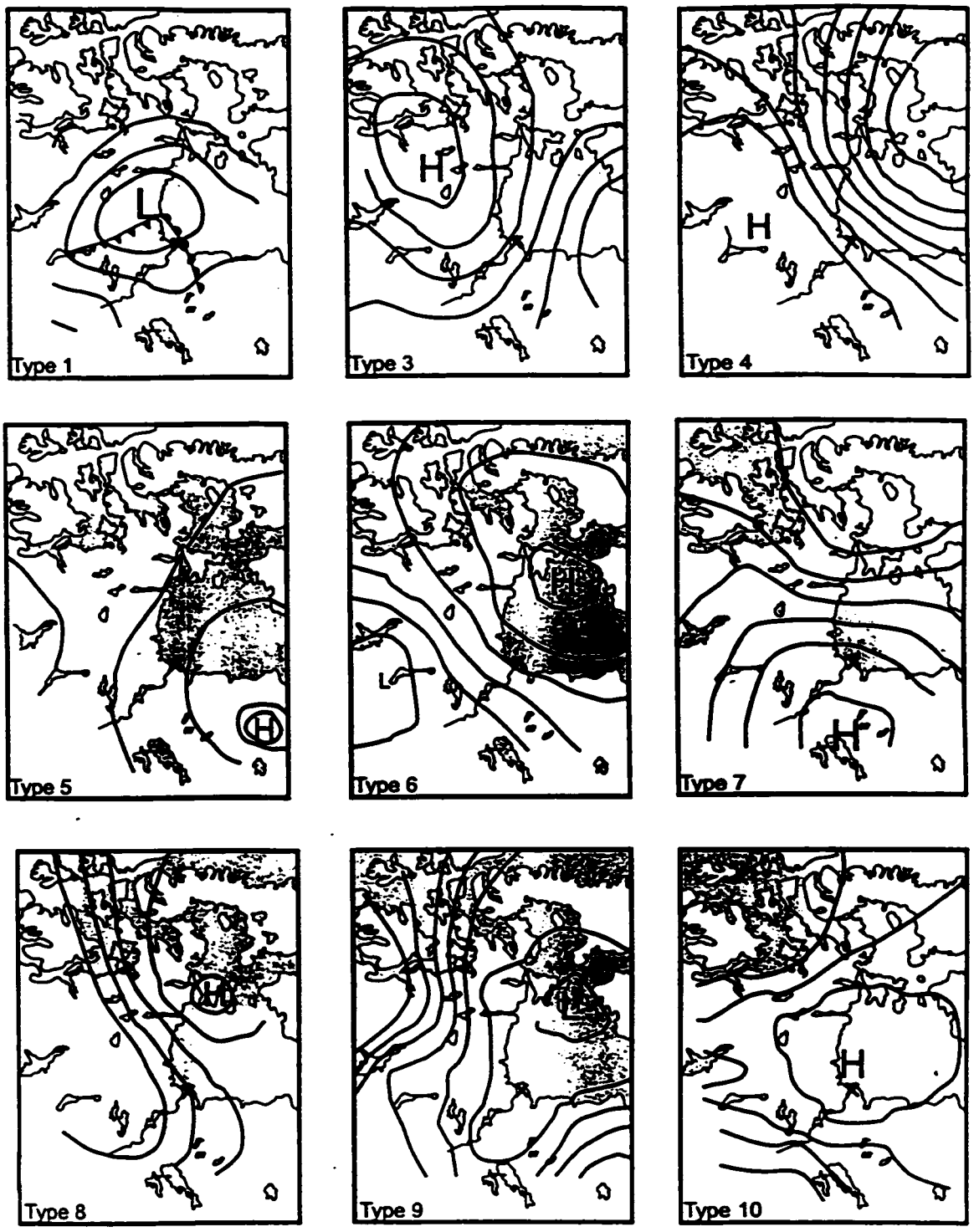

Figure 3.2: Synoptic types identified using the hybrid classification scheme during the 1996, 1997, and 1998 study seasons (April 15 to September 15) for the Churchill and central arctic region.

Table 3.3: Mean surface conditions associated with synoptic type during the period DOY 106 to DOY 260 (April 15 to September 15)

Type	Ta (Ta*)	K↓*	CC	β*	E*	P	VPD*
1	7.7 (13.5)	91	76	0.59	2.4	0.7	0.49
2	N.C.	N.C.	N.C.	N.C.	N.C.	N.C.	N.C.
3	-0.5 (7.4)	129	36	0.91	1.9	2.0	0.15
4	2.9 (12.6)	170	38	0.58	2.8	0.3	0.51
5	4.4 (15.4)	146	38	0.36	2.8	2.5	0.66
6	1.7 (10.6)	121	42	0.73	2.2	1.5	0.22
7	8.0 (15.6)	173	44	0.42	2.9	0.2	0.72
8	3.7 (8.7)	143	49	3.74	2.5	2.9	0.19
9	5.8 (11.5)	110	69	0.79	2.3	4.4	0.29
10	0.9 (11.1)	173	47	0.50	3.3	1.1	0.40

* mean conditions during the growing season (DOY 164- 238) only

Ta, air temperature (°C)
K↓, solar radiation (W m^{-2})
CC, percentage cloud cover
β, Bowen ratio
E, evaporation (mm)
VPD, vapour pressure deficit (kpa)

3.3.3.3. Type 4: Pre-high to the Southwest

Type 4 pushes northeast into the Churchill region and is dominated by northerly flow. This anticyclone is continental with a back trajectory from the southwest. The frequency distribution for Type 4 was 11% in 1996 and 1997 and 9% in 1998. Synoptic Type 4 is characterized by high solar insolation, low precipitation and relatively high evaporation rates (Table 3.3).

3.3.3.4. Type 5 and Type 6: Back of High Southeast and Back of High Northeast

Synoptic Type 5 is defined by an anticyclonic condition where the center of high pressure is situated southeast of the study region. The system has a trajectory to the east or southeast. Airflow is largely southerly. Frequencies for Type 5 were 16, 10 and 13% in the respective study years. Synoptic Type 6 is anticyclonic with the center of high pressure displaced to the northeast of the study region. The system has a trajectory to the east or northeast and flow is southerly. Type 6 frequencies were 11% in 1996 and 1997 and did not occur during the 1998 El Niño year. Synoptic Type 5 is associated with higher insolation, warmer air temperatures and higher evaporation rates than Type 6 (Table 3.3).

3.3.3.5. Type 7: High to the South

Synoptic Type 7 is defined by a high-pressure system situated to the east-southeast of the region. The flow is therefore southerly due to the back-of-the-high configuration. As a result, warm and dry continental air is advected into the study area enhancing evaporation and reducing the Bowen ratio (Petrone and Rouse, 2000).

Precipitation rates during the 3 years were about 0.2 mm per event (Table 3.3). Frequencies for the 1996, 1997 and 1998 study years were 6, 5 and 6%.

3.3.3.6. Type 8: High to the North

Low pressure to the south and high pressure to the north of the study region characterize synoptic Type 8. Surface conditions are similar to synoptic Type 3 due to the advection of cold moist air across Hudson Bay. The Bowen ratio values tend to be high and precipitation rates average about 3 mm per event (Table 3.3). The frequency of synoptic Type 8 was 7% in 1998 and did not occur in 1996 or 1997.

3.3.3.7. Type 9: Extended Low

An elongated low-pressure system extends across Hudson Bay and over the Churchill region. These systems are relatively warm and cloudy and account for the majority of Churchill's precipitation at approximately 4 mm per event (Table 3.3). The frequency distribution was 15 and 18 % in 1996 and 1997 respectively but increased to 22% in 1998.

3.3.3.8. Type 10: Elongated High

High pressure is centered over the Churchill region. Strong insolation, warm temperatures and light winds result from the weak pressure gradient across the region. Synoptic Type 10 produced the largest observed evaporation rates over the three-year study period (Table 3.3). The frequency distribution in 1996, 1997 and 1998 was 11, 16 and 9% respectively.

3.3.4. Snowmelt Synoptic Conditions

Recent studies by Griffis *et al.*, (2000b) and Lafleur *et al.*, (2000) hypothesize that the timing of snowmelt and pre-growth climatic conditions exerts a strong control on the growing-season exchange of CO_2 in northern wetlands. Pre-growth climatic conditions appear to affect the timing of leafing, nutrient availability, and the length of the growing season, which has a significant impact on the total photosynthetic flux of the canopy and therefore cumulative NEE. We examine the differences in synoptic behaviour from April 15 (DOY 105) to June 12 (DOY 163) for each of the years to explain the differences in the timing of snowmelt and the "greening" of the fen canopy. The important synoptic Types and their frequencies during snowmelt are shown in Table 3.4.

The major distinction between the 3 years is the increased frequency of synoptic Type 1 and the disappearance of Type 6 during the El Niño year. The Type 1 frequency increased from less than 2% in 1996 and 1997 to nearly 20% under El Niño conditions. Figure 3.3 indicates that atmospheric circulation during pronounced El Niño conditions causes the northwestern portion of North America to be warmer than normal from December to March (Hidore and Oliver, 1993). During these months the polar jet stream shifted north along the northwestern Pacific coast and western subarctic region preventing arctic air from penetrating south and allowing warmer southerly air to move north. Figure 3.4 verifies that this circulation pattern persisted during the 1998 late winter and spring period. During the months of April and May the polar jet was shifted north of its normal position (Figure 3.4). The polar jet returned to its normal summer position by the month of June. In 1997 (Figure 3.4) April and May show the polar jet positioned

Table 3.4: Snowmelt synoptic types for the period DOY 105 to DOY 163 (April 15 to June 12)

Synoptic Type	1996		1997		1998	
	N	F	N	F	N	F
1	N.C.	N.C.	N.C.	N.C.	11	19.6
2	N.C.	N.C.	N.C.	N.C.	N.C.	N.C.
3	14	24.1	13	23.2	13	23.2
4	3	5.3	6	10.7	3	5.4
5	9	15.8	4	7.1	9	16.1
6	9	15.8	6	10.7	N.C.	N.C.
7	1	1.8	2	3.6	3	5.4
8	N.C.	N.C.	N.C.	N.C.	2	3.6
9	12	21.1	7	12.5	6	10.7
10	5	8.8	13	23.2	9	16.1
Total Maps	**57/57**	**92.7**	**56/57**	**92.0**	**56/57**	**100.2**

N, number of days
F, frequency %
Total Maps, number of available synoptic maps analyzed over the period

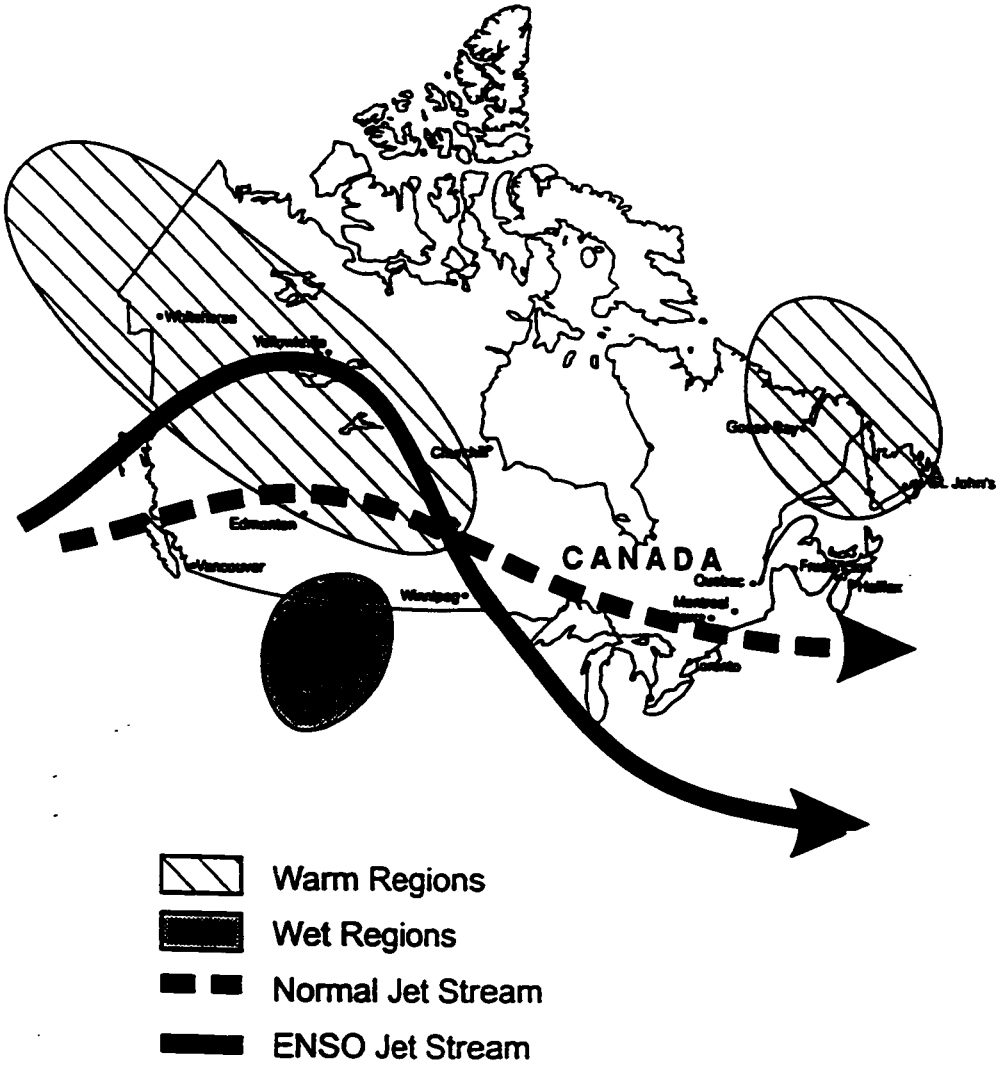

Figure 3.3: Position of the polar jet stream and depiction of source region characteristics during normal and El Niño conditions for December to March (adapted from Hidore and Oliver, 1993).

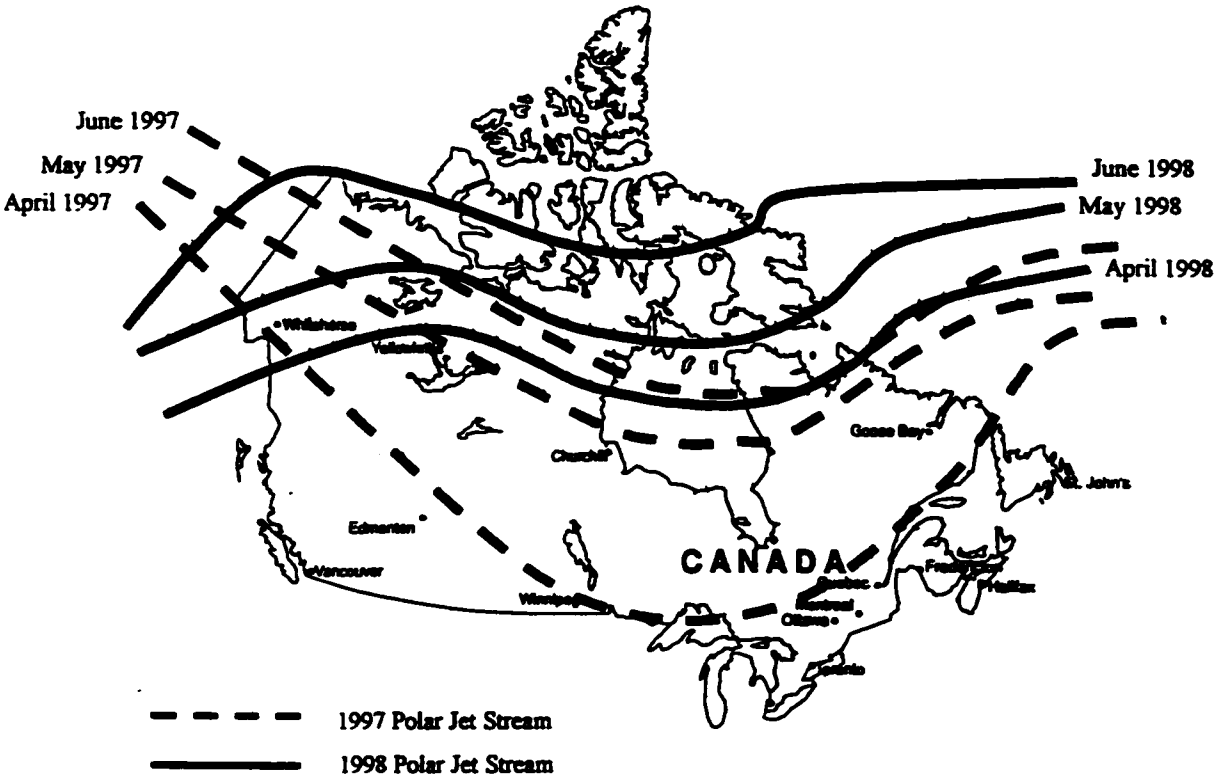

Figure 3.4: Mean position of the polar jet stream estimated from observed tropopause pressure gradient during April 1997, May 1997, June 1997, April 1998, May 1998, and June 1998 (raw data provided by the National Oceanic and Atmospheric Administration, NOAA, and the Cooperative Institute for Research in Environmental Sciences, CIRES, Climate Diagnostics Centre).

near or south of the Churchill research station.

The higher frequency of synoptic Type 1 in 1998 contributed to the early snowmelt due to the advection of relatively warm air. Differences in mean surface temperature and precipitation for each synoptic Type during the pre-growth period are presented in Table 3.5. Comparing the 3 years we see that the Type 1 synoptic pattern is associated with warmer air temperatures and greater moisture than Type 6. Therefore, the increased frequency of Type 1 in the 1998 El Niño year relative to Type 6 helped promote the early snowmelt. On average, air masses during the 1998 El Niño spring period were warmer 1996 and 1997 synoptic Types.

Precipitation totals were similar in 1996 and 1997. Snow was the major input during April and May, while rain accounted for most of the precipitation in June. Total precipitation was greatest for synoptic Types 9 and 3. The El Niño season had approximately double the precipitation with the majority occurring as rain during May and June. Precipitation totals were greatest under synoptic Types 1 and Type 3. Synoptic Type 1 accounted for 24% of the total precipitation. Type 1 appears to have played an important role in the large uptake of CO_2 in 1998 due to the warm and wet conditions associated with it.

3.3.5. Growing Season Synoptic Conditions

The growing season has previously been defined from DOY 164 to DOY 238 (Schreader *et al.*, 1998; Griffis *et al.*, 2000b). Synoptic Type 1 was important during the 1998 El Niño growing season accounting for 11% of the air masses (Table 3.6.). The

Table 3.5. Temperature and precipitation conditions associated with snowmelt synoptic Types (DOY 105 to DOY 163)

	1996		1997		1998	
Synoptic Type	**Ta**	**P**	**Ta**	**P**	**Ta**	**P**
1	N.C.	N.C.	N.C.	N.C.	3.5	19.4
2	N.C.	N.C.	N.C.	N.C.	N.C.	N.C.
3	-7.8	2.3	-10.7	12.2	-1.9	15.3
4	-4.7	0	-11.0	1.3	-6.0	8.6
5	-6.2	6.2	-10.5	0	2.8	0
6	-3.9	1.7	-9.0	0	NA	NA
7	-10.0	0	-6.0	0	-3.3	0.4
8	N.C.	N.C.	N.C.	N.C.	-0.5	11.8
9	-4.6	21.5	-5.1	11.6	0.7	10.9
10	-10.6	0	-4.3	5.0	-2.7	0.2
Average/Total	**-6.8**	**31.7**	**-8.1**	**30.1**	**-0.9**	**66.6**

Ta, air temperature (°C)
P, precipitation (mm)

Table 3.6. Synoptic Types during the growing season (DOY 164 to DOY 238)

Synoptic Type	1996		1997		1998	
	N	F	N	F	N	F
1	N.C.	N.C.	N.C.	N.C.	8	10.8
2	N.C.	N.C.	N.C.	N.C.	N.C.	N.C.
3	15	20.5	12	19.0	6	8.1
4	9	12.3	7	11.1	7	9.5
5	10	13.7	8	12.7	7	9.5
6	5	6.9	8	12.7	N.C.	N.C.
7	8	11.0	4	6.3	6	8.1
8	N.C.	N.C.	N.C.	N.C.	9	12.2
9	11	15.1	12	19.0	21	28.4
10	7	9.6	6	9.5	6	8.1
Total Maps	65/73	89.1	57/63	90.2	70/74	94.7

N, number of days
F, frequency %
Total Maps, number of available synoptic maps analyzed over the period

dominant weather pattern during the El Niño year was Type 9 at 28 %. The prevailing air mass in 1996 was Type 3 at 21%. In 1997, Type 3 and Type 9 each accounted for about 19% of the air mass Types.

3.3.6. Synoptic Influence on Gross Ecosystem Production

During the 1998 El Niño pre-growth period, early snowmelt and warm conditions promoted the early leafing of the fen canopy. Figure 3.5 shows that cumulative CO_2 exchange during the pre-green period resulted in a large uptake during the El Niño year. The 1996 season experienced a small net gain while 1997 showed a large net loss of CO_2. This indicates that the fen canopy had not developed sufficiently to counter ecosystem respiration losses (Griffis *et al.*, 2000b). Synoptic conditions have an indirect impact on CO_2 cycling by affecting the length of the growing season. However, they also directly affect CO_2 cycling by influencing the available radiation, temperature and moisture at the surface.

We examined the relationship between synoptic Type and daily photosynthetic rates using the methods of Bradley and England (1979) and Petrone and Rouse (2000) who developed precipitation and evaporation efficiency parameters associated with each synoptic Type. Photosynthetic efficiencies for each synoptic Type were computed as:

$$PS_{ij} = \frac{P_{ij} N_j}{N_{ij} P_j} \cdot 100\% \qquad (3.5)$$

Where PS_{ij} is the photosynthetic efficiency, P_{ij} is the photosynthetic flux for Type i in period j, N_{ij} is the frequency of Type i in period j, N_j is the total number of days in period j, and P_j is the cumulative photosynthetic flux in period j. The increase of a synoptic

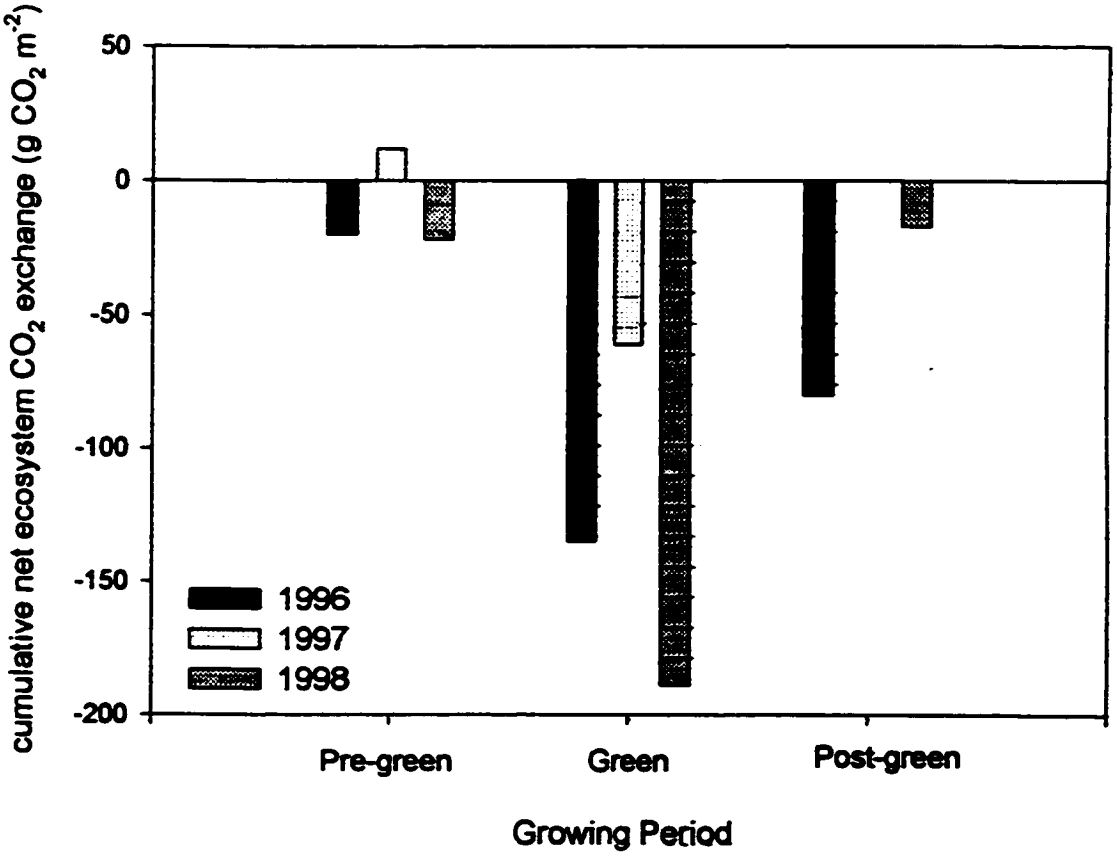

Figure 3.5: Cumulative net ecosystem CO_2 exchange at the Churchill fen during the 1996, 1997, and 1998 growing seasons. Growing periods include pre-green (DOY 164 to 172), green period (DOY 173 to 220), and post-green period (DOY 221 to 238).

type's frequency combined with a reduction in the associated photosynthetic flux will cause PS to approach 0%. Conversely, low synoptic frequency combined with a large photosynthetic rate will cause PS to approach 100%.

In 1996, photosynthesis was most efficient under Type 7 and Type 10 (Table 3.7a). In 1997, the photosynthetic efficiency was substantially higher for Type 7 than any other synoptic air mass (Table 3.7b). During the 1998 El Niño season, Type 4 and Type 7 displayed the highest photosynthetic efficiency (Table 3.7c). Each of these synoptic Types is characterized by anticyclonic conditions in the Churchill region. The mean daily surface conditions associated with these synoptic Types are moderate to high insolation (>115 to 258 W m^{-2}), warm air temperatures (12.0 to 17.6 °C), strong evaporation (>2.5 mm d^{-1}) and low rainfall (<1.0 mm d^{-1}).

The lowest photosynthetic efficiency in each year is associated with synoptic Type 3 (anticyclonic conditions approaching the region). The mesoscale influence of synoptic Type 3 on the Churchill region is pronounced cooling due to cold air advection from Hudson Bay (Rouse and Bello, 1985). Daily air temperature is typically less than 9 °C. A low-level cloud layer (CC > 71%) reduces daily solar insolation to 117 W m^{-2} on average. Rainfall ranges from 1.4 to 2.2 mm per event. Vapour pressure deficits (VPD) are low and the Bowen ratio values are large indicating that the sensible heat flux is enhanced relative to evaporation. These conditions reduce photosynthesis across the region largely due to the cold air temperatures and low solar radiation.

Table 3.7: Photosynthetic efficiency and environmental characteristics associated with synoptic Type

a) 1996 (WET) growing season.

Synoptic Type	PS_{ij}	K↓	Ta	VPD	E	β	P	CC
3	4.9	178	5.9	0.12	2.0	0.93	2.1	74
4	11.6	251	13.2	0.54	2.8	0.63	0	63
5	12.4	199	16.3	0.67	2.5	0.38	4.2	70
6	11.9	219	8.4	0.25	2.9	0.70	1.1	71
7	**16.0**	**258**	**17.1**	**0.90**	**3.3**	**0.36**	**0.2**	**63**
9	10.1	179	13.2	0.29	2.2	0.51	4.8	71
10	**16.1**	**255**	**12.7**	**0.44**	**3.3**	**0.58**	**1.0**	**64**

b) 1997 (DRY) growing season.

Synoptic Type	PS_{ij}	K↓	Ta	VPD	E	β	P	CC
3	7.3	92	8.6	0.17	1.9	0.87	2.1	72
4	9.5	119	12.5	0.40	2.5	0.64	2.3	66
5	11.6	125	17.0	0.67	3.6	0.21	2.3	64
6	11.5	82	11.7	0.20	2.0	0.81	3.8	77
7	**26.8**	**110**	**17.6**	**0.60**	**2.5**	**0.40**	**0.6**	**66**
9	8.6	85	11.4	0.32	2.3	0.48	8.6	75
10	9.6	142	12.0	0.41	3.8	0.35	0	61

c) 1998 (El Niño) growing season

Synoptic Type	PS_{ij}	K↓	Ta	VPD	E	β	P	CC
1	8.8	91	13.5	0.49	2.4	0.59	0.7	68
3	6.1	80	8.6	0.14	2.0	0.93	1.4	71
4	**13.3**	**115**	**12.0**	**0.57**	**3.2**	**0.46**	**0.3**	**61**
5	11.8	93	12.4	0.63	2.2	0.52	0.1	65
7	**12.7**	**102**	**12.2**	**0.57**	**2.6**	**0.54**	**0.2**	**61**
8	5.0	108	8.1	0.23	2.9	0.68	0.9	62
9	8.5	89	10.7	0.27	2.2	1.1	2.9	68
10	12.3	107	8.5	0.34	2.8	0.57	1.3	65

PS_{ij}, photosynthetic efficiency
K↓, solar radiation (W m^{-2})
Ta, air temperature (°C)
VPD, vapour pressure deficit (kpa)
E, evaporation (mm)
β, Bowen ratio
P, precipitation (mm)
CC, percentage cloud cover

3.4. DISCUSSION AND CONCLUSIONS

The interannual variability found in net ecosystem CO_2 exchange at the Churchill fen can be linked to large-scale variations in atmospheric circulation and synoptic climatology. Position of the polar jet and its influence on the synoptic Types that advect into the Churchill region is especially important during the early spring, pre-growing period. Under the 1998 El Niño conditions, warmer air masses and, as well, a high frequency of warm frontal systems (synoptic Type 1) moved through the Churchill region from April to June. This pattern promoted an earlier than normal snowmelt and longer than normal growing season.

Photosynthesis by mosses contributed to early carbon acquisition after snowmelt and we estimate that the vascular plants leafed 2 weeks earlier than in 1997 and 3 weeks earlier than in 1996. It is also possible that the warmer spring period increased the nutrient supply, enhancing plant growth later in the season (Lafleur *et al.*, 2000). Ample rainfall in the early spring period coincident with the timing of leafing helped promote vascular development. In 1998, canopy development was near maximum before drier conditions were established through July and August. It appears that the vascular plants were less susceptible to the droughty conditions experienced during the summer season. Furthermore, the greater canopy development earlier in the season was able to take advantage of the higher available solar radiation.

A recent study by Lafleur *et al.*, (2000) also shows similar between-year differences in NEE for open subarctic woodland for the 1997 and 1998 growing seasons. This research site is contiguous to the fen and is subject to the same meteorological

conditions. Results from the fen and open woodland provide empirical support for the model simulations of Kindermann *et al.*, (1996) showing that these northern boreal systems acquire more carbon under El Niño conditions. It appears that atmospheric circulation and synoptic activity during the winter-spring transition and their impact on phenology is more important than the synoptic effects on CO_2 exchange during the main growing period. Radiation, air temperature, energy balance, precipitation and water table differences between the 1997 and 1998 summer seasons were extremely small (Griffis *et al.*, 2000b). The earlier leafing and canopy development caused by warmer pre-growth temperatures is more important than the differences in synoptic Types during the growing season.

Daily changes in synoptic and mesoscale activity are important, largely because of the temperature dependence of the CO_2 exchange processes (dark reactions of photosynthesis, photorespiration and ecosystem respiration) operating within the system. Air temperature substantially affects the dark reaction rate of photosynthesis. Cold temperatures limit Rubisco activity (Semikhatova *et al.*, 1992), the enzyme used in fixing ambient CO_2, by reducing the transport of phosphate to chloroplasts (Taiz and Zeiger, 1991). The temperature optimum for photosynthesis in arctic plants has been reported at approximately 15 °C (Tieszen, 1973; Semikhatova *et al.*, 1992). The Churchill fen and open woodland are, therefore, forced to photosynthesize well below their temperature optimum over much of the growing season. The link between daily synoptic Type and photosynthetic efficiency indicates that photosynthesis is maximized under synoptic Types 4, 7, and 10. Each of these Types is associated with anticyclonic conditions.

Surface winds are generally west to southwest allowing advection of relatively warm air. Daily average temperatures are near the photosynthetic optimum. These are also ideal conditions for evaporation as indicated by the low Bowen ratio values (Table 3.7). Petrone and Rouse (2000) and Petrone *et al.*, (2000) show that the same synoptic Types are related to high evaporative efficiencies in 1996, 1997 and 1998 for the same fen.

Unless sufficient moisture is added to the system from other synoptic Types or from convective activity, the high rates of evaporation could eventually limit the efficiency of photosynthesis. The persistence of a single synoptic Type creating for example, droughty conditions would have adverse effects on the production of the system over time. This is an important consideration in northern wetlands where much of the surface cover is non-vascular and therefore, CO_2 acquisition is vulnerable to severe desiccation of the bryophytes. This was the reason for a strong carbon loss (+1 g CO_2 m^{-2} d^{-1}) from the Churchill fen during the 1994 growing season (Schreader *et al.*, 1998).

Expected warming of high latitude regions relative to low latitudes will act to diminish latitudinal temperature gradients. This may have the effect of weakening heat transport to the poles and may also cause the polar jet to be shifted further north. The 1998 El Niño season provided air temperatures during April, May and early June about 7 °C warmer than in 1996 or 1997. GCMs predict a warming of about 3 to 4 °C during these same months for the Churchill region under a 2xCO_2 simulation (IPCC, 1996). Models also predict increased precipitation ranging from 0.5 to 1.0 mm per day. The temperature and precipitation during the spring of 1998 El Niño event are consistent with model projections for climate warming and can serve as a simple analog for the effect of

climatic change on CO_2 cycling. In the short term, it would appear that CO_2 exchange at arctic treeline could benefit substantially from a $2xCO_2$ atmosphere.

CHAPTER FOUR

SCALING NET ECOSYSTEM CO_2 EXCHANGE FROM THE COMMUNITY TO LANDSCAPE-LEVEL AT A SUBARCTIC FEN [1]

4.1. INTRODUCTION

Northern wetlands cover approximately 346 million hectares of the earth's surface and play an important role in the global carbon cycle (Gorham, 1991). Most of these wetlands are located in high latitudes and coincide with the boreal zone. There is concern that these ecosystems will experience a net loss of stored carbon to the atmosphere in response to high latitude warming (Billings *et al.*, 1982; Billings *et al.*, 1987a; Oechel *et al.*, 1993). This biological feedback process may further amplify the greenhouse effect by releasing stored CO_2 to the atmosphere.

Many landscape-level CO_2 exchange studies (Griffis *et al.*, 2000; Schreader *et al.*, 1998; Burton *et al.*, 1996; Vourlitis and Oechel, 1997; Lafleur *et al.*, 1997) indicate that northern wetlands experience a significant reduction in net CO_2 uptake and can become a source on an annual basis when spring and summer conditions are hot and dry. Field data for a subarctic sedge fen near Churchill Manitoba, Canada, indicate that the net loss of CO_2 is caused by a strong reduction in photosynthetic activity and a small increase in ecosystem respiration (Griffis *et al.*, 2000).

[1] A modified version of this chapter, authored by T. J. Griffis, W. R. Rouse, and J. M. Waddington, will be published in *Global Change Biology*.

Over longer time scales (tens to hundreds of years), however, wetlands may display homeostatic behaviour through a number of internal feedback processes. Increased microbial activity due to warmer and drier soils may release stored organic nitrogen, thereby, enhancing the productivity of wetland systems (Shaver *et al.*, 1986, 1998) and vegetation succession, induced by climatic change, may lead to increased productivity (Waddington *et al.*, 1998). To date, field evidence of homeostatic adjustment under natural conditions remains speculative (Vourlitis and Oechel, 1997). Long-term monitoring at the appropriate scale is needed to establish baseline measurements for evaluating such system adjustment. The characteristic heterogeneity in wetness and vegetation type observed in northern wetlands suggests that carbon exchange processes vary strongly across time and space. Future changes in the energy and water balance due to climatic forcing will impact the carbon exchange processes due to changes in wetness, nutrient cycling, and vegetation succession. Thus, understanding how the ecosystem will change will require observations at the landscape, community and plant level.

Studying the balance and potential response of net ecosystem CO_2 exchange (NEE) to changing environmental conditions has most commonly been approached by using either landscape-level micrometeorological techniques (gradient and eddy covariance measurements) or community-level chamber methods (static and dynamic chambers). Landscape-level monitoring does not provide mechanistic information about the components of NEE at the community-scale since micrometeorological methods cannot differentiate between photosynthetic and respiration responses of different

vegetation communities to varying light, temperature, humidity, moisture, and nutrient conditions. This lack of resolution is important because individual vegetation communities respond differently to changing environmental conditions (Bubier *et al.*, 1998). Consequently, the ability to predict changes in NEE to climatic change could be biased. For example, communities characterized by mosses may experience a large reduction in photosynthesis under dry surface conditions, while vascular dominated communities continue to photosynthesize near their potential because of roots in the deeper saturated zone. More importantly, changes in community composition and distribution within a wetland could result in poor estimates of NEE if model parameters do not account for plant or community scale processes.

Measurements at the community/chamber-level have their own limitations as they can directly influence the plant and soil environment (Norman *et al.*, 1997, Dugas, 1993; Knapp and Yavitt, 1992; Moore and Roulet, 1991; Matthias *et al.*, 1978). Moreover, calculating landscape-scale budgets from chamber data can be problematic due to the uncertainty associated with lower temporal and spatial sampling (Waddington and Roulet, 1999; Moore *et al.*, 1998). Gaining a better understanding into the response of northern wetland carbon cycling to climate change therefore requires studying these systems at a variety of spatial scales. However, to our knowledge, scaling CO_2 fluxes from the community to the landscape-level has never been attempted for this environment. The objective of this study, therefore, is to combine both landscape and community-scale approaches simultaneously in order to: 1) understand the scale

complexity of net ecosystem CO_2 exchange at a subarctic fen in Churchill, Manitoba and 2) help substantiate the growing season CO_2 budget.

4.2. MATERIALS AND METHODS

4.2.1. Research Site

The experimental area is located on the southwestern shore of Hudson Bay, within the Hudson Bay Lowland (Figure 4.1). Patches of open woodland near the experimental area mark the edge of the northern boreal tree line and the transition to open tundra. Continuous permafrost begins to the south of the region. The Hudson Bay has a strong influence on the regional climate and energy balance during the growing season through the advection of cold moist air (Rouse, 1991).

The research site is an extensive fen and is located 20 km east of the town of Churchill Manitoba (58° 45'N, 94° 04'W), and 12.5 km south of the Hudson Bay shoreline. This fen is characterized by non-patterned, hummock-hollow terrain. Detailed surveying within a 150 m radius of the main micrometeorological measurement tower indicates that small hummocks comprise 47%, hollows 48% and large hummocks 5% of the landscape with respect to the water table position. The maximum difference in vertical height between large hummocks and hollows is approximately 0.75 m. The configuration and height of the hummocks and hollows determines the depression storage of surface water. A maximum amount of water storage occurs at a mean height of 0.08 m above the base of the hollows (depression storage surface)(Rouse, 1998). As the water table rises above this equilibrium level, lateral drainage of water begins. The water table

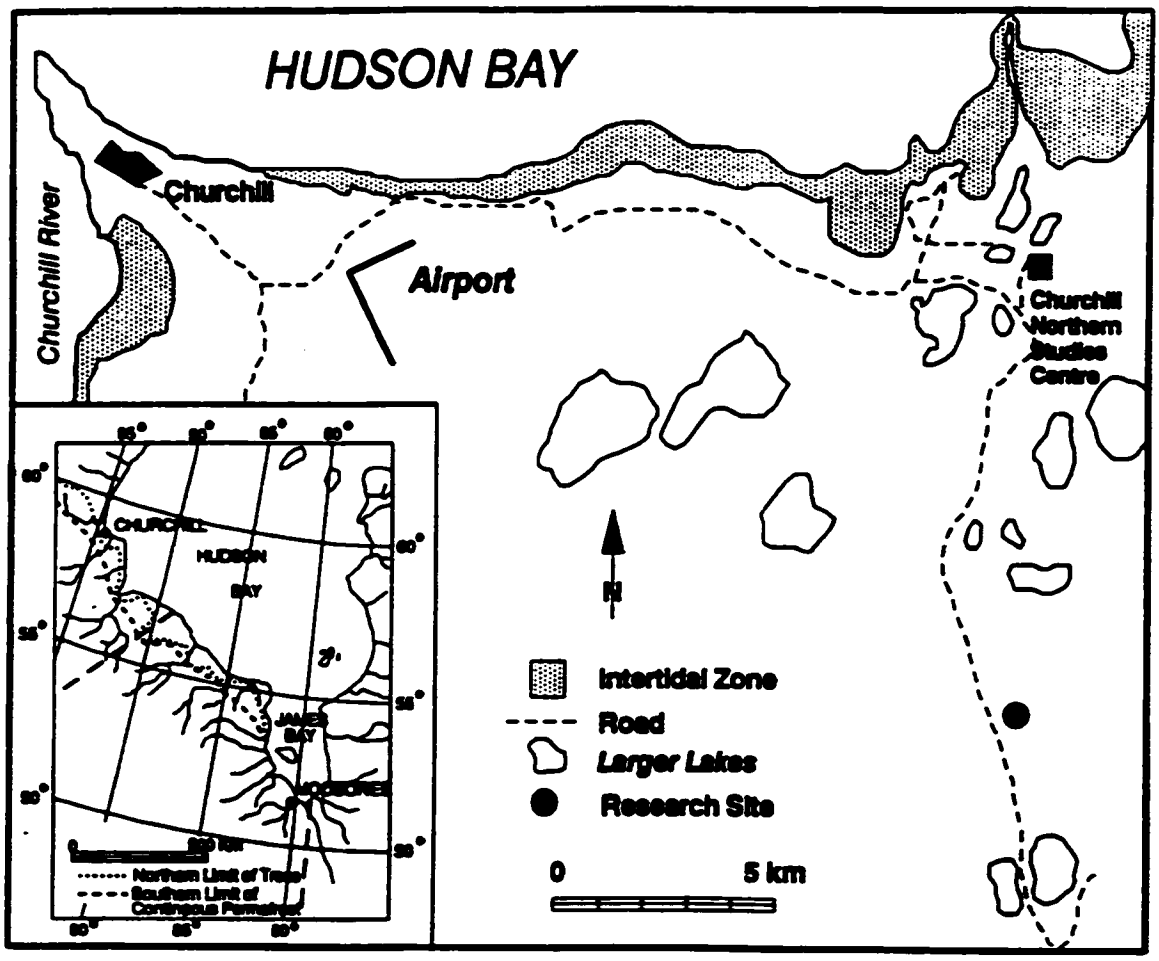

Figure 4.1: Research area and study site.

falls below the hollow surfaces at a height of –0.08 m relative to the equilibrium storage level.

Average water table height relative to the hummocks and hollows has an important influence on the distribution of vegetation (Billings, 1987b; Bubier *et al.*, 1995). At this fen, brown moss (*Scorpidium turgescens*) is the dominant vegetation found in the wet hollows. Small hummocks exhibit a limited moss cover (*Tomenthypnum nitens*) but are dominated by the vascular species (*Carex aquatilis, C. Limosa, C. Saxatilis and C. Gynocrates*). Larger hummocks support vascular species *(Betula glandulosa, Ledum decumbens Salix arctophila or Carex* spp.) and non-vascular species of lichen (*Cladina stellaris, C. rangiferina*) and moss (*Dicranum undulatum*).

The fen has a mean peat depth of 0.25 m and is underlain by glaciomarine till, consisting of fine silts and clays with interspersed layers of carbonate shingles. The regional landscape continues to respond to isostatic rebound following the last glaciation. Elevation increase at the research site is about 0.01 m y^{-1}. At present, the fen is approximately 22 meters above sea level, and therefore, it is estimated that vegetation and peat development was initiated about 2200 years ago. Combining this with peat depth, bulk density, and carbon content, we estimate the long-term rate of carbon accumulation for this fen at 11 g CO_2 m^{-2} y^{-1}.

4.2.2. Study Periods

CO_2 fluxes are examined over the measurement period DOY 164 (June 13) to DOY 238 (August 26). This includes the majority of the growing season at this tundra location. Each growing season has been divided into three periods following Griffis *et al.* (2000). Period one (pre-green) extends from DOY 164 to DOY 172 (June 21). At this time the vascular species emerge but are immature. Period two (green) includes DOY 173 to DOY 220 (August 8). In this period vascular species reach full maturity and leaf area index (LAI) reaches a maximum. Period three (post-green) extends from DOY 221 to DOY 238. The post-green period generally coincides with the onset of senescence but this varies substantially from year to year.

4.2.3. Landscape-Level Instrumentation and Measurements

Measurements during the 1997-growing season are similar to those described in Griffis *et al.*, (2000). The Bowen ratio energy balance approach (BREB) was used to calculate the energy balance over the fen. Temperature and vapour pressure profiles were measured with wet and dry-bulb psychrometers. The sensors were mounted at heights of 0.35, 0.70, 1.10, 1.60, 2.30 and 3.20 m. A wind speed profile was measured using cup anemometers mounted at the same heights. Data logger sampling was every 2 seconds, and the averaging period was 0.5 hour. Precipitation was recorded daily using a standard rain gauge, and half-hourly with a tipping bucket rain gauge. Water table position was measured relative to the equilibrium water storage level at a manual well and recorded continuously with a float-potentiometer system. Net radiation Q^* was measured at a height of 3 m above ground using a Middleton net pyrradiometer. Incoming $K\downarrow$ and

reflected $K\uparrow$ solar radiation were measured with Eppley pyranometers. Photosynthetic active radiation PAR was measured with a Licor Quantum sensor. Surface temperature was monitored using a series of thermocouple arrays. Ground heat flux was measured with 4 Middleton heat flux plates, which were arranged to give a spatially representative flux. The calorimetric ground heat flux calculation was used to correct the heat flux plate measurements following Halliwell and Rouse (1987) to correct for inconsistencies in thermal conductivity and poor thermal contact between the heat flux plates and the organic soil.

4.2.4 Landscape-Level Net CO_2 Flux Measurements

The theory and methodology for calculating the net CO_2 flux F_c using gradient techniques has been described previously in Burton *et al.*, (1996), Schreader *et al.*, (1998) and Griffis *et al.*, (2000). F_c is derived from the following expression

$$F_C = -K_C \frac{\partial \rho_C}{\partial z} \qquad (4.1)$$

where K_c is the turbulent transfer coefficient for CO_2 and $\partial \rho_c / \partial z$ is the time averaged vertical gradient of CO_2 concentration. K_c is assumed identical to the turbulent transfer coefficient for sensible heat K_h and is derived from the Bowen ratio energy balance approach.

Atmospheric gradients of CO_2 concentration were measured from the same height intervals as for temperature, vapor pressure and wind speed. Due to the remote location of the research site, all instrumentation was powered by 12-V storage batteries and charged with a wind generator and solar panels. Air from the six levels was drawn through equal length tubing into 1-L buffer sample volumes. Buffer volume air was

continuously replenished by the pumping system. Sequential sampling from the six buffer volumes was controlled with a solenoid-actuated valve manifold system. Samples were analyzed on an infrared gas analyzer (LI-COR 6262). A time interval of 1 minute was used to determine the CO_2 concentration from the six buffer volumes. The net CO_2 flux was calculated from 0.5 hr time averaging and corrected for density variations resulting from the latent heat flux (Webb *et al.*, 1980).

4.2.5. Estimating Landscape-Level Ecosystem Respiration and Photosynthesis

Ecosystem respiration (ER) consists of heterotrophic soil respiration and dark autotrophic plant respiration. Both soil and plant respiration has been shown to vary strongly with soil and plant temperatures respectively. As well, soil respiration is a function of water table position, which has a direct affect on redox potential and therefore microbial activity. Plant respiration is proportional to the amount of biomass present and also varies with phenological stage. Despite these complexities, some success has been achieved in estimating total respiration fluxes from tower and chamber data as functions of temperature and or water table position (Waddington *et al.*, 1998; Kim and Verma, 1992; Oberbauer *et al.*, 1991; Shurpali *et al.*, 1995). We used nighttime ($K\downarrow = 0$) net CO_2 tower data from 4 different growing seasons to estimate respiration as a linear function of surface temperature. From this bulk relationship, we adjusted the y-intercept of the function until it matched the measured half-hourly nighttime respiration recorded at the tower for each period during the 1997 season. Adjusting the linear fit as the season progressed was necessary since ER varied with changes in water table, amount of

biomass, and phenology. The goal was not to model respiration explicitly, but to separate respiration from NEE in order to provide a best estimate of the photosynthetic flux.

4.2.6. Community-Level Instrumentation and Measurements

A semi-dynamic chamber system (surface area 0.05 m^2, volume 20 l) was constructed from clear Plexiglas. The chamber was outfitted with circulation fans and a water-bath-cooling unit to help maintain ambient conditions. On average, chamber temperatures were maintained to within ± 0.3 °C. However, in a few instances chamber temperatures differed from ambient by 5 °C. PAR extinction resulting from the Plexiglas material was approximately 13%. PVC collars were inserted into the peat to maintain a seal between the ground surface and chamber, and as well, to reduce the chance of episodic CO_2 release during measurement. Boardwalks were placed near each of the collars to help reduce site disturbance. During CO_2 sampling the chamber was placed on a collar for a 5-minute interval. The relatively short interval was chosen to reduce the effect of the chamber on the plant and soil environment. CO_2 concentrations were measured every minute on a PP-systems portable EGM-1 infrared gas analyzer (PP Systems, UK.). The chamber CO_2 flux was calculated as

$$F_C = \frac{\Delta CO_2}{\Delta t} \quad , \qquad (4.2)$$

where ΔCO_2 is the change in CO_2 concentration over the Δt, 5 minute interval. Fluxes were corrected for volume changes resulting from temperature variations within the chamber. NEE was measured using a clear semi-dynamic chamber while ecosystem respiration was measured using a dark version of the semi-dynamic chamber.

Photosynthesis was then estimated by subtracting ecosystem respiration from NEE. Site selection included 3 hollows (H), 6 small hummocks (SH) and 3 large hummocks (LH). The total number of chamber observations for ER and photosynthesis during the pre-green, green and senescence period was 155, 475 and 361 respectively. Chamber measurements were taken between 0800 and 1630 solar time. The sign convention for community and landscape-level CO_2 fluxes is, (+) respiration; (-) photosynthesis; (+) net loss of CO_2 from the wetland to the atmosphere and, (-) net gain of CO_2 to the wetland from the atmosphere.

4.2.7. Measurement Accuracy of CO_2 Flux Calculations

CO_2 flux measurements derived from the gradient approach are prone to substantial errors resulting from fetch limitations, determination of the turbulent transfer coefficient K_c and systematic bias in one or more of the measuring sensors. Schreader *et al.*, (1998) give a detailed discussion of these errors, which is summarized as follows.

The measurements were made over a large homogeneous fen with a minimum fetch of 2500 m in the southerly direction. Analysis indicates that 80% of the flux footprint lies within 238 m of the tower and that the most sensitive distance is at 26.5 m. Calculating the turbulent transfer coefficients K_h and K_c from BREB-Q_h can be problematic when Q^* is small such as at night or during sunrise or sunset. At these times, temperature and humidity gradients tend to be small and β may become unreliable. Under these conditions K_h has been derived from either the aerodynamic or eddy covariance calculation of Q_h. This approach has been successful due to the relatively vigorous nocturnal wind speeds typically experienced at Churchill. Systematic bias in the sensors

has been remedied by using a multiple level flux calculation scheme and a software package originally described by Halliwell and Rouse (1989) to test for measurement error and boundary layer problems. Maximum error in daytime F_c can approach 30%. Errors associated with chamber measurements are difficult to quantify due to the uncertainty of their effect on the soil and plant environment. For consistency we have estimated that the error is similar to the tower measurements.

4.3. RESULTS

4.3.1. Environmental Conditions

The 1997 growing season was drier and warmer than the Churchill 30-year normal (Griffis *et al.* 2000). Total precipitation during the growing season was 125 mm (4 mm below average) and mean air temperature was 12.7 °C (1.9 °C above average). Precipitation events occurred on average every 3 days and were generally more frequent at the beginning of the season (Figure 4.2a). Water table depth remained above the depression storage surface until DOY 180 (June 29) and reached a maximum depth of -0.32 m on DOY 217 (August 5) (Figure 4.2b). Leaf area index (LAI) was 0.47 by DOY 192 and decreased to 0.28 ten days following the start of the post-green period. Photosynthetically active radiation and net radiation was typical for the season.

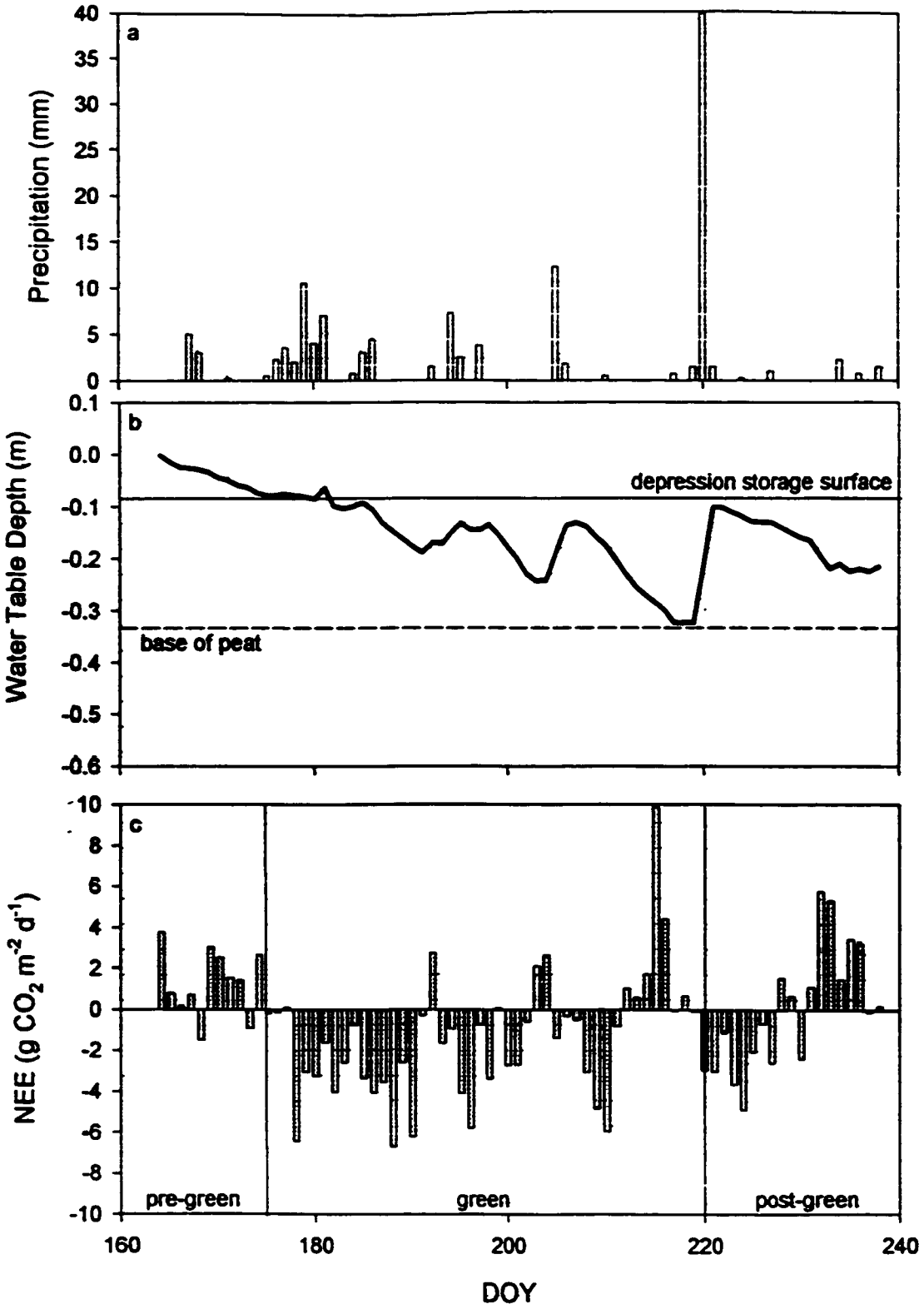

Figure 4.2: a) Seasonal precipitation; b) Seasonal water table position; c) Daily landscape-level net ecosystem CO_2 exchange.

through the pre-green period (Figure 4.2c). Evaporation was the dominant energy sink, consuming 57% of the net radiation. The Bowen ratio averaged 0.49 over the growing season (Griffis *et al.*, 2000).

4.3.2. Landscape-Level CO_2 Exchange

The fen represented a net sink of -0.7 g CO_2 m^{-2} d^{-1}, accumulating a total of -49 g CO_2 m^{-2} over the measurement period. Daily losses of CO_2 were experienced during the pre-green period. Peak uptake occurred early in the green period. Day to day variability in NEE increased during the mid-green period and large losses of CO_2 occurred near the end of the green period. The early post-green period experienced a net gain of CO_2 while late post-green CO_2 exchange showed frequent losses. The seasonal diurnal curve of NEE (Figure 4.3) indicates maximum CO_2 uptake in the morning (0700 hr) and a strong reduction through the afternoon hours. Losses of CO_2 were observed from early evening (1900 hr) to early morning (0530 hr).

Ecosystem respiration and photosynthesis were both relatively small during the pre-green period. Respiration averaged +4.7 g CO_2 m^{-2} d^{-1} and photosynthesis averaged -3.3 g CO_2 m^{-2} d^{-1} (Figure 4.4). Green period respiration and photosynthesis increased to +6.6 g CO_2 m^{-2} d^{-1} and -7.6 g CO_2 m^{-2} d^{-1} respectively. Post-green respiration decreased to +6.3 g CO_2 m^{-2} d^{-1} while photosynthesis decreased to -6.0 g CO_2 m^{-2} d^{-1}.

4.3.3. Community-Level CO_2 Exchange

The majority of the chamber measurements from this study were taken between (1030 and 1530 h) and therefore exhibit lower photosynthetic and higher respiration rates than would be expected if integrated over the entire daytime period. However, it is the

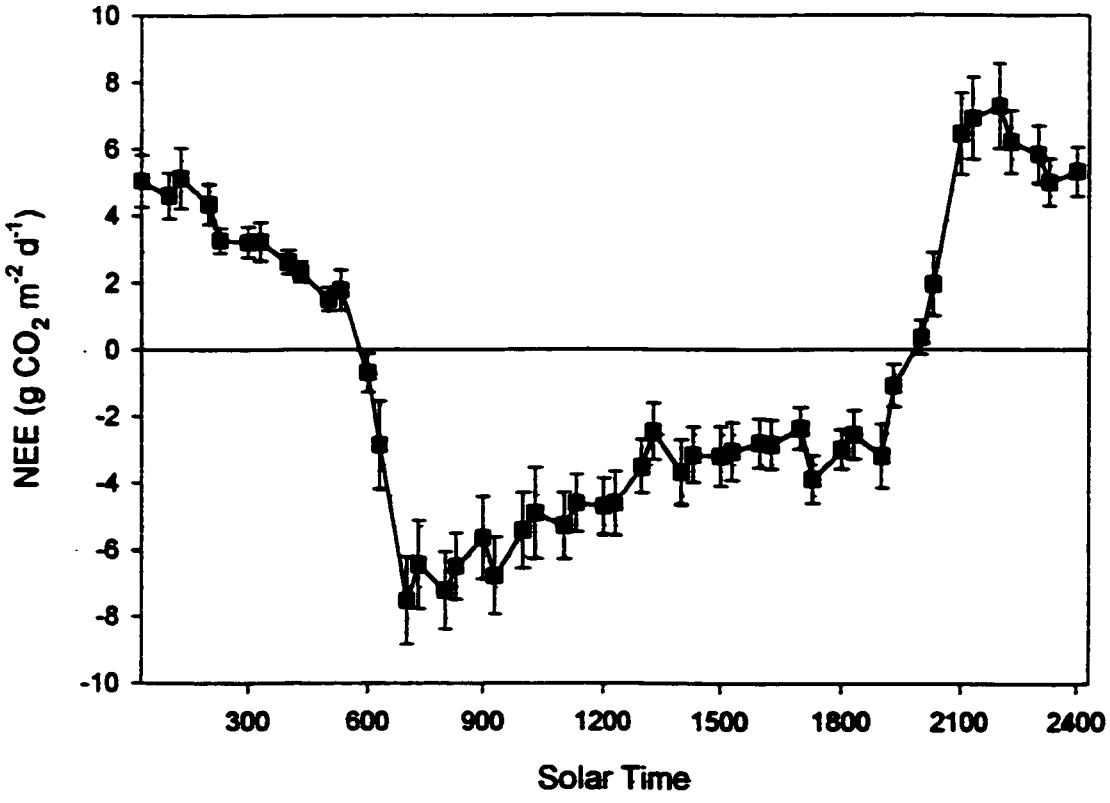

Figure 4.3: Diurnal landscape-level net ecosystem CO_2 exchange.

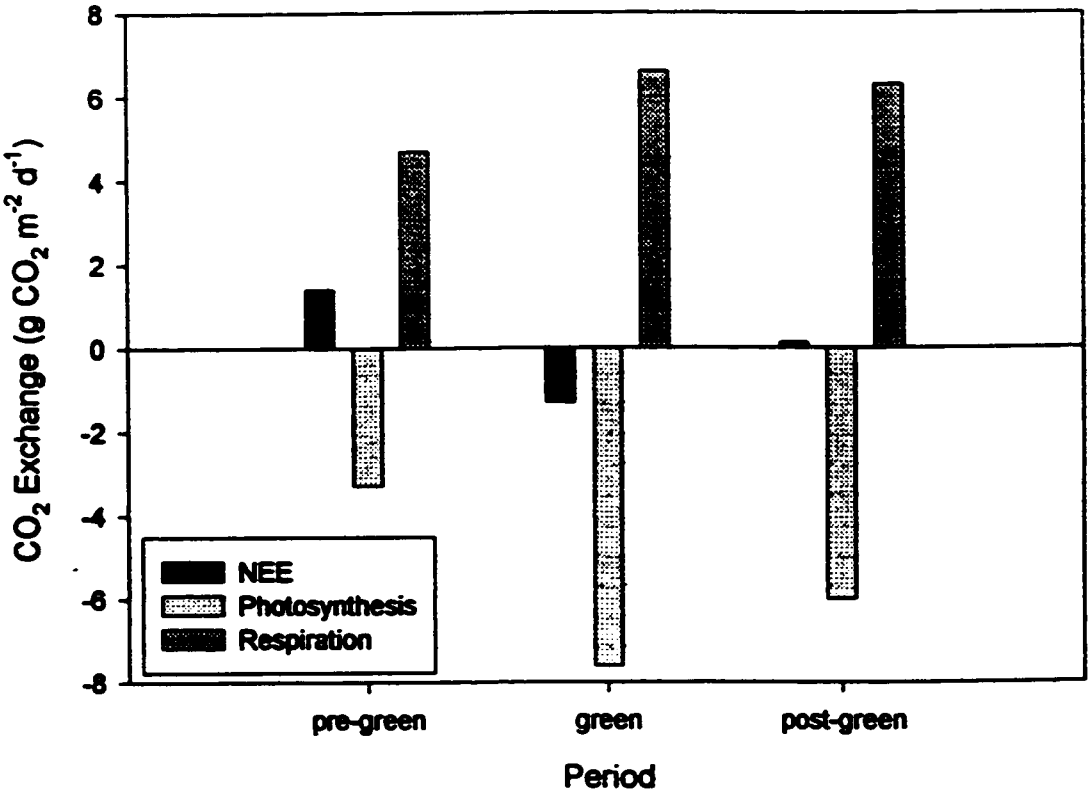

Figure 4.4: Mean landscape-level ecosystem respiration, photosynthesis, and NEE by phenological study period.

relative difference in CO_2 exchange between the community types that is of primary interest. At the hollow sites respiration averaged +3.4 g CO_2 m^{-2} d^{-1} with a coefficient of variation (C.V.) 51%. Pre-green, green and post-green respiration averaged +0.9, +3.8, and +3.3 g CO_2 m^{-2} d^{-1} (Figure 4.5a). Seasonal photosynthesis averaged -2.1 g CO_2 m^{-2} d^{-1} and showed a large amount of spatial and temporal variability (C.V.=83%). Pre-green, green and post-green photosynthesis averaged -0.9, -2.5, and -2.1 g CO_2 m^{-2} d^{-1} respectively (Figure 4.5b). Small hummock respiration averaged +9.9 g CO_2 m^{-2} d^{-1}. Pre-green, green, and post-green respiration averaged +8.1, +10.6, and +9.5 g CO_2 m^{-2} d^{-1} (Figure 4.5a). The C.V. for small hummock respiration at 32% was smaller than for the hollows. Seasonal photosynthesis averaged -8.8 g CO_2 m^{-2} d^{-1}. The variability in photosynthesis was also lower (C.V. = 52%) than for the hollows. Pre-green, green, and post-green photosynthesis averaged -5.0, -9.7 and -9.7 g CO_2 m^{-2} d^{-1} respectively (Figure 4.5b). Pre-green photosynthetic rates were relatively large due to the wet mosses and as well the contribution from the emerging vascular plants. Photosynthesis remained large during the early post-green period as senescence had just been initiated. As well, complete senescence had not occurred when the 1997 field study ended on DOY 238. Large hummock respiration rates averaged +5.5 g CO_2 m^{-2} d^{-1}. Pre-green, green, and post-green respiration averaged +3.9, +5.6, and +4.0 g CO_2 m^{-2} d^{-1} (Figure 4.5a). Seasonal photosynthesis averaged -5.1 g CO_2 m^{-2} d^{-1}. Pre-green, green, and post-green photosynthesis averaged -4.2, -4.7 and -6.4 g CO_2 m^{-2} d^{-1} respectively (Figure 4.5b). The coefficient of variation for large hummock respiration and photosynthesis was 70% and 66% respectively.

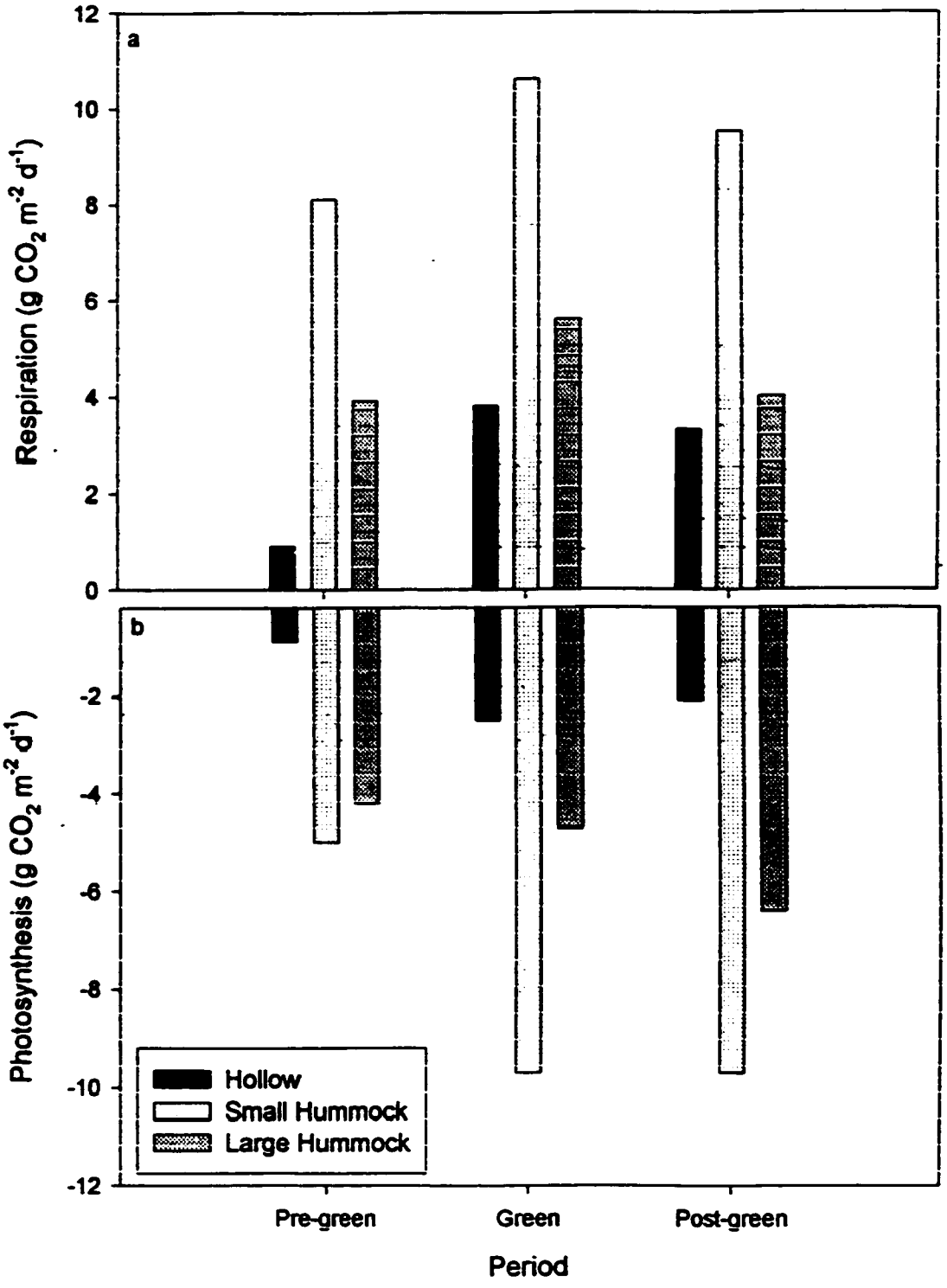

Figure 4.5: Mean community-level CO_2 exchange. a) Community respiration by phenological study period; b) Community photosynthesis by phenological study period.

4.3.4. Scaling from the Community to Landscape-Level

A priori selection of the community scale was based on the strong patterning of vegetation type with respect to microtopography. Community and landscape-scale CO_2 fluxes were analyzed to: compare the differences between chamber and tower measurements; examine the CO_2 exchange differences between community types; and, assess how the process of photosynthesis and ecosystem respiration differs between the communities and landscape-level.

4.3.4.1. Comparison of Chamber and Tower Data

Simultaneous chamber measurements of photosynthesis, respiration, and NEE over each terrain type was not possible. Therefore, in order to scale from the community to landscape-level, it was necessary to integrate all chamber measurements within each of the three phenological study periods. Pre-green, green, and post-green chamber fluxes were scaled as follows:

$$Fc_{total} = 0.48 \cdot (Fc_{HW}) + 0.47 \cdot (Fc_{SH}) + 0.05 \cdot (Fc_{LH}) \quad (4.3)$$

where, Fc_{total}, is the scaled-sum of chamber photosynthesis, respiration or NEE resulting from the individual terrain units. The scaling factor is the percentage areal coverage of each terrain unit type determined from the detailed survey. Figure 4.6 shows comparisons between scaled chamber fluxes with tower measurements for common half-hour time intervals during each of the phenological periods. Figure 4.6a indicates good agreement between chamber and tower photosynthesis and respiration in the pre-green period. The scaled chamber method produced lower photosynthetic rates by 4% and

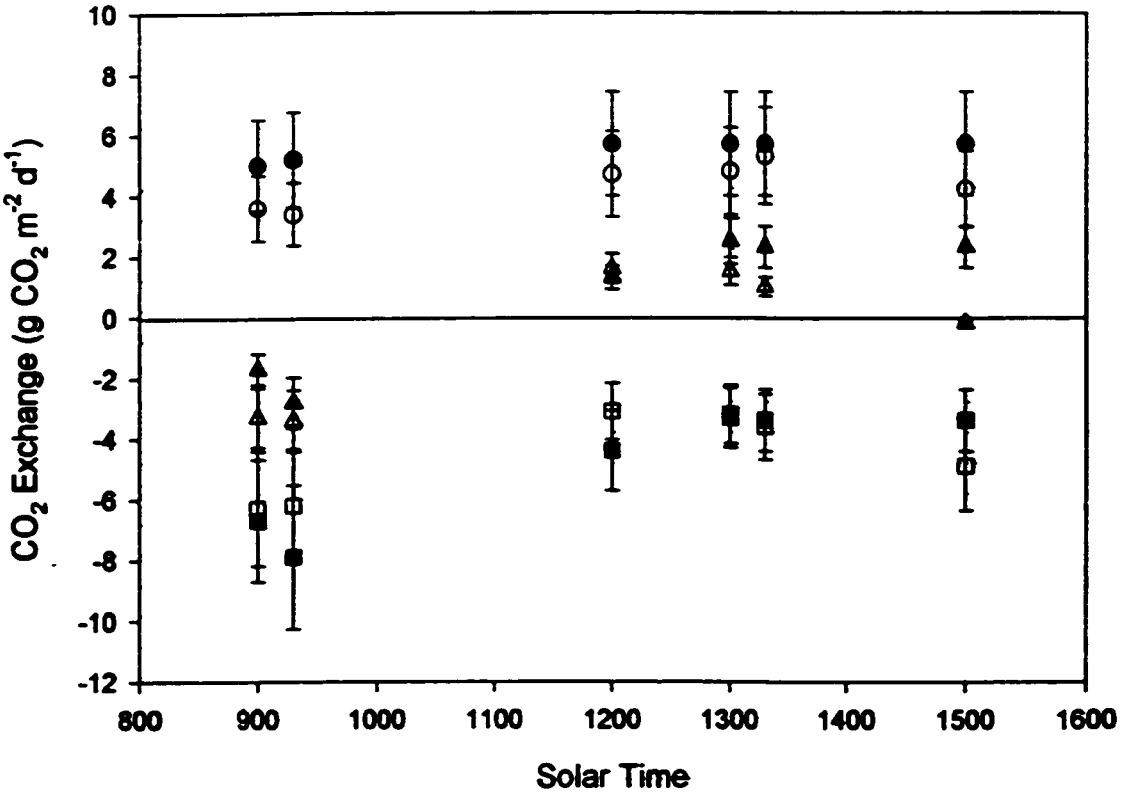

Figure 4.6: a) Pre-green period comparison of scaled chamber and landscape-level CO_2 fluxes (square indicates photosynthesis, circle indicates respiration, triangle indicates NEE, dark symbols indicate landscape-level measurements, open symbols indicate community scale chamber measurements.

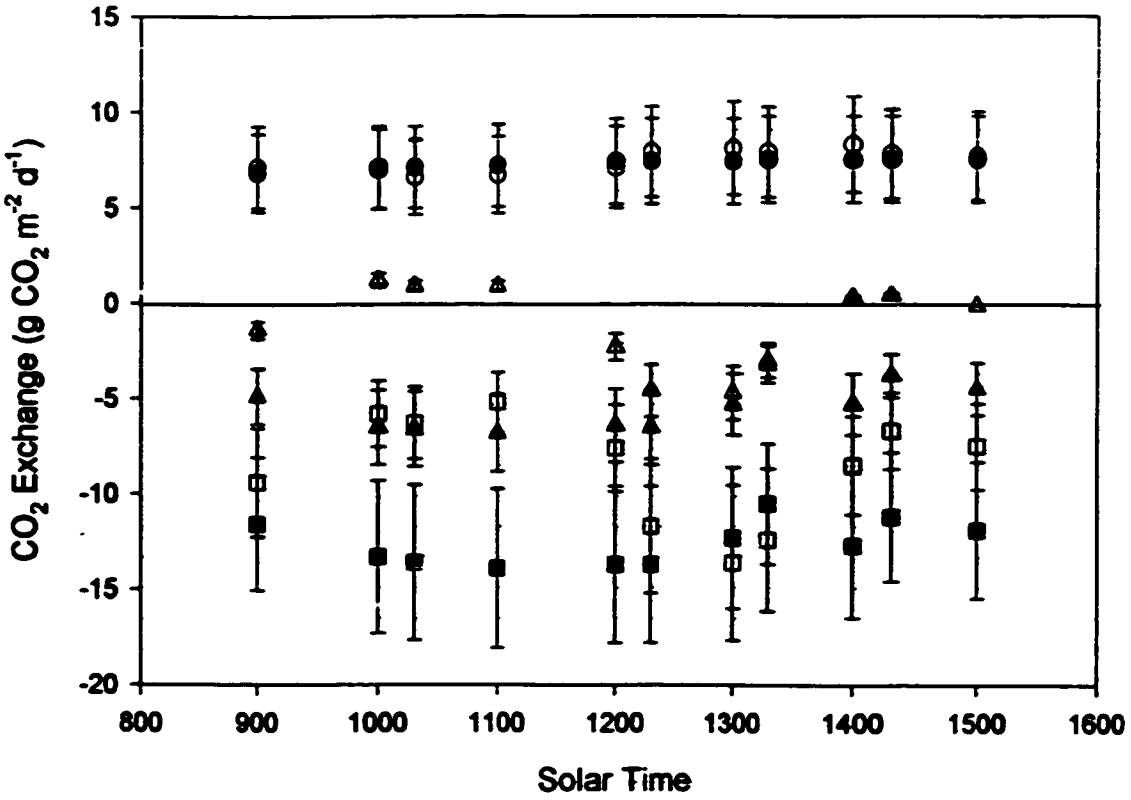

Figure 4.6: b) Green period comparison of scaled chamber and landscape-level CO_2 fluxes (square indicates photosynthesis, circle indicates respiration, triangle indicates NEE, dark symbols indicate landscape-level measurements, open symbols indicate community scale chamber measurements.

respiration by 28%. Figure 4.6b displays the half-hour comparisons for the green period. Scaled chamber photosynthesis was lower than tower photosynthesis by 32% and chamber respiration was greater than the tower respiration by 3%. Photosynthesis estimates between 1230 and 1330 hr however, showed only a 3% difference. Consequently, there was a substantial difference in NEE during the morning and afternoon hours. Post-green comparisons of photosynthesis, respiration and NEE show good agreement and are within the maximum expected error (Figure 4.6c). Chamber measurements were lower than tower photosynthesis, respiration and NEE by 28%, 17%, and 37% respectively during this period. It appears that the best agreement between scaled chamber and tower measurements is during mid-day for all periods.

4.3.4.2. Estimating the Community Contribution to Landscape-Level CO_2 Exchange

Expected changes in mean water table position resulting from global warming is likely to shift the distribution of plant types within this fen. It is essential therefore to understand how each community type within the larger landscape influence CO_2 exchange. The contribution of each community to landscape-scale NEE was estimated by computing an effective scaling factor (ESF) for each terrain unit. In doing so, we identify the communities that have the largest control on CO_2 exchange within the fen. This scaling method is especially useful when the physical processes operating in a system are not completely understood. One caveat to this approach, however, is the assumption that the relative difference between photosynthesis and ecosystem respiration between each community type is conserved diurnally. This potential error has been

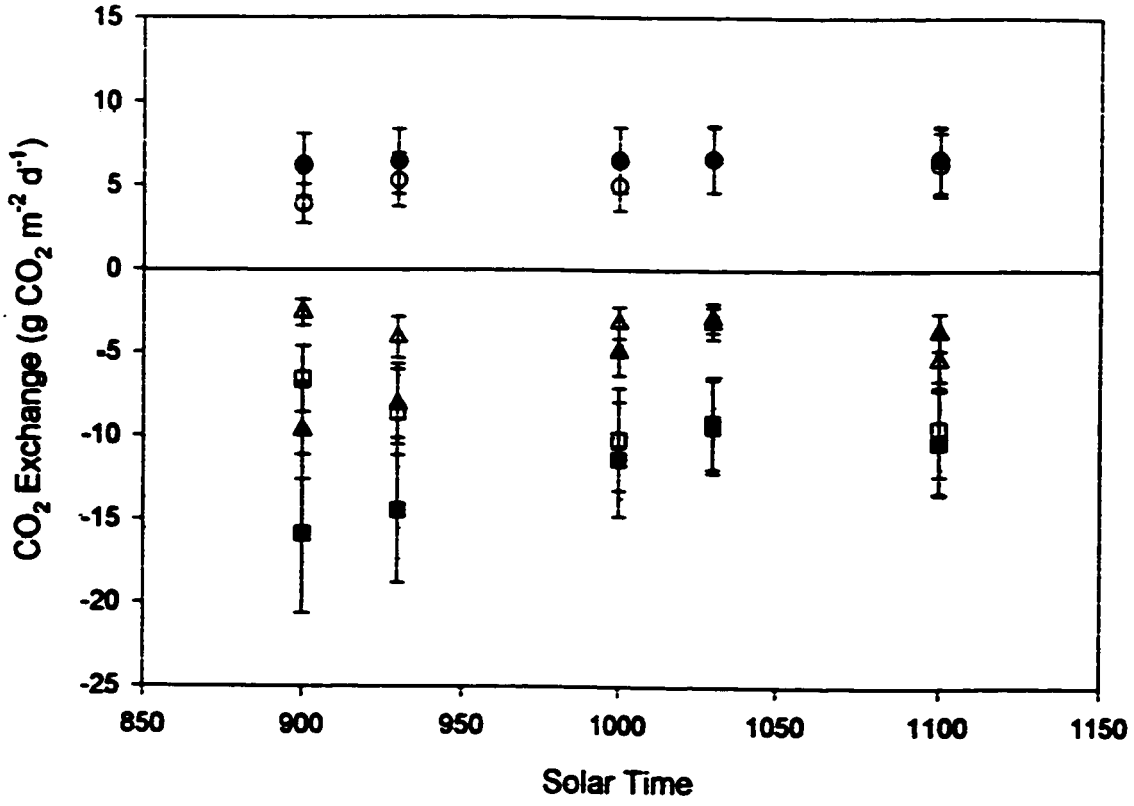

Figure 4.6: c) Post-green period comparison of scaled chamber and landscape-level CO_2 fluxes (square indicates photosynthesis, circle indicates respiration, triangle indicates NEE, dark symbols indicate landscape-level measurements, open symbols indicate community scale chamber measurements.

reduced by using a large number of chamber observations and by developing the effective scaling factor for different phenological periods.

The ESF was calculated by multiplying the terrain unit-scaling factor by the relative difference in respiration and photosynthesis observed for each community (hollow, small hummock, large hummock) (Table 4.1).

$$ESF = ASF \frac{Fc_{CT}}{Fc_{total}} \quad , \qquad (4.4)$$

where, *ESF* is the effective scaling factor, *ASF*, the areal scaling factor for each terrain unit or community type, Fc_{CT} is the mean CO_2 flux observed from a community type. The *ESF* was then applied to the landscape-scale NEE measurements to obtain the relative contribution from each community. Figure 4.7a shows the contribution of each terrain unit type to respiration. Over the growing season, small hummocks accounted for +4.4 g CO_2 m^{-2} d^{-1}. Hollows and large hummocks contributed +1.5 and +0.3 g CO_2 m^{-2} d^{-1}. Figure 4.7b displays the contribution of individual terrain units to photosynthesis. Small hummocks dominated the overall production of the fen and averaged -5.3 g CO_2 m^{-2} d^{-1}. Hollows and large hummocks contributed significantly less to the overall production of the fen. Their average estimated production was -1.3 and -0.3 g CO_2 m^{-2} d^{-1} respectively. Therefore, it appears from this analysis that the *Carex* spp. portion of the landscape represents the major sink of CO_2 to the fen. Small hummock terrain units gave a net balance of -0.9 g CO_2 m^{-2} d^{-1} while hollows experienced a net loss of +0.2 g CO_2 m^{-2} d^{-1}. Large hummock photosynthesis and respiration balanced over the season. Summation of all the contributing fluxes results in a net balance of -0.7 g CO_2 m^{-2} d^{-1}.

Table 4.1: Effective Scaling Factors of Community Contribution to Landscape-Level CO_2 Exchange

Terrain Unit	Pre-green R	Pre-green P	Green R	Green P	Post-green R	Post-green P
Small hummock	0.75	0.79	0.70	0.76	0.71	0.77
Hollow	0.18	0.14	0.26	0.20	0.25	0.17
Large hummock	0.07	0.07	0.04	0.04	0.03	0.05

*Respiration (R), Photosynthesis (P)

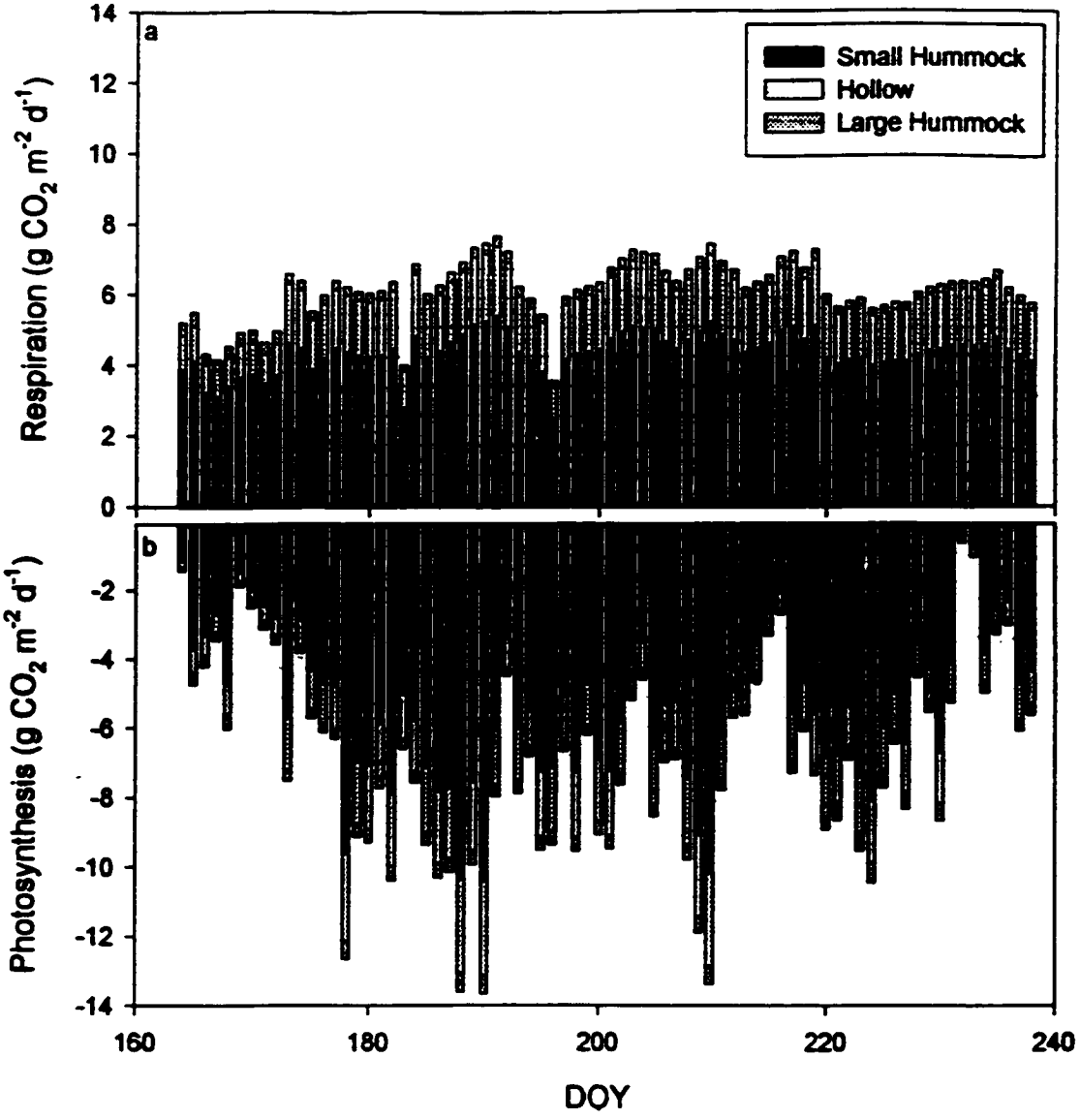

Figure 4.7: Community-level contribution to landscape-scale CO_2 flux. a) Ecosystem respiration; b) Gross ecosystem production.

4.3.5. Landscape and Community-Scale Processes

Results from the community level CO_2 exchange and effective scaling factor analysis indicate that photosynthesis and ecosystem respiration behave differently both between communities and at the landscape level. Net photosynthesis and ecosystem respiration was examined at the landscape and community-scale from a simple process perspective.

4.3.5.1 Net Photosynthesis

NEE and net photosynthesis is commonly described as a function of photosynthetically active radiation (Prioul and Chartier, 1977; Whiting, 1994; Waddington *et al.*, 1998; Frolking *et al.*, 1998). However, the process is complicated by a number of other environmental factors including leaf temperature, soil and leaf water potential, atmospheric moisture deficit, internal and ambient CO_2 concentrations, and nutrient status (Lambers *et al.*, 1998). Here, we examine the relationship between net photosynthesis and light using the basic model proposed by Prioul and Chartier (1977):

$$A = \frac{\phi \cdot Q + A_{\max} - \sqrt{(\phi \cdot Q + A_{\max})^2 - 4 \cdot \phi \cdot Q \cdot k \cdot A_{\max}}}{2 \cdot k} - R_{day} \quad (4.5)$$

where A is the net photosynthetic flux , ϕ is the apparent quantum efficiency (AQE) describing the conversion of light to photochemical products. Q, is the photosynthetically active radiation, A_{max}, the maximum light saturated net photosynthetic rate, R_{day}, the daylight respiration rate resulting from non-photorespiration processes and k, is a scaling parameter describing the change of slope between the light limited and light saturated region of the curve.

Growing season net photosynthesis at the landscape-level and at each community type show unique relationships with respect to light levels (Figures 4.8). The parameters for each curve-fit and the net photosynthetic flux value (A) for Q=1000 μmol m^{-2} s^{-1} are listed in Table 4.2. In general, each curve-fit exhibits a low correlation coefficient and only the small hummock and landscape-level parameters are statistically significant at the 95% confidence interval. This can be attributed to the fact that a large number of the controlling environmental factors are not included in the above algorithm. Furthermore, we expect a large amount of scatter in the net photosynthetic data due to spatial (biomass) and temporal (phenological stage) heterogeneity within the fen. For the landscape-scale, small hummock, hollow and large hummock communities correlation coefficients were 0.40, 0.50, 0.25, and 0.32 respectively. The curve-fits show higher correlation at the landscape-level and small hummock community compared to the hollow and large hummock community. This may be due to the small flux values at the hollow and large hummock sites relative to the errors involved in the measuring process. As well, since the hollow and large hummock communities are dominated by bryophytes, variations in plant water potential and atmospheric moisture content may lead to large variability in net photosynthesis over a wide range of PAR levels.

At the community scale, small hummock net photosynthesis yielded the smallest AQE and the largest A_{max} rate. Hollows and large hummock communities experienced higher AQEs and lower A_{max} rates compared to the small hummocks. Landscape-level net photosynthesis exhibited an AQE and A_{max} value that was within the range of the

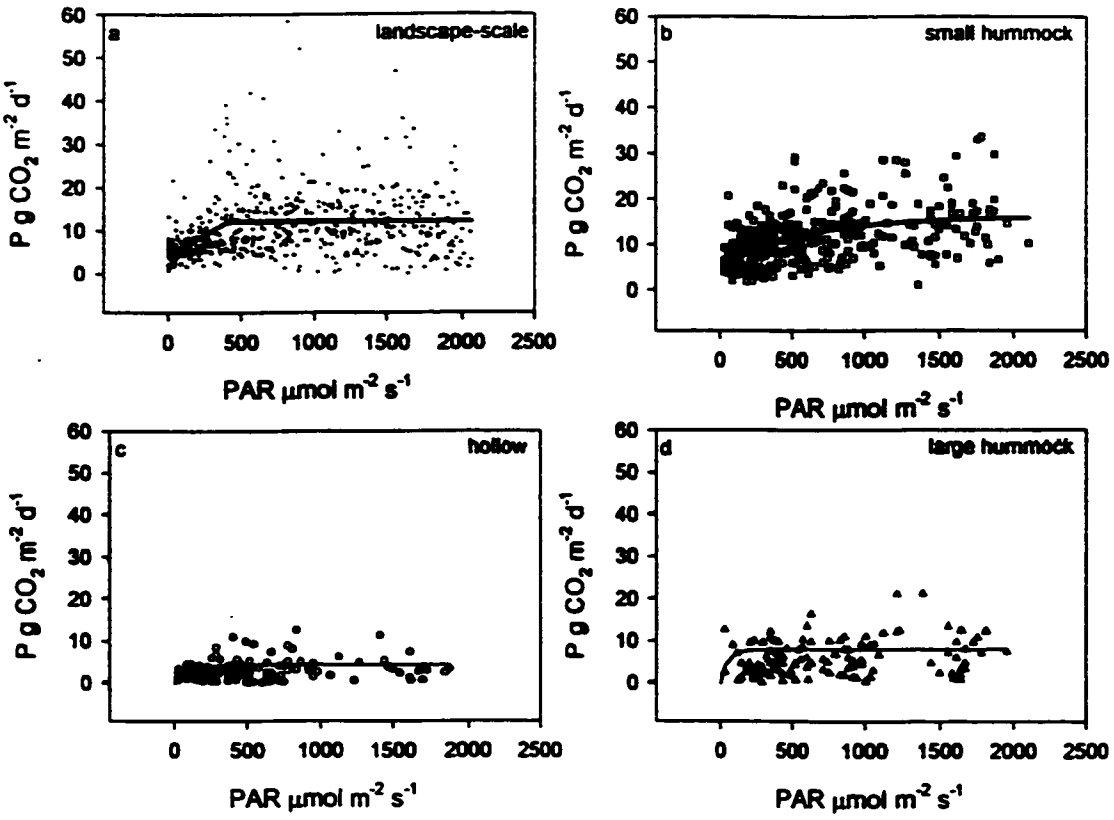

Figure 4.8: Landscape and community-scale net photosynthesis as a function of photosynthetically active radiation.

community values. Each of the community parameters was scaled according to the areal coverage of the community type:

$$Pp_{total} = 0.48 \cdot (Pp_{HW}) + 0.47 \cdot (Pp_{SH}) + 0.05 \cdot (Pp_{LH}) \quad , \qquad (4.6)$$

where P_p is the areal weighted sum of the net photosynthesis community parameters ϕ, A_{max}, R_{day} and k. The scaled community relationship yields parameters that are close to those found at the landscape-level. For comparative purposes we determined the net photosynthetic rate for the landscape-level, individual community types, and the scaled community parameters for Q=1000 μmol m^{-2} s^{-1}. The observed difference in net photosynthesis between the landscape-level and scaled community composite is about 21%.

4.3.5.2. Ecosystem Respiration

Empirical approaches to estimating ER fluxes from functions of soil temperature and or water table position have been adopted by numerous authors (Waddington *et al.*, 1998; Kim and Verma, 1992; Oberbauer *et al.*, 1991; Shurpali *et al.*, 1995). In general, these relationships have performed poorly due to the large amount of spatial and temporal variability observed in the fluxes. ER plotted as a function of surface temperature for the landscape-scale and each community type is shown in Figures 4.9. The landscape-scale ER fluxes have been grouped into small temperature intervals and averaged. This classification was necessary in order to smooth the large number of data points and better depict the relationship with surface temperature. A similar approach was employed by Waddington *et al.*, (1998) for ER at the community scale. Also note that the nighttime temperature range is small (-1.4 to 15.5°C) relative to each of the community types where

Table 4.2: Curve-fit parameters for landscape and community-scale net photosynthesis described as a function of photosynthetically active radiation.

Terrain Type	ϕ	A_{max}	R_{day}	k	$A_{(Q=1000)}$
Small hummock	0.014	11.3	5.8	0.76	14.2
Hollow	0.026	3.0	1.5	0.84	4.4
Large hummock	0.040	5.0	3.1	0.96	8.1
Landscape	0.019	7.9	4.3	1.0	12.2
Scaled Community	0.021	7.0	3.6	0.81	10.1

ϕ, g CO_2 m^{-2} d^{-1} μmol^{-1} PAR
A_{max}, g CO_2 m^{-2} d^{-1}
R_{day}, g CO_2 m^{-2} d^{-1}
k, dimensionless

*All curve fit parameters are statistically different at the 95% confidence interval.

measurements were made during the daytime. A linear equation was fit to each of the data sets to estimate ER as a function of surface temperature

$$ER = \alpha \cdot T_S + R_{\max} \quad , \qquad (4.7)$$

where α is the slope of the *ER* vs surface temperature relationship describing microbial and plant response to surface temperature change and R_{max} is the maximum *ER* rate at a surface temperature of 0 °C. R_{max} can be viewed as a relative measure of microbial activity and is also dependent on plant biomass and phenological stage. Each of the parameters along with Q_{10} factors are listed in Table 4.3.

The correlation coefficient for the landscape, small hummock, hollow and large hummock communities was 0.83, 0.46, 0.58 and 0.29 respectively. ER at the small hummock community yields the largest respiration rate at the freezing temperature. Hollows experience small respiration rates under cold conditions. The large hummock communities experienced slightly higher respiration rates than hollows at freezing. The Q_{10} sensitivity factor indicates that the hollow communities respond the most rapidly to surface temperature change. This is likely autocorrelated with lower water table position given higher surface temperature, however, no significant relationship was found between ER and water table position or soil moisture content. The landscape and community-scale parameters were within the same order of magnitude. Each of the community parameters was scaled according to the areal coverage of the community type:

$$P_{R}total = 0.48 \cdot (PR_{HW}) + 0.47 \cdot (PR_{SH}) + 0.05 \cdot (PR_{LH}) \quad , \qquad (4.8)$$

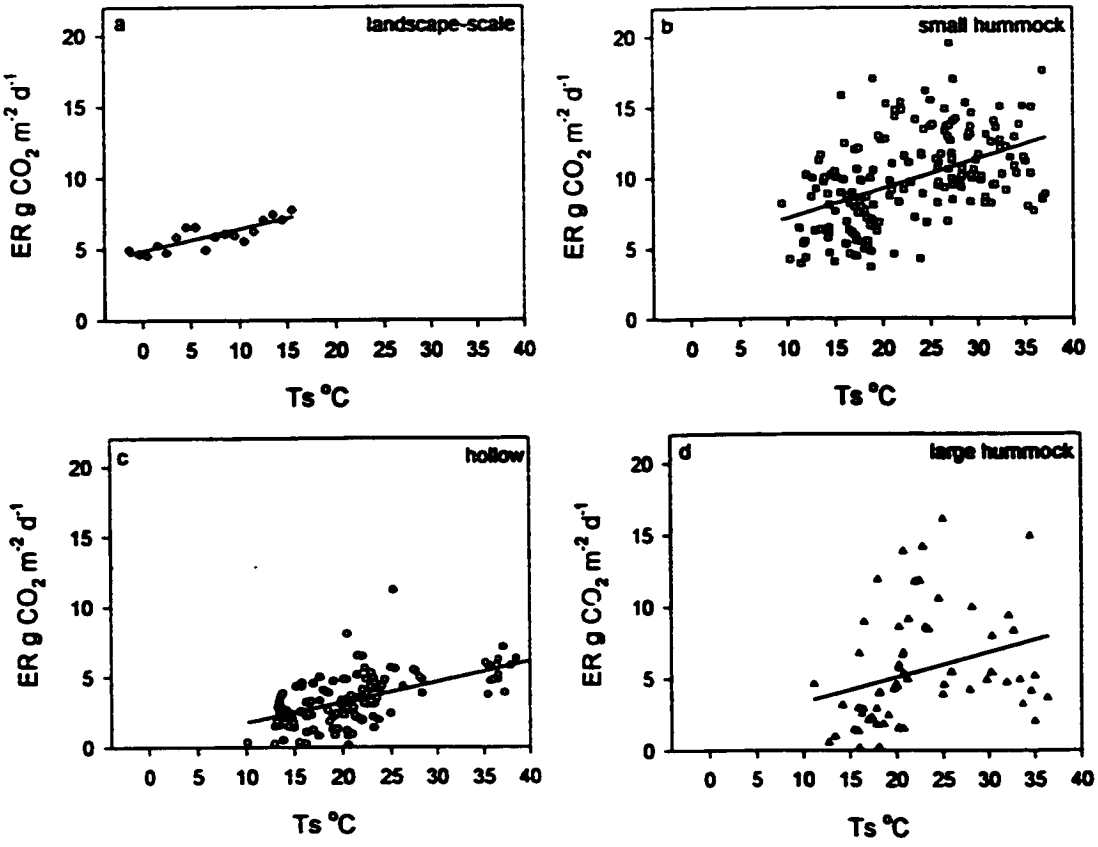

Figure 4.9: Landscape and community-scale ecosystem respiration as a function of surface temperature.

where P_R is the areal weighted total of the ecosystem respiration community parameters α, and R_{max}. The scaled community composite resulted in similar parameters, however, overestimated α and underestimated R_{max}. For a surface temperature of 25 °C the community composite relationship underestimated landscape-level respiration by about 26%. The landscape-level and the community-scaled composite revealed a similar Q_{10} response.

4.4. DISCUSSION

4.4.1. Landscape-Level NEE

During the relatively dry and warm growing season the Churchill fen experienced a small net gain of CO_2. The daily photosynthetic flux did not exceed ecosystem respiration until about DOY 178 when leafing had commenced. Maximum uptake of CO_2 occurred early during the green period when LAI reached near maximum and coincided with relatively wet surface conditions. As the season progressed the water table position dropped and NEE became more variable. Maximum draw down in the water table near the end of the green period coincided with five days of large CO_2 losses from the wetland. However, CO_2 uptake increased following a large rain event that occurred at the end of the green period. The data suggest that NEE may become more sensitive to precipitation events as the water table is lowered. Consequently, synoptic conditions exert an important control on the CO_2 exchange at the fen.

Table 4.3: Parameters for landscape and community-scale ecosystem respiration described as a function of surface temperature.

Terrain Type	α	R_{max}	Q_{10}
Small hummock	0.21	5.1	1.3
Hollow	0.14	0.32	1.6
Large hummock	0.17	1.6	1.4
Landscape	0.15	4.9	1.2
Scaled Community	0.17	2.6	1.3

α, g CO_2 m^{-2} d^{-1} $°C^{-1}$
R_{max}, g CO_2 m^{-2} d^{-1}
*All curve fit parameters are statistically different at the 95% confidence interval.

4.4.2. Scaling

At the community-scale, all fluxes showed a large amount of spatial and temporal variability as indicated by the large coefficients of variation. However, respiration rates were less variable than photosynthesis. This observation supports the findings of Griffis *et al.*, (2000) where the inter-annual variability in landscape-scale NEE at a subarctic fen was attributed to large seasonal and daily differences in photosynthesis. Furthermore, Kindermann *et al.*, (1996) using the Frankfurt Biosphere Model, attributed global–scale inter-annual variability in atmospheric CO_2 concentrations to differences in photosynthesis.

The small hummock community (*Carex* spp.) exerted the strongest control on landscape-scale NEE. This is due to their relatively large surface coverage but more importantly, the large flux value observed for both photosynthesis and respiration. Small hummocks exhibited the largest effective scaling factor during all periods of study. Therefore, the observed diurnal pattern in landscape-scale NEE is largely driven by CO_2 exchange at the small hummock sites. Strong reduction in CO_2 uptake through the late morning and afternoon hours is likely due to a reduction in stomatal conductance at the small hummock sites. Blanken and Rouse (1996) and Schreader *et al.*, (1998) provide evidence of water conservation in *Carex* species. Furthermore, estimates of landscape-scale photosynthesis (Griffis *et al.*, 2000) show a strong reduction through the late morning and afternoon hours especially during warm and dry years. Positive NEE (losses of CO_2) from the wetland following the maximum draw down in the water table is likely due to a large reduction in photosynthesis and a small increase in ecosystem respiration.

Scaling the chamber measurements to the landscape-level over the season indicates that estimates of tower photosynthesis and respiration, as well as, measured NEE is within the maximum margin of error of both methods. This helps substantiate that the fen was a net sink of -49 g CO_2 m^{-2} over the measurement season. There is a need for detailed analysis of the error associated with chamber measurements. It is apparent that chambers tend to underestimate the fluxes. This may be due to three factors 1) lack of spatial representation; a limited number of sampling points was available for the early morning and late afternoon hours. 2) gradient problems; build-up of CO_2 in the chamber could have suppressed the respiration flux while depletion of CO_2 might have reduced the photosynthetic flux. Re-examination of the photosynthesis CO_2 gradients from our data suggests that the 5-minute sampling interval is too long for some sites. 3) Chamber heating may have enhanced photorespiration rates. Better results might have been achieved with a more sophisticated dynamic chamber.

4.4.3. Ecological Implications

Previous studies of landscape-scale NEE (Griffis *et al.*, 2000; Lafleur, 1997) indicate that the transient response of northern wetlands to hot and dry spring-summer conditions is a net loss of CO_2 while warm and wet summers enhance CO_2 uptake. Based on the results of the community and landscape scale analysis it is possible to hypothesize about the equilibrium response of this fen to climatic warming.

A water balance model developed by Rouse (1998) for the Churchill fen suggests that soil moisture will decrease during the main growing season given a future $2xCO_2$ warming of 4 °C and a substantial 20% increase in precipitation. In time, this small

reduction in water table position at the fen could enhance its productivity by 1) changing the vegetation distribution within the fen, and 2) increasing the mineralization of organic nitrogen. The strong patterning of vegetation in relation to microtopography and mean water table position suggests that a long-term reduction in the water table position at the fen would allow for the invasion of vascular species into the drier hollows. For example, a similar distribution of *Carex* spp. at the hollow and small hummock sites would have changed the 1997 NEE dramatically (Table 4.4). In effect, this vegetation feedback would approximately double the LAI of the fen from 0.47 to 0.94. Moreover, this analysis may also serve as a simple analogue for increased productivity resulting from greater nitrogen availability due to drier soil conditions. It is well known than the productivity of arctic ecosystems is strongly limited by either nitrogen and or phosphorous (Shaver *et al.*, 1991; Shaver and Chapin, 1995; Shaver *et al.*, 1998). In this scenario, *Carex* spp. would not necessarily change their distribution but increase their leaf blade dimension. Experiments by Shaver *et al.*, (1998) demonstrated that increased nitrogen and or phosphorous supply to wet sedge tundra in northern Alaska caused significant increases in above and below ground biomass; changed species composition and increased both ecosystem production and respiration on an areal basis. Leaf area increased 4 to 6 times in nitrogen plus phosphorous addition experiments. Communities dominated by sedges showed significant increases in the abundance of *Carex corrdorrhiza*, a species that yielded the highest nutrient concentrations in control treatments. Ecosystem photosynthesis and respiration fluxes increased mainly due to changes in biomass. Recent work by Rolph (1999) has shown similar findings for the

Table 4.4: Potential change in landscape-scale NEE resulting from vegetation feedback

Current Distribution	**Small Hummocks**	**Hollows**	**Large Hummocks.**
Cumulative P	-394	-98	-23
Cumulative R	+328	+115	+19
P-R	-66	+17	-4
Seasonal NEE	**-53 g CO_2 m^{-2}**		
Daily NEE	**-0.7 g CO_2 m^{-2} d^{-1}**		
Scenario 1			
Cumulative P	-788		-23
Cumulative R	+656		+19
P-R	-132		-4
Seasonal NEE	**-136 g CO^2 m^{-2}**		
Daily NEE	**-1.8 g CO_2 m^{-2} d^{-1}**		

P, Photosynthesis g CO_2 m^{-2} d^{-1}
R, Ecosystem Respiration g CO_2 m^{-2} d^{-1}
*Results based on 1997 Environmental Characteristics

Churchill fen. In this 4-year nitrogen addition experiment (FERTEX), significant changes were found in both species composition and above ground biomass. Higher abundance of *Carex aquatilis* and *Carex limosa* was found for fertilized plots in both hollow and small hummock environments. LAI reached 1.5 at the peak of the growing season, which was approximately 3 times larger than at the control site. The effects of community composition and biomass changes on chamber-level CO_2 exchange are currently under investigation at the FERTEX study site.

It is possible that one or both of the above feedbacks could occur. Based on the 1997 climatic conditions, a doubling of LAI would have amplified net CO_2 uptake by about 2.6 times resulting in a net sink of -136 g CO_2 m^{-2}. However, our analysis assumes that soil respiration and stomatal conductance would respond conservatively to the changing water table position. Current modelling efforts (Griffis and Rouse, 2000) are examining the sensitivity of these potential feedbacks.

4.4.4. Modelling Implications

Combination of community and landscape-level observations reveals the complex nature of CO_2 cycling at the Churchill fen. While predicting the future response of NEE will require detailed physical representation of the exchange processes at the appropriate scales, this paper has shown that landscape-level monitoring is critical to verifying that all the important community-level processes have been identified and described accurately. While it was not the goal of this paper to describe in detail the physical processes regulating CO_2 exchange at the community and landscape-level, we provide two simple examples that demonstrate how photosynthesis and ecosystem respiration

behave differently at each scale and between community types. Community scale analysis indicates that stomatal control on photosynthesis is a key variable influencing CO_2 exchange at the Churchill fen. Mechanistic models of NEE should, therefore, be developed from lower-order processes (plant-level) and scaled to the landscape-level using community information. This would provide an opportunity to use satellite data to monitor community distribution changes and allow for the adjustment of model scaling parameters.

CHAPTER FIVE

MODELLING THE INTER-ANNUAL VARIABILITY OF NET ECOSYSTEM CO_2 EXCHANGE AT A SUBARCTIC SEDGE FEN [1]

5.1. INTRODUCTION

It is estimated that northern peatlands cover 346 million hectares of the earth's surface and represent a soil carbon sink of 455 Pg (Gorham, 1991). Northern peatland development has reduced atmospheric CO_2 concentrations and provided feedback to the global climate system by reducing the greenhouse effect (Moore *et al.*, 1998). Recent evidence, however, suggests that these ecosystems have experienced a reduction in net CO_2 acquisition and in some cases are releasing more CO_2 back to the atmosphere (Vourlitis and Oechel, 1997; Griffis *et al.*, 2000a).

These northern environments are unique since they are typically underlain by permafrost, maintain a water table near the surface, and have a diverse vegetation cover consisting of both vascular and non-vascular plants. Climatic change, therefore, is anticipated to have pronounced effects on these landscapes (Gorham, 1991). Future warming of northern latitudes is expected to lengthen the snow free period, increase precipitation, enhance evaporation, promote surface drying, increase the length of the growing season, and have a significant impact on photosynthesis, plant respiration,

[1] A modified version of this chapter, authored by T. J. Griffis and W. R. Rouse, will be published in *Global Change Biology*.

and organic decomposition rates (Gorham, 1991; Oechel and Billings, 1992; Rouse *et al.*, 1997). Resulting changes to energy, water, and carbon dioxide exchange of northern peatlands will provide significant feedback to the global climate system given their unique physical and biological properties and vast spatial coverage.

Field studies show that northern peatlands can change from a sink to source of atmospheric CO_2 both seasonally and interannually (Shurpali *et al.*, 1995; Griffis *et al.*, 2000a). This large variability is due to the impact of hydroclimatic conditions on plant growth, photosynthesis, and soil and plant respiration. Few studies (Vourlitis and Oechel, 1997; Joiner *et al.*, 1999; Griffis *et al.*, 2000a) have examined the magnitude and cause of interannual variability in net ecosystem CO_2 exchange (NEE) in northern peatlands. Recently Griffis *et al.*, (2000a) hypothesized that the interannual variability in NEE is largely manifest in the year to year variability in gross ecosystem photosynthesis (GEP), and speculate that the timing of snowmelt and spring hydroclimatic conditions has an important impact on phenology and the biological vigor of the vascular canopy through the entire growing season. Although their study estimated the variability in landscape-scale GEP and ecosystem respiration (ER), their analysis did not explicitly account for the processes and feedbacks affecting photosynthesis, ecosystem respiration, plant growth, and their combined impact on NEE. In an eight-year study involving field manipulations, Johnson *et al.*, (2000) demonstrated that plant photosynthesis and plant respiration were more variable than soil respiration and, therefore, a larger determinant of NEE. These rather surprising results illustrate the need for a better understanding of the

feedbacks involving photosynthesis, plant respiration, soil respiration, NEE, and climatic change in these northern environments.

Modelling the interannual variability in NEE for these peatlands is needed, therefore, to increase the understanding of the feedback processes controlling NEE, to provide better temporal and spatial estimates of NEE, and to help understand the impact of climatic change on the local and global carbon cycle. Vourlitis *et al.*, (2000) have shown that it is possible to extend simple physiological models of photosynthesis and ecosystem respiration using a "minimum data" approach to estimate NEE at the landscape scale. Further modelling studies are needed in order to test their reliability at predicting longer-term interannual variation in NEE.

The goal of the present paper is to synthesize a number of studies involving energy balance, plant physiological, and gas flux experiments conducted at a subarctic sedge fen near Churchill, Manitoba from 1976 to present, in order to model the CO_2 exchange. The model presented here is empirical and consists of number of algorithms describing the energy, water, and CO_2 exchange of the Churchill fen. The model is developed in an attempt to 1) help better understand the complex interrelationship between climate and phenology and their influence on NEE; 2) explore the causes of interannual variability of NEE; 3) examine how CO_2 cycling will vary given a changing climate; 4) identify processes that require better biophysical explanation.

Although there is a need to move toward more physically based models our approach is to highlight the processes and feedback mechanisms that are needed to explain the interannual variability in CO_2 exchange.

5.2. RESEARCH SITE AND METHODS

The experimental area is located on the southwestern shore of Hudson Bay, within the Hudson Bay Lowland (Figure 5.1). The research site is an extensive fen, located 20 km east of the town of Churchill Manitoba (58° 45' N, 94° 04' W), and 12.5 km south of the Hudson Bay shoreline. This fen is characterized by non-patterned, hummock-hollow terrain with hummocks comprising 47%, hollows 48% and large hummocks 5% of the landscape (Griffis *et al.*, 2000b). Brown moss (*Scorpidium turgescens*) is the dominant vegetation found in the wet hollows. The moss (*Tomenthypnum nitens*) and vascular species (*Carex aquatilis, C. limosa, C. saxatilis and C. gynocrates*) cover the small hummock sites. Larger hummocks support vascular species (*Betula glandulosa, Ledum decumbens Salix arctophila or* Carex spp.) and species of lichen (*Cladina stellaris, C. rangiferina*) and moss (*Dicranum undulatum*). The fen has a mean peat depth of 0.25 m and is underlain by glaciomarine till, consisting of fine silts and clays with interspersed layers of carbonate shingles.

5.2.1. Field Measurements

Ongoing field experiments at the Churchill fen and other wetlands within the experimental area began in 1976. Summer season energy and water balance measurements have been continuous at the fen since 1987 and landscape-scale CO_2 measurements were initiated in 1991. The Bowen ratio and aerodynamic gradient methods, and robust eddy covariance measurements have been used to estimate the energy balance and carbon dioxide budget of the fen. Non steady-state chamber measurements of CO_2 exchange were made frequently during the 1997 growing season

and were compared to micrometeorological flux estimates of CO_2 exchange in 1997 (Griffis et al., 2000b). Methodological approaches to the energy, water, and carbon dioxide flux measurements and associated sources of error have been described previously in Halliwell and Rouse, (1989); Burton et al., (1996); Schreader et al., (1998) and Griffis et al., (2000a). The daytime average error in the gradient-derived CO_2 flux can approach 30%.

5.2.2.Power Spectral Analysis

We used power spectral analysis to examine the half-hour gradient-derived CO_2 flux from five growing seasons to help identify the underlying processes influencing the variability in NEE. The technique used is the power spectral density "psd" function available from The MATLAB Signal Processing Toolbox (MATLAB V5.2, The Math Works, Inc., Natick, MA, U.S.A.), which employs Welch's method (Welch, 1967) of averaging periodograms. A Fast Fourier Transform (FFT) was performed on 15 day windows to compute the mean spectrum of the 375 day signal (18000 half-hour flux measurements). The 95% confidence intervals were also computed to identify the frequencies statistically different from random noise.

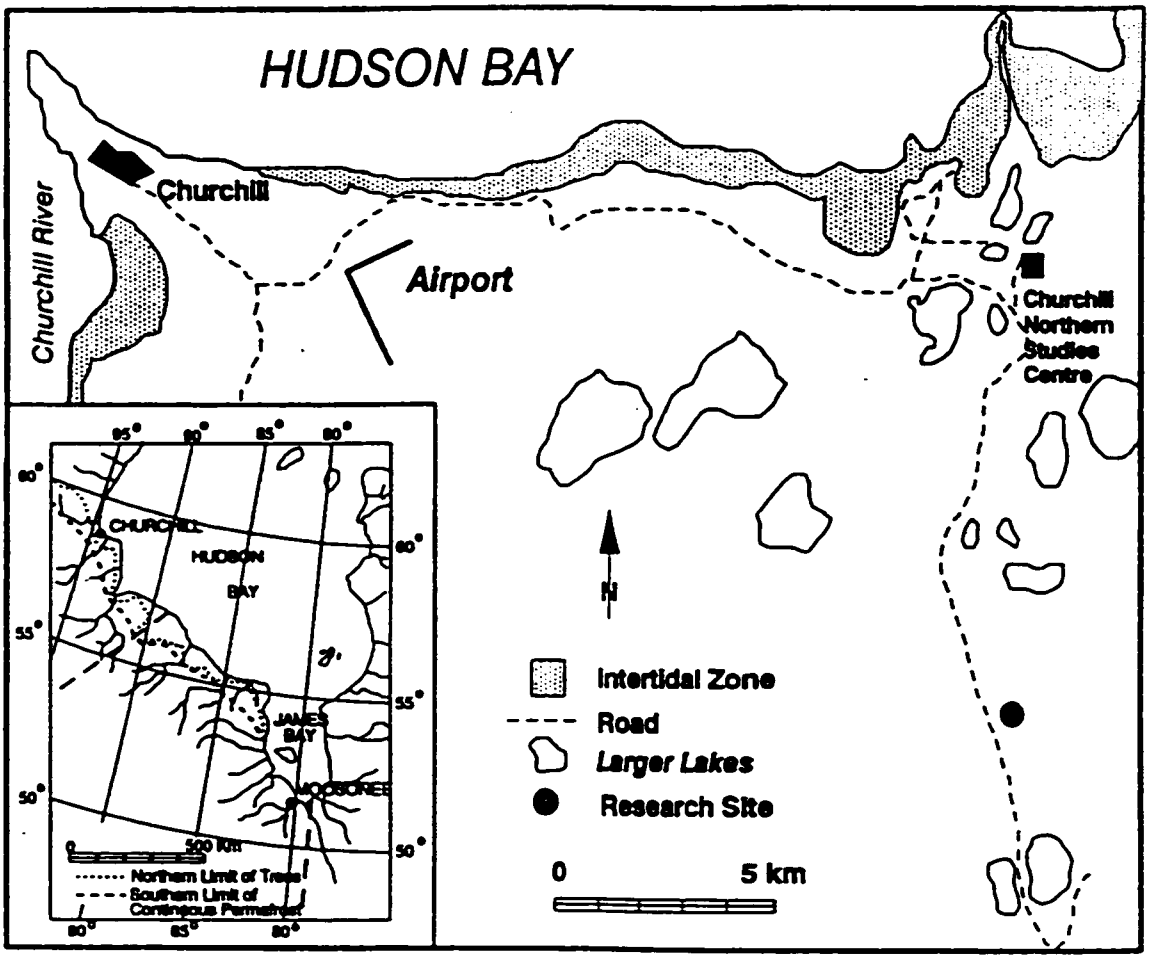

Figure 5.1: Research area and study site

5.2.3. Climatic Conditions and Net Ecosystem CO_2 Flux Data

Table 5.1 summarizes the general climatic conditions and NEE data for the five growing seasons examined in this study. The 1994 season was uncharacteristically dry and experienced a net loss of +76 g CO_2 m^{-2} to the atmosphere over the measurement period (June 13 to August 28, DOY 164 to 238). In 1996 climatic conditions were wetter than normal and NEE showed a net gain of -235 g CO_2 m^{-2}. The 1997 and 1998 seasons were similar climatically through the measurement period. Both seasons were warmer than the 30-year Churchill normal with near-normal precipitation. Each season was a sink of CO_2. In 1999 growing season precipitation was near normal with a pronounced dry spring period. The fen was a weak net sink of -34 g CO_2 m^{-2} (Griffis *et al.*, 2000a).

5.3. MODEL DEVELOPMENT

The power spectrum (Figure 5.2) of the measured tower-flux data revealed significant power in frequencies ranging from 1 to 4 days. High power in the 1 day frequency is related to diurnal changes in photosynthetically active radiation and air temperature, and we hypothesize that the significant power in lower frequencies (>1day) result from synoptic weather events, fluctuations in water table position, the wetting and drying cycle of mosses, and their combined influence on photosynthesis, respiration and plant growth. The energy of each of the frequencies was calculated by integrating the power magnitude over the frequency interval. From the 5-year record of NEE we find that the 1-day frequency accounts for 12% of the total spectrum energy and that frequencies ranging up to 3 days account for 98% of the spectrum energy. The broad-band behaviour (significant power in a number of frequencies), combined with the energy

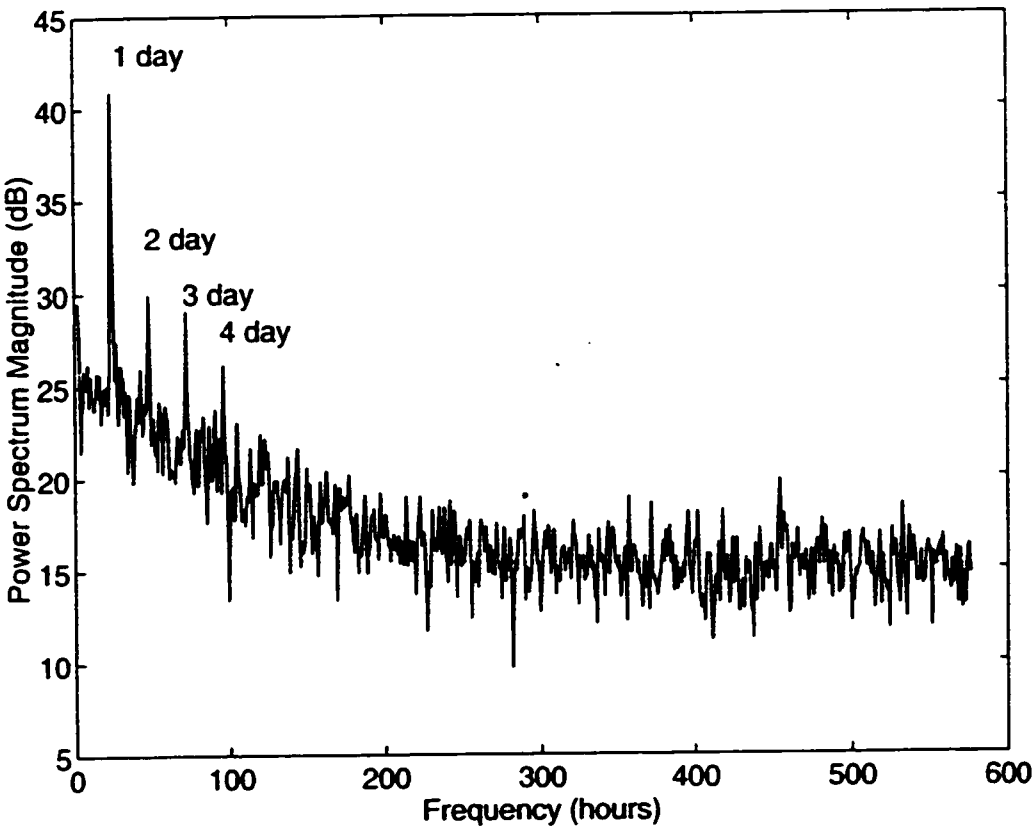

Figure 5.2: Power spectrum of five growing seasons (1994, 1996-1999) of net ecosystem CO_2 exchange at the Churchill fen. The power spectrum is given as a function of frequency from time scales of one-half hour to 600 hours (25 days). The spectrum was computed from 18000 half-hour periods (375 days) using a 15 day window. Labeled frequencies are statistically significant at the 95% confidence interval. These data were measured using micrometeorological gradient techniques and are provided by Schreader et al., (1998) and Griffis et al., (2000a).

level of each frequency, provide an important set of diagnostics in which to test model dynamics.

The model presented here uses a half-hour time step in order to simulate the observed NEE time series. Model inputs include: net radiation (Rn), photosynthetically active radiation (Q), air temperature (Ta), precipitation (P), and vapour pressure deficit (vpd). Model variables, parameters, and model coefficients (a-v) are listed in Appendix A1.

5.3.1 Water Balance

The water balance functions were developed and tested by Rouse (1998). A brief description is given here along with new developments in its formulation. The model is initialized with a known water table depth (WT_i) following snowmelt and begins calculating the potential latent heat flux (QeP) as a bilinear function of net radiation and air temperature

$$QeP = a_1 Rn + a_2 Ta \ . \qquad (5.1)$$

The actual latent heat flux (Qe) is estimated by relating QeP to a surface resistance (R_s). R_s is the ratio of $\frac{Qe}{QeP}$ as it varies with the change in water table depth

$$R_s = b_1 + b_2 WT \ . \qquad (5.2)$$

R_s increases as the water table drops below the surface of the wetland since less surface water is exposed to the atmosphere and the soil water molecules must travel a longer path length before entering the atmosphere. The actual latent heat flux is therefore

Table 5.1: Growing season climatological and NEE characteristics

(a) Mean Daily Air Temperature by Growing Period and Season (°C).

Year	Pre-green	Green	Post-green	Season
1994	12.5 (+5.7)	12.3 (+1.0)	11.1 (-0.4)	12.0 (+1.2)
1996	7.0 (+0.2)	13.0 (+1.7)	11.5 (0.0)	11.9 (+1.1)
1997	6.1 (-0.7)	13.8 (+2.5)	13.0 (+1.5)	12.7 (+1.9)
1998	5.5 (-1.3)	14.1 (+2.8)	12.9 (+1.4)	12.8 (+2.0)
1999	13.0 (+6.2)	12.6 (+1.3)	12.1 (+0.6)	12.5 (+1.7)
Normal	6.8	11.3	11.5	10.8

*bracket indicates departure from normal

(b) Total Precipitation by Growing Period and Season (mm).

Year	Pre-green	Green	Post-green	Season
1994	4 (-9)	32 (-47)	37 (0)	73 (-56)
1996	35 (+22)	70 (-9)	41 (+4)	145 (+16)
1997	8 (-5)	109 (+30)	7 (-30)	125 (-4)
1998	23 (+10)	58 (-21)	35 (-2)	118 (-11)
1999	0 (-13)	72 (-7)	45 (+8)	118 (-11)
Normal	13	79	37	129

*bracket indicates departure from normal

(c) Cumulative Net Ecosystem CO_2 Exchange and Estimate of Maximum Probable Error (g CO_2 m^{-2})

Year	Pre-green	Green	Post-green	Season
1994	+55 (± 17)	-12 (± 4)	+33 (± 10)	+76 (± 23)
1996	-20 (± 6)	-135 (± 41)	-80 (± 24)	-235 (± 71)
1997	+12 (± 4)	-61 (± 18)	0 (± 0)	-49 (± 15)
1998	-22 (± 7)	-189 (± 57)	-17 (± 5)	-228 (± 68)
1999	-0.6 (± 0.2)	-41 (± 12)	+8 (± 2)	-34 (± 10)
Days	9	48	18	75

*bracket indicates maximum probable error (Griffis et al. 2000a)

$$Qe = QePf(R_s) \tag{5.3}$$

with the cumulative half-hour water budget, ds, calculated as

$$ds = (P - E) \tag{5.4}$$

where P, is precipitation and E, the amount of water evaporated in meters. The water table position is updated according to the half-hour change in ds. In order to calculate the effect of ds on WT position it is necessary to know the percentage area of the wetland that is submerged. A detailed survey of the site was used to estimate the proportion of the wetland residing above and below the relative water table position (Figure 5.3) from the following sigmoid relationship

$$w_a = \frac{Wa_{max}}{c_1 + e^{\left(-\left(\frac{WT - c_2}{c_3}\right)\right)}} \tag{5.5}$$

where w_a represents the fractional area of wetland submerged. Given the initial position of the water table, the relative surface area of water, the change in ds, and the specific yield of the soil SY, the new water table position can be estimated as

$$WT_{t+1} = WT_t + \frac{ds}{SY}(1 - w_a) + dsw_a . \tag{5.6}$$

From equation 5.6, when the entire wetland is submerged (WT > 0.50 m), SY equals 1.0. SY varies from 0.36 at the peat surface and decreases to 0.06 in the deeper marine clay soil layers at a depth below 0.25 m.

Volumetric soil moisture (SM) at the base of the moss layer (0.025 m) at the edge of small hummock sites can be predicted from an exponential relationship with WT position (Figure 5.4). The soil moisture content is predicted as

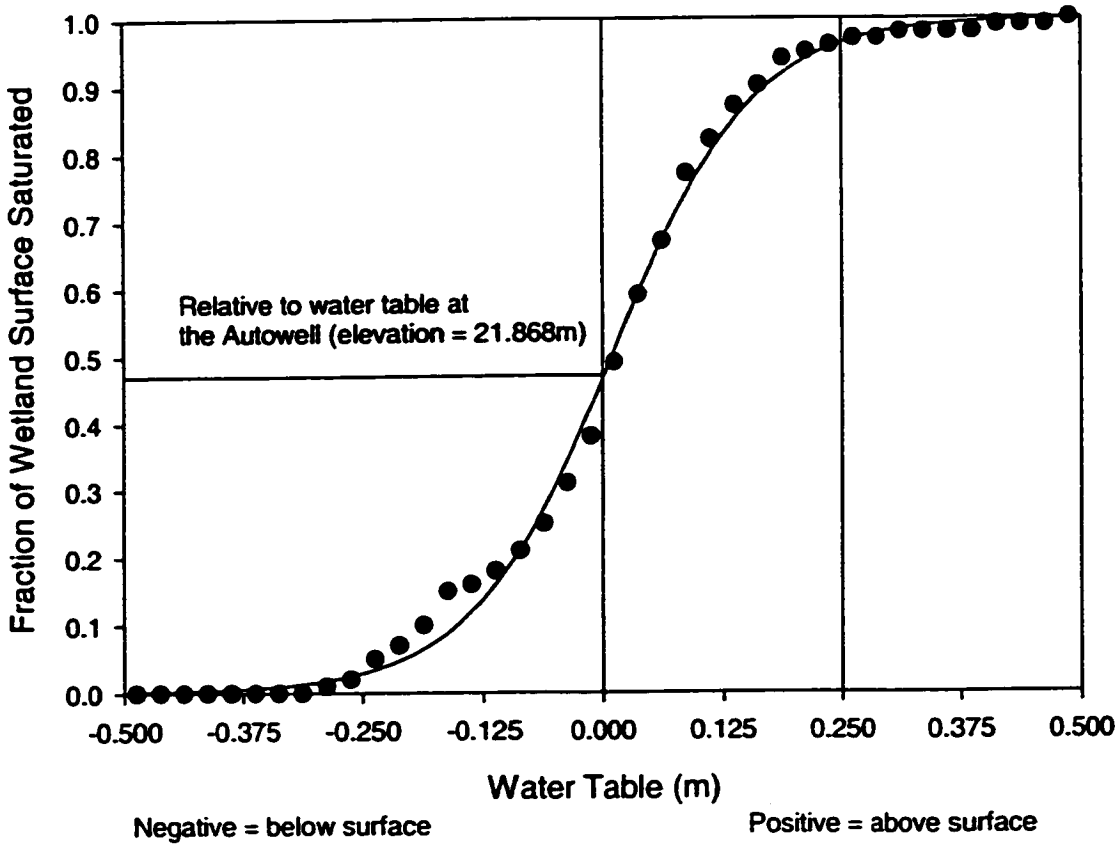

Figure 5.3: Modelled fractional area of wetland surface submerged below the water table level. Data points represent surveyed topography from 4 cardinal directions within a 150 m radius of the main micrometeorological tower site.

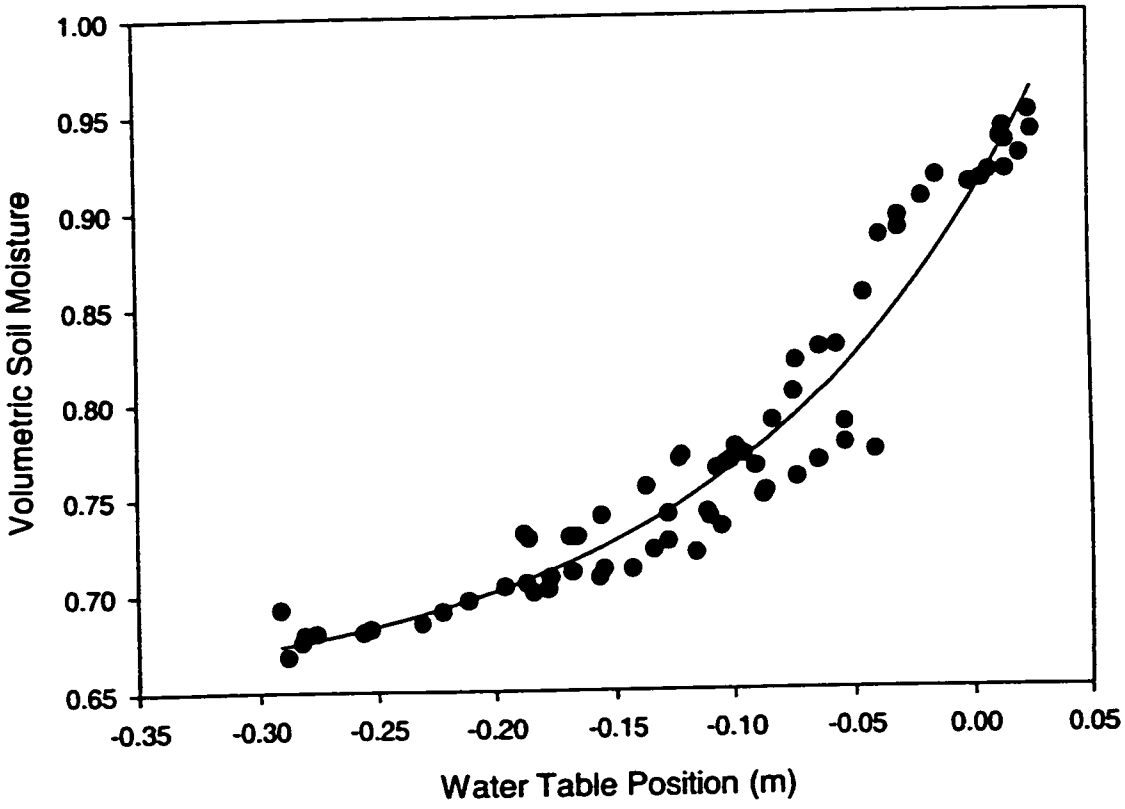

Figure 5.4: Relationship between surface volumetric soil moisture and water table position. Soil moisture was measured during the 1997 and 1998 growing season using water content reflectometry (CS615, Campbell Scientific).

$$\theta_s = d_1 + d_2 e^{(d_3 WT)} \qquad (5.7)$$

5.3.2. Phenology and Plant Fitness

There is a scarcity of information regarding the phenology, and fitness characteristics of Carex spp. The timing of events such as germination, breaking of dormancy and flowering has been shown to have important consequences on plant fitness (Kalisz, 1986; Purrington and Schmitt, 1998). Purrington and Schmitt (1998) have shown that the timing of seedling emergence can affect plant mortality rates and reproductive performance. In the plant *Silene latifolia* early emergence caused high mortality rates through the growing season. Optimum fitness (low mortality rates and high flower production) was attained for seedlings that experienced intermediate emergence times. The sedge species *Eriophorum vaginatum* has been shown to germinate rapidly following snowmelt at surface temperatures between 23 and 27 °C (Gartner et al., 1986). As well, Gerritsen and Greening (1989) have shown that Carex spp. have higher germination rates at low water table positions in marsh environments since lower water table permits greater oxygen diffusion to the vicinity of dormant seeds. To our knowledge, information does not exist on the relationship between the timing of *Carex aquatilis* emergence and its impact on fitness or mortality rates.

Estimating leaf area index is difficult due to temporal and spatial variability in above ground biomass. The number of shoots produced each season depends on a number of factors ranging from predation on seeds and rhizomes (Srivastava and Jefferies, 1996; Jano et al., 1998) to the failure of seeds and rhizomes to break dormancy given

unfavorable spring or winter conditions (Vleeshouwers et al., 1995). We assume that all shoots emerge at the time our model is given the initial LAI.

At the Churchill fen, shoot densities have been shown to vary between 1000 and 1500 shoots m^{-2}, reaching maximum density between mid June and mid July (Petrone, 1996; Schreader et al., 1998; Rolph 1999). We assume that all seed germination commences after snowmelt once surface temperatures exceed freezing. When dormancy has been broken, the model estimates the initial leaf area index (LAI). The initial LAI and fitness of the vascular canopy is based on the timing of snowmelt and the water table position. Three initial conditions are used to describe the state of the phenology and its fitness consequences to the vascular plants. These estimates are based on personal field observations at the study site and are currently being investigated with on going remote sensing studies (Appendix A2).

Fitness Condition 1: Normal to late snowmelt

Snowmelt commences ± 1 week of June 1. Water table position is above the surface causing low soil oxygen diffusion. As a result, breaking of seed and rhizome dormancy is delayed and shoot emergence is slow. When the water table position recedes and hummock tops become exposed the initial LAI is set to 0.001. The maximum LAI given these initial growing conditions (a descriptor of plant fitness) ranges between 0.47 and 0.60.These values are supported by field observations (Petrone, 1996; Rolph, 1999; Griffis et al., 2000b).

Fitness Condition 2: early snowmelt and dry spring

Snowmelt is completed at least 1 week prior to May 27, precipitation events are infrequent and the growing season begins with a water deficit (Rouse, 1998). Water table position is below -0.01 m. Vascular vegetation does not reach maturity before experiencing considerable drought stress. In this case the phenology and climatic conditions adversely affect the fitness of the vascular species. The dry conditions experienced during this intense period of plant development cause many of the shoots to have high mortality rates. The initial LAI is 0.001 but a lower maximum LAI of 0.35 is attained (Schreader et al., 1998).

Fitness Condition 3: early snowmelt and no-water deficit

Snowmelt commences at least 1 week earlier than May 27, however, ample precipitation prevents the water table level from dropping to levels that would adversely affect germination and plant growth. The early snowmelt and ideal water table position increase the fitness of the vascular plants. The initial LAI is set to 0.15 (Brown, 1999) due to the longer growing period leading up to the start of model calculations, which due to our data collection start June 13 (DOY 164). A maximum LAI is set at 0.60. We hypothesize that the longer growing period allows greater root development and the ability of the vascular canopy to avoid drought stress later in the season.

Although these fitness parameters are at the present time gross assumptions, they provide a qualitative starting point to the problem of phenology vs fitness and biological vigor in these ecosystems. Phenology and fitness is also relevant to bryophytes (Johanson *et al.*, 1995), however, these characteristics have received relatively little attention in the

scientific literature and have not been studied at the Churchill fen. Moreover, the change from net source to net sink at the Churchill fen is correlated with the timing of leaf-out (Schreader *et al.*,1998).

Once LAI and fitness have been described, plant growth is controlled by the rate of photosynthesis, respiration, and carbon allocation parameters. The LAI is updated half-hourly and typically attains a maximum value within 3 to 4 weeks of emergence. Drought stress and cold temperatures bring about the onset of dormancy and senescence. We use sustained levels of highly negative soil moisture potentials (<-400 ∑Mpa, cumulated half-hourly) to trigger the onset of dormancy based on observations from the 1994 growing season (Schreader et al., 1998). Sub-freezing temperatures also initiate plant dormancy. Once senescence has been initiated the process is irreversible and the remaining leaf area decays at an assumed rate of 1% per day.

5.3.3. Carbon Economics and Plant Growth

One of the greater challenges in modelling and understanding the carbon budgets of ecosystems is accounting for the transport and allocation of photosynthetic products to the different plant organs and partitioning those products into new growth structures, storage, and the respiration resulting from biosynthesis, maintenance of biomass and the maintenance of ion gradients (Penning de Vries, 1975; Heide et al., 1985; Van der Werf et al., 1988; Poorter et al., 1990; Atkin et al., 1996).

Carbon economics differ between plants and relatively little information is available for *Carex aquatilis*, and, *Scorpidium turgescens* remains uninvestigated. However, studies have examined some Carex spp. (Van der Werf et al., 1999) and

generalizations can be made between fast and slow growing plant species (Poorter et al., 1990). Poorter et al., (1990) report on the carbon and nitrogen economics of 24 different wild species with respect to relative growth rate (RGR). Slow growing (RGR<110 mg g^{-1} d^{-1}) species in their study showed approximately 27% of the daily photosynthate products were allocated to new leaf growth, 13% shoot growth, 18% root growth, 24% above ground respiration, 19% below ground respiration. Allocation patterns are even more complex in natural settings. Heide et al., (1985) has shown that day length can have a significant effect on the allocation to below and above ground structures. During long days, a greater portion of carbon is invested in shoot and leaf growth whereas short days result in greater carbon partitioning into root structures. Larger respiration rates have also been found in slow growing alpine and lowland *Poa* spp. (Atkin et al., 1996). Their study showed that 45 to 60% of the daily photosynthetic flux is lost to respiration. The greater expense of respiration in slow growing and arctic species has been hypothesized to be related to a lower efficiency in producing respiratory products, or alternatively, that the respiratory energy efficiency is low. Tenhunen et al., (1992) hypothesized a greater need for protein turnover to adapt to the cold conditions.

In our parameterization, 24% of the photosynthate production is used to form new shoot and leaf growth and 74% is used for root growth. This assumption is based on the above and below ground biomass findings of Rolph (1999). 2% of the photosynthetic production is stored as sugars in the plant structures. Leaf and shoot respiration resulting from maintenance and growth processes (autotrophic respiration, R_a) account for 30% of the photosynthetic production. The effect of environmental conditions (day length effects

and nutrient conditions) on transport and distribution of photosynthate carbon to above and below ground structures is currently ignored. However, the amount of R_a from the plant is increased by 1% for every 1-degree increase above the optimum temperature of 15 °C. This parameter value is arbitrarily assigned but justified by the fact that warmer temperatures increase protein turnover in plants and the amount of energy production used in respiration.

From the carbon budget of the plant, the growth of the vascular leaf area is estimated as

$$LAI_{t+1} = LAI_t + G_l \tag{5.8}$$

where G_l is a growth parameter describing the conversion of leaf photosynthate into leaf biomass.

5.3.4. Gross Photosynthesis

Photosynthetic activity of the moss community can occur when the air temperature exceeds freezing. Based on chamber measurements from the 1997-growing season we used a boundary analysis approach and scaled the maximum observed chamber flux (P_{mmax}) according to PAR (Figure 5.5) and volumetric water content. The moss contribution to gross ecosystem photosynthesis can be described as

$$P_m = P_{m\max} f(A_{mQ}) f(A_{m\theta}) \tag{5.9}$$

where

$$f(A_{mQ}) = \left(\frac{\phi_m Q + P_{m\max} - \sqrt{(\phi_m Q + P_{m\max})^2 - 4\phi_{mQ} k P_{m\max}}}{2kP_{m\max}} \right) \tag{5.10}$$

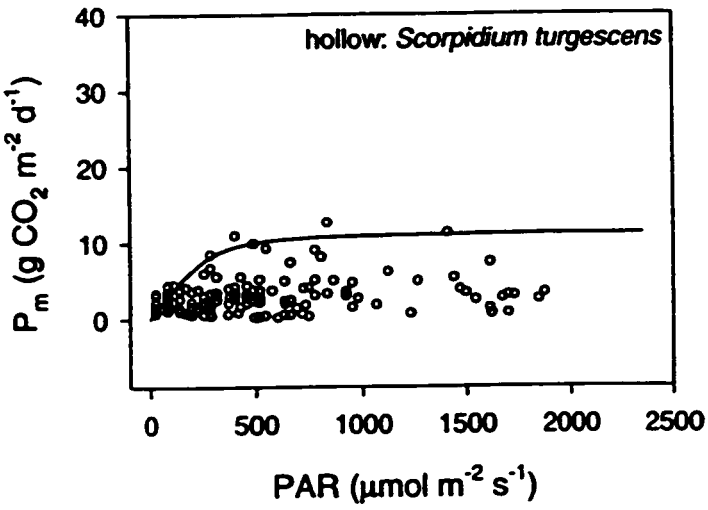

Figure 5.5: Boundary curve describing moss community photosynthesis as a function of photosynthetically active radiation. These data (n = 128) were acquired from non steady-state chamber measurements made at the Churchill fen during the 1997 growing season (Griffis et al., 2000b).

and

$$f(A_{m\theta}) = \frac{\left(h_1 + h_2 e^{(h_3 \theta_m)}\right)}{P_{m\max}}. \qquad (5.11)$$

A_{mQ} describes the response of moss net photosynthesis to variations in Q. Equation 5.10 was proposed by Prioul and Chartier (1977). The parameter ϕ_m is the apparent quantum efficiency for moss (ϕ_v for vascular plants) describing the conversion of light to photochemical products and k is the scaling parameter defining the change in slope between the light limited and light saturated region of the curve.

Equation 5.11 describes the limitation of decreased volumetric moisture on moss gross photosynthesis. This relationship is idealized and not supported by empirical data at present from the Churchill fen. However, previous research investigations supports that water content of bryophytes play an important role in their photosynthetic capacity (Tenhunen et al., 1992; Green and Lange, 1994). Moss moisture content, θ_m, is estimated from the water table soil moisture curve (equation 5.7).

Vascular photosynthesis is based on chamber measurements made during the 1997 growing season (Griffis et al., 2000b) combined with a stomatal conductance model developed for Carex *aquatilis* by Blanken and Rouse (1995). Gross photosynthesis is described as

$$P_v = (P_{v\max} - P_m) f(A_{vQ}) f(g_s) \qquad (5.12)$$

$$f(A_{vQ}) = \left(\frac{\phi_v Q + P_{v\max} - \sqrt{(\phi_v Q + P_{v\max})^2 - 4\phi_v Q k P_{v\max}}}{2k(P_{v\max} - P_m)} \right) \qquad (5.13)$$

$$f(g_s) = \frac{LAI}{LAI_{\max}} f(Ts) f(VPD) f(\psi_s) \tag{5.14}$$

$$f(T_s) = \frac{m_1 + m_2 T_s + m_3 T_s^2}{gs_{\max}} \tag{5.15}$$

$$f(vpd) = \frac{n_1 + n_2 VPD}{gs_{\max}} \tag{5.16}$$

$$f(\psi_s) = \frac{p_1 + p_2 \psi_s}{gs_{\max}} \tag{5.17}$$

Since bryophytes carpet the entire fen landscape, equation 5.13 separates the modelled moss net photosynthesis from the vascular community. Vascular photosynthesis, P_v, is described as a function of Q following Prioul and Chartier (1977) (Figure 5.6).

The conductance model (g_s) is described in detail by Blanken and Rouse (1995). We have adapted the model so that it is used to scale the photosynthetic flux and not as an absolute conductance value. The conductance model was also developed from a boundary analysis approach and is a function of surface temperature (Ts), vapor pressure deficit, soil water potential (ψ_s) and the ratio of the observed leaf area (LAI) to the maximum potential leaf area (LAI_{max}). The maximum observed conductance value (g_{smax}) is used to scale each of the stomatal conductance functions to a fraction of 1.0.

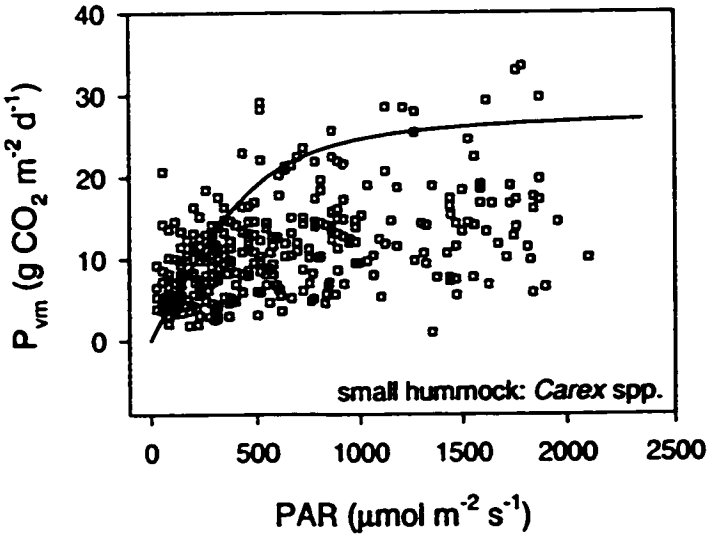

Figure 5.6. Boundary curve describing vascular community photosynthesis as a function of photosynthetically active radiation. These data (n = 332) were acquired from non steady-state chamber measurements made at the Churchill fen during the 1997 growing season (Griffis et al., 2000b).

5.3.5. Soil Respiration

We separate soil respiration (heterotrophic respiration, R_h) from plant respiration despite the complexities in the relationship between them and, as well, the difficulties of measuring these fluxes in the field. Based on chamber measurements where the vegetation was removed at the beginning of the growing season we developed a soil respiration relationship based on temperature (Figure 5.7) and soil moisture (Figure 5.8).

$$R_h = R_{h\max} f(T_s) f(\theta_s) \tag{5.18}$$

$$f(T_s) = \frac{q_1 + q_2 T_s}{R_{h\max}} \tag{5.19}$$

$$f(\theta_s) = \frac{v_1 + v_2 \theta_s}{R_{h\max}} \tag{5.20}$$

R_{hmax} is the maximum observed soil respiration flux from chamber measurements.

5.3.6. Net Ecosystem Exchange

The net ecosystem exchange of carbon dioxide at the fen is the net balance between production and decomposition processes. Gross ecosystem photosynthesis includes production from the mosses (P_m) and vascular plants (P_v). Ecosystem respiration comprises the dark respiration from the mosses (R_m) and vascular plants (R_v) and also the respiration from soil microbial decomposition (R_h).

$$GEP = P_m + P_v \tag{5.21}$$

$$ER = R_m + R_v + R_h \tag{5.22}$$

$$NEE = GEP - ER \tag{5.23}$$

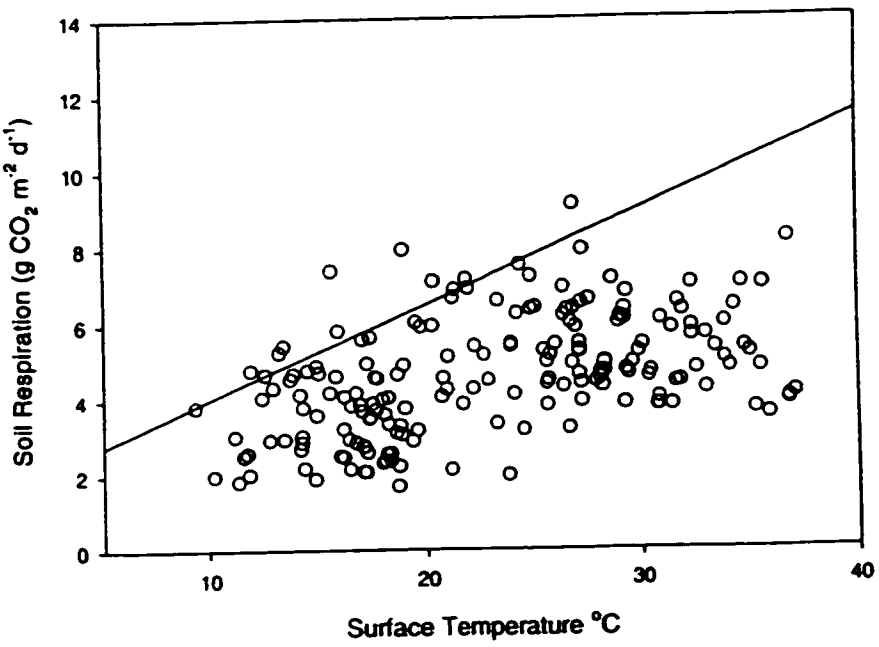

Figure 5.7: Boundary curve describing soil respiration as a function of surface temperature. These data (n = 190) were acquired from non steady-state chamber measurements made at the Churchill fen during the 1997 growing season. Soil respiration was estimated by removing the surface vegetation prior to sampling.

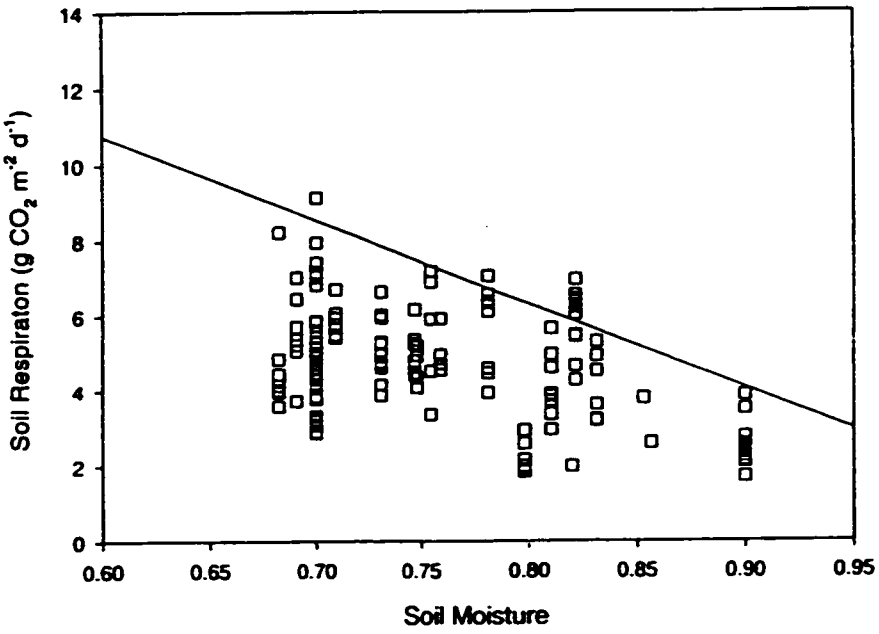

Figure 5.8: Boundary curve describing soil respiration as a function of surface moisture. These data (n = 190) were acquired from non steady-state chamber measurements made at the Churchill fen during the 1997 growing season. Soil respiration was estimated by removing the surface vegetation prior to sampling.

5.4. MODEL TESTING

5.4.1 Sensitivity Analysis of Model Parameters

A sensitivity analysis of the model parameters listed in Appendix A1 was performed to help identify potential causes of model bias. Sensitivity was examined by varying each of the parameters by ± 5% and assessing their effect on the model simulations for the 1996 season. The sensitivity of NEE to the estimate of θ_m caused a 20% change in the modelled seasonal cumulative CO_2 exchange. Simultaneous increases in LAI_{max} and G_l caused a 13% change in seasonal NEE. Varying P_{vmax} showed an 8% difference in the seasonal NEE. Testing of all other parameters resulted in changes of less than 5% for the simulated seasonal NEE. The sensitivity analysis indicates that the assumptions surrounding estimate of moss moisture content and vascular plant growth have the strongest influence on the modelled seasonal NEE.

5.4.2. NEE Simulations

The behaviour of the model is tested against five years of growing season NEE data. These data have been described previously in Griffis et al., (2000a). The five-year series of NEE, cumulative seasonal NEE, diurnal NEE, and the time series of half-hour fluxes for 1996 and 1997 are examined in order to evaluate model performance.

The power spectrum for the continuous series of the five modelled data years is presented in Figure 5.9. Frequencies with high relative power are similar to those shown in Figure 5.2 for the observed data series. However, the model exhibits significantly higher power in additional low frequencies of up to 8 days. It is encouraging that the model captures the broad-band behaviour at frequencies less than 3 days. The energy of

the model spectra, however, is concentrated (>90%) in the 1 day frequency. Greater attention is needed, therefore, in improving the model dynamics beyond the 1 day frequency. This may require better simulation of the wetting and drying cycle of mosses and phenology of both vascular and moss species.

5.4.3. Seasonal Net Ecosystem Exchange

The model accurately predicts those years that experienced a net gain and a net loss of CO_2. Figure 5.10 displays the actual and modeled cumulative NEE for the five test years. On a seasonal basis the model performs reasonably well in four of the five years. In 1994 the model underestimates the net loss of CO_2 during the early portion of the growing season (Figure 5.10a). Although the magnitude of the modeled flux disagrees with the measured data, the behaviour of the model shows strong similarities to the observed trend. During the mid growing season, the observed and modeled net loss of CO_2 from the wetland reach a near equilibrium due to the emergence of the vascular species. Following an early vascular senescence, initiated in mid July, both signals experience an increase in the loss of CO_2 from the wetland. The model over estimated the net loss by 10 g CO_2 m^{-2}; however, this is within the maximum margin of error in the flux measurements. Figure 5.11a indicates that the net loss of CO_2 during the 1994 growing season was due to low photosynthetic rates from both the moss and vascular species relative to ecosystem respiration.

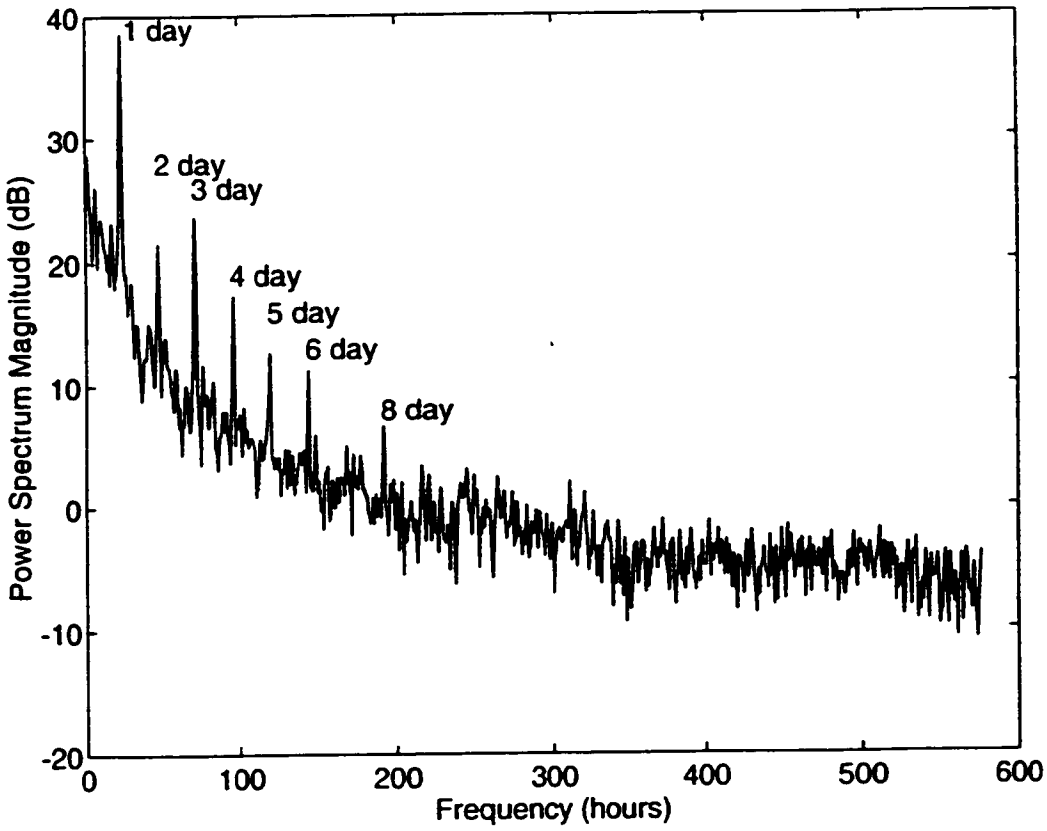

Figure 5.9: Power spectrum of five growing seasons (1994, 1996-1999) of modelled net ecosystem CO_2 exchange at the Churchill fen. The power spectrum is given as a function of frequency from time scales of one-half hour to 600 hours (25 days). The spectrum was computed from 18000 half-hour periods (375 days) using a 15 day window. Labeled frequencies are statistically significant at the 95% confidence interval.

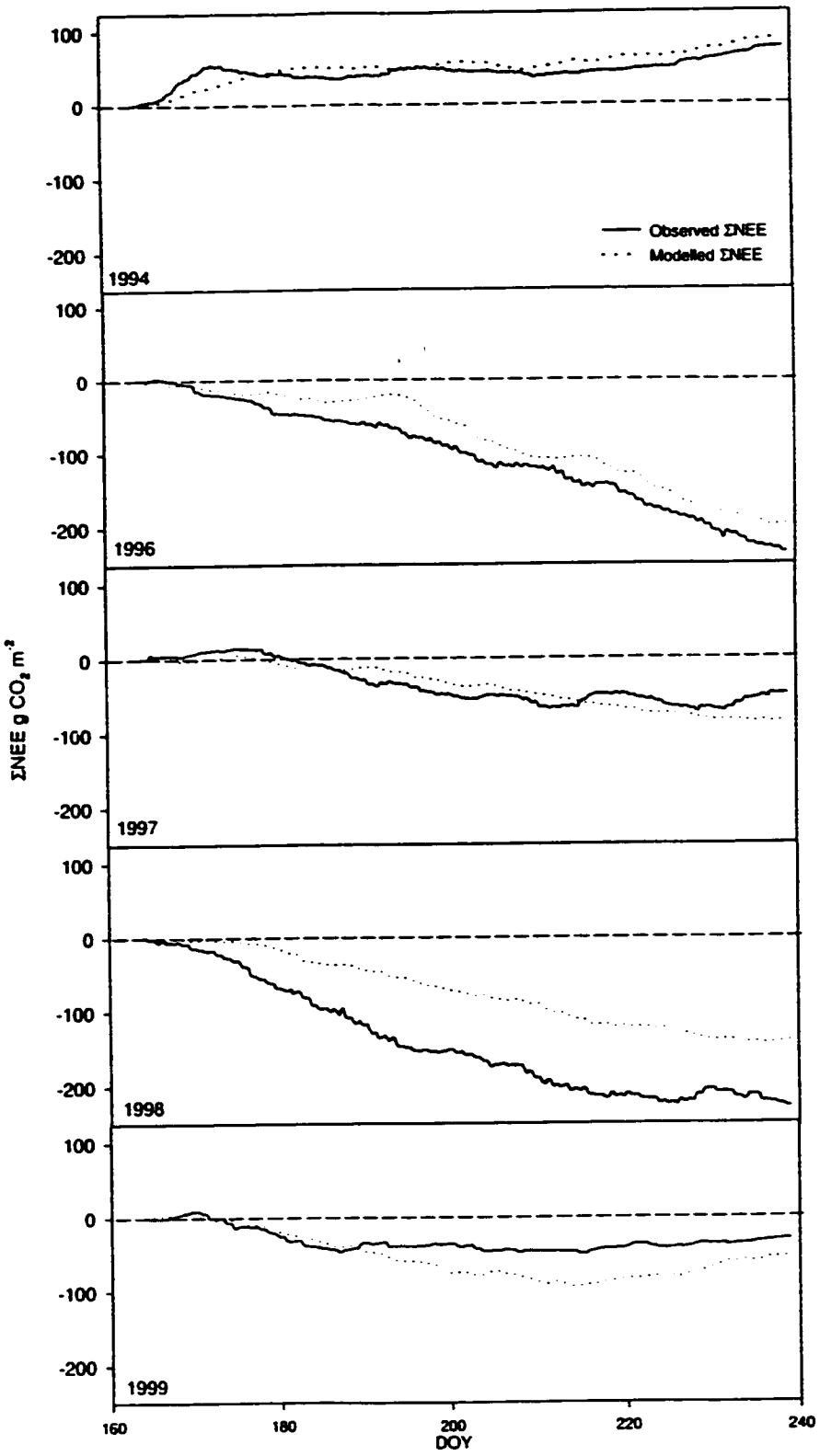

Figure 5.10: Comparison of modelled and observed cumulative net ecosystem CO_2 exchange for five growing seasons at the Churchill fen. Observed data are tower-flux measurements provided by Schreader et al., 1998 and Griffis et al., 2000a.

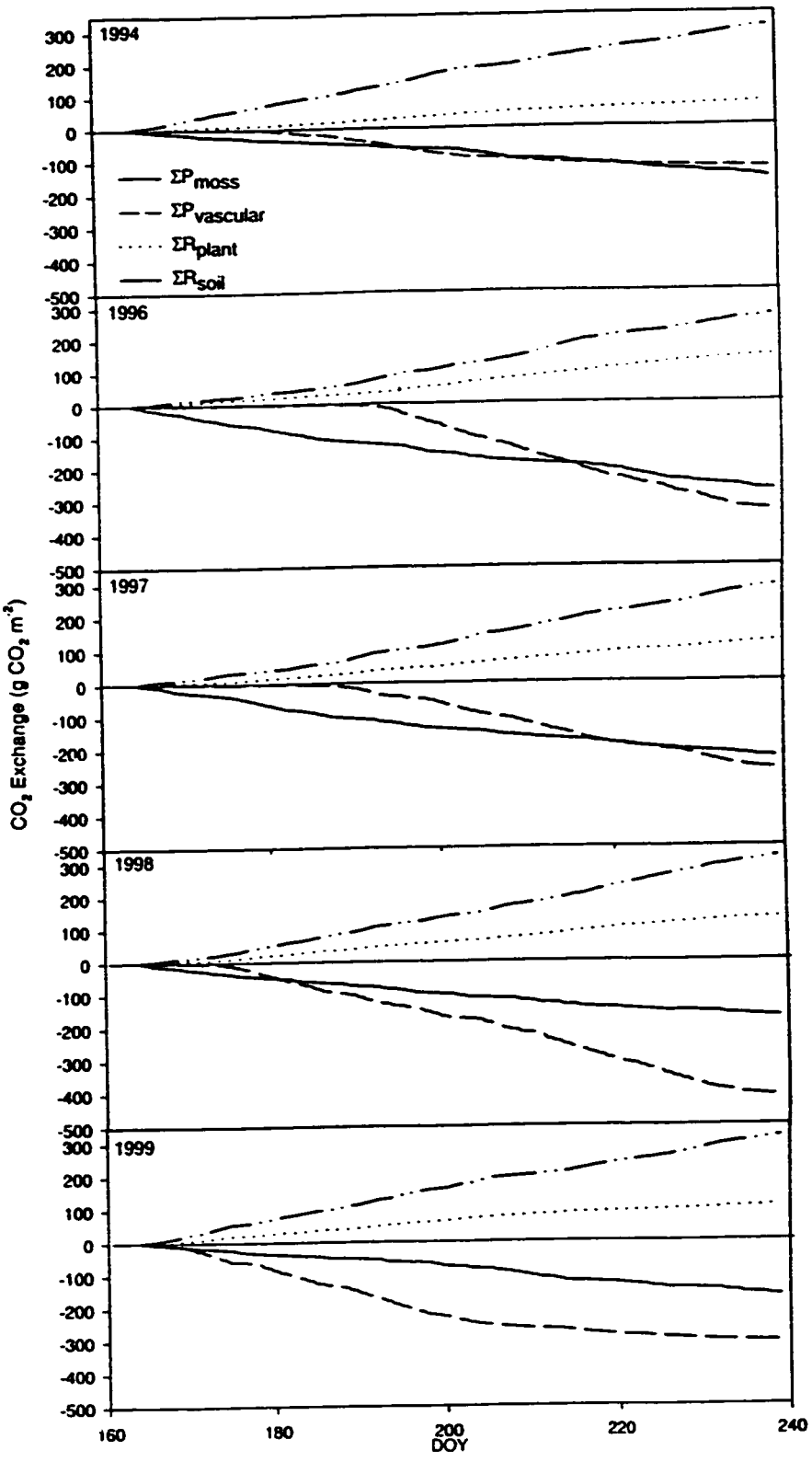

Figure 5.11: Modeled cumulative CO_2 fluxes of moss and vascular gross photosynthesis, plant respiration, and soil respiration.

In 1996 the model accurately estimates a strong sink year (Figure 5.10b). Acquisition of CO_2 is rapid during the early part of the growing season attributed to the wet spring conditions that promoted a large photosynthetic flux from the mosses (Figure 5.11b). However, the model does not maintain the rate of CO_2 acquisition and begins to underestimate the cumulative gain in early July (DOY 180 and DOY 200). The underestimate is likely caused by the large reduction in moss gross photosynthesis due to the drier surface conditions and, as well, a low vascular net photosynthetic flux. Model behaviour improves once the vascular leaf area has reached its maximum of 0.6 at mid season. By the end of the growing season the modeled cumulative CO_2 exchange underestimated the actual by 37 g CO_2 m^{-2}. Although this is a significant underestimate it is within the error of the flux measurements.

There is good agreement between the modeled and observed cumulative CO_2 flux in 1997 (Figure 5.10c). During the early growing season the model under predicts the loss of CO_2 to the atmosphere and switches from a net source to a net sink earlier in the season. Model behaviour is similar to the observed data during the mid growing period; however, there is some departure between the simulated and observed data near the end of the growing season. Figure 5.11c supports that the divergence is due to strong vascular photosynthetic activity late in the growing season. Modelling the shoulder season components appear to be problematic due to the current description of phenology. The simulation overestimated the net gain by 37 g CO_2 m^{-2}, which is within the maximum probable error of the measured cumulative flux.

The model simulation for the 1998 growing season performed poorly during the early growth period which lead to a gross underestimate of the observed cumulative NEE (Figure 5.10d). It is possible that the vascular photosynthetic contribution is underestimated in the model (Figure 5.11d). During independent tests, model performance improved when a larger starting vascular leaf area was prescribed. However, at the present time we cannot justify this large LAI value, as early growing season leaf area data are not available. The model underestimated the observed cumulative NEE flux by 88 g CO_2 m^{-2} and exceeded the error in the measurements.

The simulated cumulative NEE for 1999 shows realistic behaviour during the early growing season but diverges later in the season (Figure 5.10e). This suggest that the fitness parameter describing the maximum LAI is incorrect or that senescence was initiated earlier due to the dry surface conditions (Figure 5.11e). The model overestimated the net acquisition by 23 g CO_2 m^{-2} and was with the error of measurement.

5.4.4. Diurnal Patterns of CO_2 Exchange

On a half-hour time step the model failed to reproduce the mean diurnal pattern of net ecosystem CO_2 exchange for each of the seasons (Figure 5.12). The best comparison is observed for the 1997 season (Figure 5.12c). The half-hour variability in NEE is generally noisy in the measured signal and the model fails to reproduce this variability. Large bias is apparent for the nighttime respiration and for the early morning maximum peak in net CO_2 acquisition.

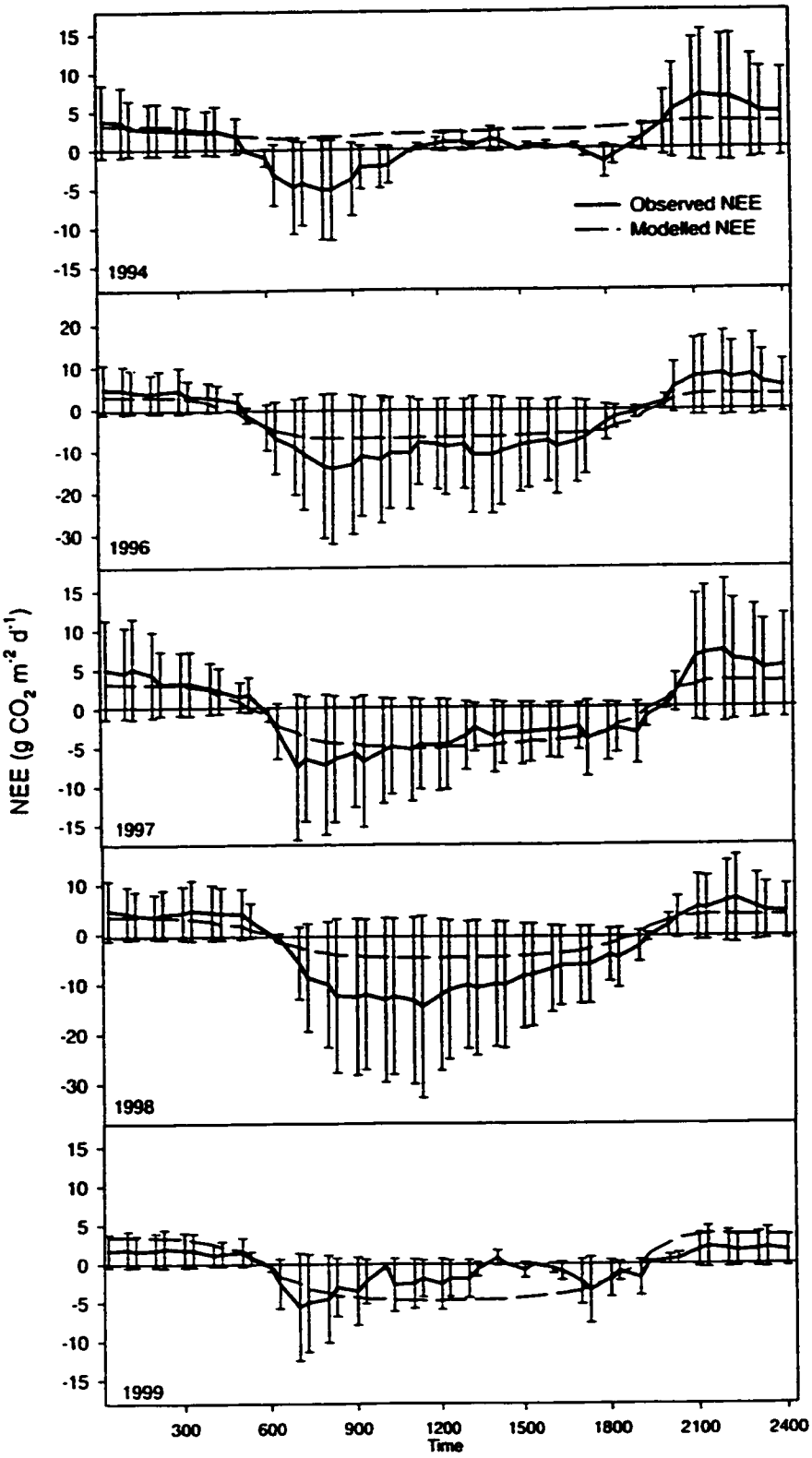

Figure 5.12: Comparison of modelled and observed mean diurnal patterns of net ecosystem CO_2 exchange. Observed data are tower-flux measurements provided by Schreader et al., 1998 and Griffis et al., 2000a. Error bars represent the maximum probable error in the measured data.

The diurnal variation in moss moisture content may be causing some of the bias in NEE. The GEP values do not decrease as expected through the midday period. Because mosses are prone to surface drying we would expect a significant reduction in GEP through the day. Furthermore, Blanken and Rouse (1995) and Schreader et al., (1998) have shown that Carex aquatilis exhibit evidence of water conservation. Modelled diurnal patterns of stomatal conductance do not show similar patterns to the observed NEE. It is possible, therefore, that the midday reduction in carbon acquisition is a result of photoinhibition of both the moss and vascular species. Murray et al., (1993) have shown that *Sphagnum* moss production decreases at high PAR levels (>800 μmol m^{-2} s^{-1}), which may be related to low tissue nitrogen.

5.4.5. Time Series of Half-hour Fluxes

Observed and simulated half-hour fluxes of NEE for 21 days (DOY 170 to DOY 190) from the 1996 and 1997 seasons are presented in Figure 5.13. The time period includes the beginning of leaf-out to approximately full canopy at the fen. In 1996, the model simulation between DOY 177 and 179 is particularly problematic. This period coincides with warm and sunny conditions, which ended an 8- day period of relatively cold and wet conditions in Churchill. Since this period occurs early in the growing season, the inability of the model to capture the abrupt change in NEE may be attributed to underestimation of moss GEP under these potentially optimal conditions. In 1997, the model simulation is especially poor between DOY 187 and 189. This period was characterized by relatively warm daytime temperatures (>25°C), with a single precipitation event 7 days prior. The simulation indicates an overestimate of nighttime

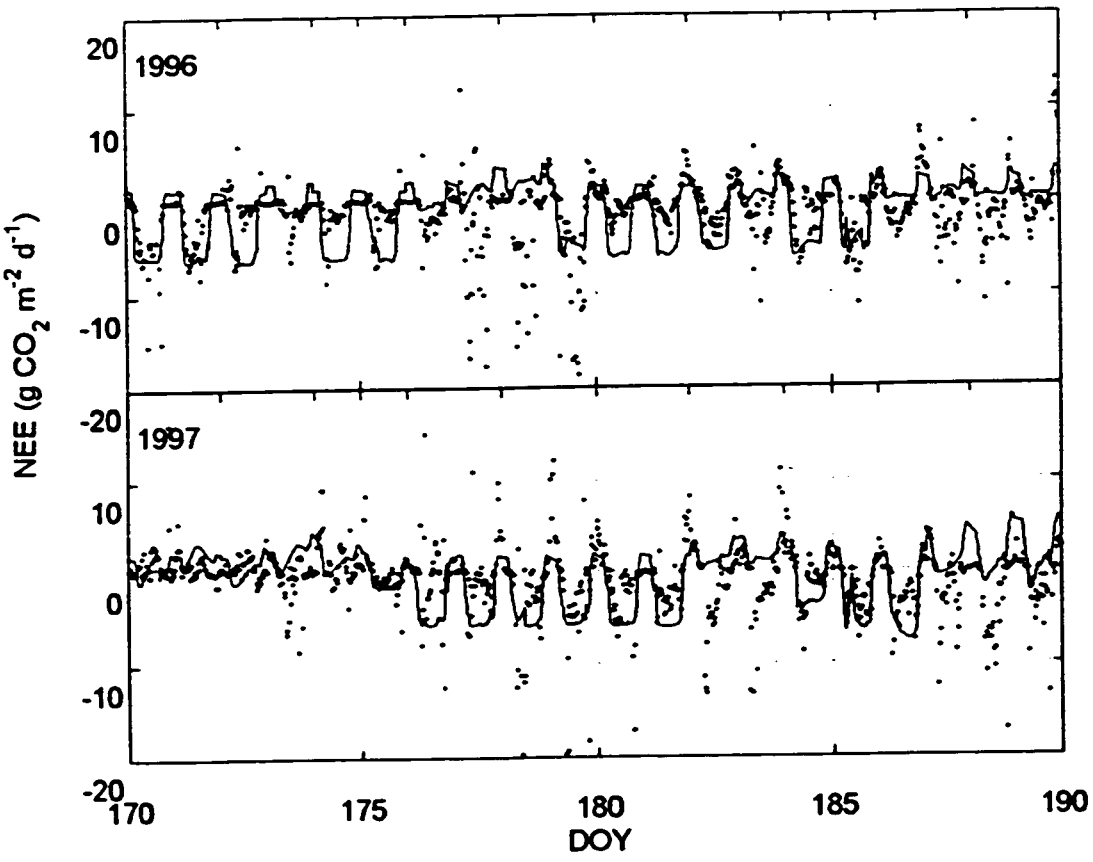

Figure 5.13: Comparison of half-hour modelled and measured net ecosystem CO_2 exchange for a 21 day period during the 1996 and 1997 growing seasons. Boxes represent half-hour tower-flux measurements (Griffis et al., 2000a).

ecosystem respiration and underestimate of daytime NEE in response to drying surface conditions. Although tower flux measurements are prone to errors at night (Schreader et al., 1998), the disparity between daytime fluxes illustrates the strong sensitivity of the model to surface moisture conditions.

5.4.6. Sensitivity Analysis

In this section we examine the sensitivity of NEE to changes in air temperature, precipitation, leaf area index, and explore the potential response of the Churchill fen to transient and equilibrium changes in climate.

5.4.6.1. Air Temperature

Changes in air temperature are expected to influence NEE by affecting soil respiration, plant respiration, and photosynthesis. Many of the algorithms used in our model are temperature dependent. We expect, therefore, that modeled GEP, ER, and NEE will show high sensitivity to temperature change in the system. In our analysis we changed the observed temperature of each year by ± 4 °C in order to assess the sensitivity of NEE, GEP and ER to temperature change (Table 5.2).

In general gross photosynthesis was enhanced between 15 and 20% for warmer air temperatures and decreased between 24 and 26% for cooler air temperatures. The response is largely attributed to the higher conductance values under warmer temperatures. It has been argued that arctic plants photosynthesize below their optimum temperature over the majority of the growing season (Tieszen, 1973; Semikhatova *et al.*, 1992). The largest increase in gross photosynthesis was observed in 1996, which was the coldest season. Increased temperature generally results in higher stomatal conductance

and larger photosynthetic rates. The smallest increase in gross photosynthesis was observed in 1997, which experienced the highest daytime temperatures. The decrease in gross photosynthesis resulting from colder air temperatures showed strong similarity between all seasons.

Ecosystem respiration showed a similar response to the ± 4 °C temperature change in all years. Efflux of CO_2 under the warmer scenario increased by about 20% and decreased by a similar amount for the colder scenario in each year.

The effect of temperature change on NEE is due to the differences caused in GEP and ER. Increasing temperature caused NEE to vary between 3 and 25%. In 1994 the loss of CO_2 from the wetland was increased by 25%. Although GEP was enhanced by 17% the increase in ER resulted in an increased net loss of carbon from the wetland. Lower temperatures caused NEE to change between 1 and 61%. Lower temperatures caused substantial reductions in gross photosynthesis. This was due to a higher frequency of air temperatures below the temperature optimum of photosynthesis. Photosynthesis decreased more than the ecosystem respiration in all seasons causing an increase in the observed carbon loss in 1994 and reducing the carbon acquisition in the other years.

5.4.6.2. Precipitation

We explored the sensitivity of CO_2 exchange to changes in precipitation by varying the magnitude of the observed precipitation events in each year by ± 30%. Climate simulations from GCMs indicate a 20% increase in precipitation for $2xCO_2$ scenarios in the central arctic (Maxwell, 1992). Our larger value of 30% is used to accentuate the NEE response in the model simulations. We also examined the effects of

Table 5.2: Sensitivity of GEP, ER, and NEE to changes in air temperature

Year	GEP			ER			NEE		
	+4°C	P	-4°C	+4°C	P	-4°C	+4°C	P	-4°C
1994									
Σ	341	291	218	448	377	306	↑108	↑86	↑87
Δ	+17%		-25%	+19%		-19%	+25%		+1%
1996									
Σ	729	607	450	496	410	326	↓234	↓198	↓124
Δ	+20%		-26%	+21%		-21%	+18%		-37%
1997									
Σ	570	494	371	486	408	328	↓84	↓86	↓44
Δ	+15%		-25%	+19%		-20%	-3%		-49%
1998									
Σ	687	587	443	531	446	359	↓156	↓141	↓84
Δ	+17%		-25%	+19%		-20%	+11%		-40%
1999									
Σ	551	474	362	501	420	341	↓51	↓53	↓21
Δ	+16%		-24%	+19%		-19%	-5%		-61%

P, Present Condition
GEP, gross ecosystem production
ER, ecosystem respiration
NEE, net ecosystem exchange
Σ, cumulative seasonal flux (g CO_2 m^{-2})
Δ, percentage change in flux
↑, net exchange of CO_2 to the atmosphere
↓, net exchange of CO_2 to the wetland

precipitation distribution and frequency of rain events on CO_2 exchange. To accomplish this we distributed the total observed seasonal precipitation in each year to either the early summer season (ES: DOY 164 to DOY 201) or the late summer season (LS: DOY 202 to DOY 238) while employing an artificial rainfall frequency of 2 days to examine the impact of a wet spring/ dry summer versus a dry spring/wet summer on NEE.

5.4.6.2.1. Precipitation Magnitude

Increasing the magnitude of precipitation events enhanced GEP in all years between 1 and 4% (Table 5.3). ER decreased between 0 and 2% despite the greater productivity of the plants. This indicates that soil respiration was reduced relative to plant respiration. Changes in NEE varied between 6 and 24% for all years.

Reducing the magnitude of precipitation events by 30% caused GEP to decrease between 2 and 20%. The largest change occurred in 1998 due to the onset of an early senescence. The smallest change was observed for 1996, which is attributed to the wet surface conditions that persisted through that season. ER increased between 0.3 and 4%. Changes in NEE were large and ranged from 10% in 1996 to 71% in 1998.

5.4.6.2.2.Precipitation Distribution and Frequency

Changing the distribution and frequency of the observed rainfall in each year caused substantial differences in GEP and NEE. The model is highly sensitive to the timing of rainfall events. Given frequent early summer precipitation events (wet

spring/dry late summer), GEP increased by 32% in 1994 and decreased by 4% in 1996 (Table 5.4). ER increased in all years excluding 1998.

The wet late summer scenario caused a reduction in GEP for all years ranging between 4 and 30%. The largest decrease was observed in 1998 due to the onset of a premature senescence. The changes in ER are complex. In some cases, ER increases as a result of greater plant respiration while in other cases ER decreases due to higher soil water contents.

The influence of precipitation distribution and frequency on NEE is pronounced and depends on the initial conditions of the wetland. In 1994 the frequent early season rainfall delayed the senescence of the vascular canopy and caused the net loss of CO_2 from the system to be reduced by 85%. In 1996 the simulated wet spring reduced the net gain of carbon by 17%, which resulted from desiccation of the moss canopy occurring later in the season. In 1999 there was a 70% increase in net carbon acquisition due to more frequent wetting of the moss surface and, as well, the delayed senescence of the vascular canopy. This analysis indicates the high level of complexity in NEE and shows that it can largely manifest itself in GEP.

5.4.6.3. Leaf Area Index

The sensitivity of NEE to a ±10% change in LAI was high in all cases, varying from 11% in 1994 to 45% in 1999 (Table 5.5). This demonstrates the need for better estimates of LAI. GEP increased from 4% in 1994 to 6% in 1998 and 1999. ER increased 0.5 to 2% due to greater plant production. Reducing LAI caused similar changes in the opposite direction for all years.

Table 5.3: Sensitivity of GEP, ER, and NEE to change in precipitation magnitude

Year	GEP			ER			NEE		
	+30%	P	-30%	+30%	P	-30%	+30%	P	-30%
1994									
Σ	303	291	278	375	377	378	↑72	↑86	↑100
Δ	+4%		-5%	-0.5%		+0.3%	-12%		+16%
1996									
Σ	615	607	594	404	410	415	↓211	↓198	↓179
Δ	+1%		-2%	-2%		+1%	+6%		-10%
1997									
Σ	505	494	480	400	408	415	↓107	↓86	↓65
Δ	+2%		-3%	-2%		+2%	+24%		-24%
1998									
Σ	598	587	470	441	446	430	↓157	↓141	↓41
Δ	+2%		-20%	-1%		-4%	+11%		-71%
1999									
Σ	482	474	462	420	420	422	↓62	↓53	↓41
Δ	+2%		-3%	0		+ 0.5%	+15%		-23%

P, Present Condition
GEP, gross ecosystem production
ER, ecosystem respiration
NEE, net ecosystem exchange
Σ, cumulative seasonal flux (g CO_2 m^{-2})
Δ, percentage change in flux
↑, net exchange of CO_2 to the atmosphere
↓, net exchange of CO_2 to the wetland

Table 5.4: Sensitivity of GEP, ER, and NEE to change in precipitation distribution and frequency

Year	GEP			ER			NEE		
	ES	P	LS	ES	P	LS	ES	P	LS
1994 Σ	384	291	275	397	377	377	↑13	↑86	↑101
Δ	+32%		-6%	+5%		0%	-85%		+17%
1996 Σ	582	607	556	418	410	422	↓165	↓198	↓135
Δ	-4%		-8%	+2%		+3%	-17%		-32%
1997 Σ	494	494	466	413	408	418	↓80	↓86	↓49
Δ	0%		-7%	+1%		+3%	-7%		-43%
1998 Σ	610	587	414	442	446	410	↓167	↓141	↓4
Δ	+4%		-30%	-1%		-8%	+18%		-97%
1999 Σ	623	474	454	444	420	419	↓179	↓53	↓35
Δ	+31%		-4%	+5%		-0.2%	+70%		-34%

P, Present Condition
ES, wet early summer and dry late summer
LS, wet late summer and dry spring
GEP, gross ecosystem production
ER, ecosystem respiration
NEE, net ecosystem exchange
Σ, cumulative seasonal flux (g CO_2 m^{-2})
Δ, percentage change in flux
↑, net exchange of CO_2 to the atmosphere
↓, net exchange of CO_2 to the wetland

Table 5.5: Sensitivity of GEP, ER, and NEE to change in LAI

Year	GEP			ER			NEE		
	+10%	P	-10%	+10%	P	-10%	+10%	P	-10%
1994									
Σ	302	291	279	379	377	374	↑77	↑86	↑95
Δ	+4%		-4%	+0.5%		-0.8%	-11%		+11%
1996									
Σ	638	607	576	415	410	403	↓223	↓198	↓173
Δ	+5%		-5%	+1%		-1%	+13%		-13%
1997									
Σ	518	494	469	413	408	403	↓105	↓86	↓66
Δ	+5%		-5%	+1%		-1%	+22%		-23%
1998									
Σ	626	587	548	453	446	438	↓173	↓141	↓109
Δ	+6%		-7%	+2%		-2%	+23%		-23%
1999									
Σ	502	474	445	425	420	415	↓77	↓54	↓30
Δ	+6%		-6%	+1%		-1%	+45%		-44%

P, Present Condition
GEP, gross ecosystem production
ER, ecosystem respiration
NEE, net ecosystem exchange
Σ, cumulative seasonal flux (g CO_2 m^{-2})
Δ, percentage change in flux
↑, net exchange of CO_2 to the atmosphere
↓, net exchange of CO_2 to the wetland

5.4.6.4. Climate Change Scenario

Climate models forecast warming at high latitudes given a $2xCO_2$ scenario. There is great uncertainty surrounding the expected changes in precipitation both in magnitude and frequency. In these scenarios we assume a 4 °C warming with a ± 30% increase in precipitation of the observed rainfall from each season. The transient response considers conditions where no change in above ground biomass occurs. The equilibrium response case assumes that the vascular canopy has adjusted to a lower water table position, longer growing season, and increased nutrient turnover. Although our model does not account for nutrient changes explicitly we assume that LAI is enhanced under a $2xCO_2$ scenario due to greater nutrient availability (Griffis *et al.*, 2000b). The Equilibrium change assumes a 50% increase in LAI.

5.4.6.4.1. Transient $2xCO_2$ Response

The warm and wet scenario (WW) produced greater carbon sequestration in all years excluding the 1994 season. Increases ranged from 10% in 1999 to 25% in 1996 (Table 5.7). The large increase in 1996 is attributed to the increase in air temperature resulting in more frequent optimum conditions for photosynthesis. GEP increased by 21% and ER increased by 19%. Increases in GEP were larger than ER in all years excluding the 1999 season.

The warming and drying scenario (WD) accelerated the net loss of carbon at the fen in 1994. Increased ER exceeded the gains in GEP. During 1996, the fen gained carbon despite the drier conditions. This substantiates that cold temperatures limited GEP. However, 1997, 1998 and 1999 all experienced large reductions in net carbon

acquisition. This was due to large increases in ER relative to GEP. In 1998, the decreased moisture and higher temperatures caused an earlier senescence of the vascular canopy causing GEP to decrease by 4%.

5.4.6.4.2. Equilibrium $2xCO_2$ Response

In all cases the equilibrium response (EQ) showed substantial increases in carbon acquisition. In each of the sink years carbon acquisition increased between 43 and 240% (Table 5.8). GEP increased between 28 and 54%. Again, the largest increase in GEP was observed in the 1996 season owing to the warmer temperatures and more frequent optimum photosynthetic temperature. Increases in ER were substantial and ranged from 23 to 33%. The 1994 season remained a net source of CO_2 to the atmosphere. Despite having greater leaf area, the dry surface conditions caused ER to exceed GEP. This suggests that increased above ground biomass in response to drier conditions may not be sufficient to change these ecosystems from sources to sinks of atmospheric carbon under extremely dry conditions.

5.5. DISCUSSION

5.5.1 Model Performance

The NEE model presented here can predict, on a seasonal basis, the strong sink and source years and, therefore, can be used as a tool to help explain our observations and hypotheses surrounding the interannual variability of CO_2 exchange. The model performance is highly sensitive to our assumptions surrounding moss moisture content and its impact on photosynthesis, and as well, our description of phenology, fitness, and

Table 5.6: Transient and equilibrium response of GEP, ER, and NEE to climatic change scenarios

Year	GEP				ER				NEE			
	WW	P	WD	EQ	WW	P	WD	EQ	WW	P	WD	EQ
1994												
Σ	351	291	328	410	446	377	450	466	↑95	↑86	↑122	↑57
Δ	+21%		+13%	+41%	+18%		+19%	+24%	+11%		+ 42%	-34%
1996												
Σ	736	607	716	932	489	410	502	547	↓247	↓198	↓215	↓386
Δ	+21%		+18%	+54%	+19%		+22%	+33%	+25%		+9%	+95%
1997												
Σ	581	494	556	715	477	408	494	527	↓104	↓86	↓62	↓188
Δ	+18%		+13%	+45%	+17%		+21%	+29%	+17%		-28%	+119%
1998												
Σ	701	587	561	753	527	446	512	550	↓175	↓141	↓49	↓202
Δ	+16%		-4%	+28%	+18%		+15%	+23%	+19%		-65%	+43%
1999												
Σ	559	474	540	720	500	420	503	539	↓59	↓53	↓38	↓181
Δ	+15%		+14%	+52%	+19%		+20%	+28%	+10%		-28%	+240%

P, Present Condition
GEP, gross ecosystem production
ER, ecosystem respiration
NEE, net ecosystem exchange
Σ, cumulative seasonal flux (g CO_2 m^{-2})
Δ, percentage change in flux
WW , warm and wet scenario (+4 °C and +30% P)
WD , warm and dry scenario (+4 °C and –30% P)
EQ, equilibrium climate change (+4 °C and –30% P and +50% LAI)
↑, net exchange of CO_2 to the atmosphere
↓, net exchange of CO_2 to the wetland

plant growth. These factors will require further field study in order to improve these model algorithms.

5.5.2. Inter-annual Variability

The inter-annual variability in NEE at the Churchill fen results from phenological and hydroclimatic variations. In an environment with a relatively short growing season, the impact of daily weather and climate on phenology is pronounced. During 1993, fall and winter precipitation at Churchill failed to restore the summer water deficit (Rouse, 1998; Schreader *et al.*, 1998). Early snowmelt, coupled with high evaporation rates in the spring of 1994 magnified the water deficit. Low water table position and persistent dry summer conditions reduced the photosynthetic capacity of the wetland and the vascular species experienced premature dormancy (Figure 5.11a). The reduction in both bryophyte and vascular photosynthesis caused ER to dominate the CO_2 balance of the fen. Consequently, the fen experienced a net loss of +76 g CO_2 m^{-2} over the measurement period.

The 1998 growing season provides a marked contrast to the 1994 season. Heavy rains during the 1997 fall season recharged the soil moisture reservoir prior to freeze back. Relatively warm winter and spring temperatures due to the 1997/1998 El Niño phenomenon (Griffis *et al.*, 2000c) caused an early snowmelt and greater than normal spring precipitation. The wet and warm surface conditions during the pre-green and early green period caused large photosynthetic fluxes from the moss-covered surfaces and also allowed early leaf development in the vascular plants (Figure 5.11d). The early breaking of dormancy during favorable growing conditions appears to have helped the vascular

canopy withstand the drier summer conditions experienced later in the growing season (Griffis *et al.*, 2000a). Scott *et al.*, (1997) has also suggested that early spring hydroclimatic conditions are critical to the growth of trees at treeline in the vicinity of Churchill.

Strong sink years, however, are not always associated with early leaf development. In 1996, late snowmelt and cool spring conditions prevented early leaf development. Carbon acquisition in this particular year was large due to the high productivity of the mosses early in the season and from the vascular plants later in the season (Figure 5.11b).

Water table position and soil moisture content play a key role in controlling the dormancy and phenology of the fen vegetation. Dry surface conditions can cause mosses to lie dormant until rewetting, and low soil moisture content can trigger the dormancy of vascular plants as in 1994 and 1999. The idea of plant fitness or biologic vigor (the relation of phenology to hydroclimatic conditions) is a qualitative parameter used in our model to help explain the complex interaction between plant growth and mortality rates as determined by the early season hydroclimatic conditions during the time that dormancy is broken. There is currently a lack of understanding of these fitness relationships.

Our model of NEE can predict, on a seasonal basis, the strong sink and source years and, therefore, can be used as a tool to help explain our observations and hypotheses surrounding the inter-annual variability of CO_2 exchange.

5.5.3. Sensitivity of NEE

Model sensitivity analysis illustrates that the response of NEE to changes in the environmental variables is dependent on the initial conditions of the wetland. The strength of the NEE response to individual variables varies considerably between the years. In general, warmer temperatures act to increase GEP more than ER. This evidence supports the hypothesis of Griffis *et al.*, (2000a) and the explanation of inter-annual variability in NEE. The effect of increased temperature on GEP is more pronounced in cooler and wetter years such as the 1996 season. These results support that arctic ecosystems photosynthesize below their temperature optimum over the majority of the growing season.

Precipitation distribution and frequency of precipitation events are important factors controlling the inter-annual variability in NEE. In seasons such as 1994, 1997 and 1999, mid to late season precipitation events failed to increase the CO_2 acquisition of the fen (Griffis *et al.* 2000a). However, 1998 illustrates how wet spring conditions can lead to greater CO_2 acquisition through much of the growing period even when drier conditions persist. The sensitivity of the modeled NEE agrees with these field observations. In all simulations, excluding the 1996 season, increased frequency of precipitation events early in the growing season lead to greater carbon acquisition over the course of the growing season.

5.5.4. Source-Sink Reversal

Based on field and model evidence it is now possible to examine how the fen can switch from a carbon sink to a carbon source. Given the initial conditions for the 1994

season and its strong CO_2 source characteristic, we explored how the precipitation regime from the 1996 season would affect the outcome of the 1994 carbon budget in an attempt to understand how the season could be switched from a source to a sink. We increased the observed precipitation total to the 1996 level (145 mm) with a similar seasonal frequency distribution of 2.3 days. The new precipitation regime caused the 1994 season to become a net sink of -66 g CO_2 m^{-2}. Furthermore, starting the 1994 season with a positive water deficit as in the 1996 season (0.058 m) and retaining the observed precipitation from 1994 we simulated a net acquisition of -26 g CO_2 m^{-2}. Finally, if the model is run for the 1994 season using both the starting water table position and precipitation for 1996 we simulate a net acquisition of -106 g CO2 m^{-2}. Using a similar analysis, we reduced the precipitation in 1996 to the observed 1994 levels (72 mm) with a frequency of 3 days. The effect was a reduction in net acquisition by about 40 g CO_2 m^{-2}. The fen, however, remained a large sink of -160 g CO_2 m^{-2}. These simulations further illustrate the importance of the early growing season conditions and the interrelationship between phenology and the hydroclimatic conditions.

5.5.5. Climatic Change and Net Ecosystem CO_2 Exchange

The historical rate of carbon acquisition by northern peatlands has been estimated at about -29 g C m^{-2} y^{-1} (Gorham, 1991). At the Churchill fen, carbon gain has been approximately -7 g C m^{-2} y^{-1}over its 2200 year history. However, the contemporary annual CO_2 balance of the Churchill fen is potentially a net loss based on the five growing seasons of data and the estimated non-growing season respiration losses reported in Griffis *et al.*, (2000a). The recent trend suggests that carbon loss is proceeding at a rate

of nearly 3x's the historical gain. It would appear, therefore, that hydroclimatic conditions have changed resulting in reduced carbon acquisition and frequent net loss at the fen. This hypothesis assumes that vegetation has not changed significantly and that inter-annual differences in phenology and plant fitness balance over longer time scales. Preliminary macrofossil analyses (Coristine, 1998) support that the fen has been composed of mosses and sedges throughout its history. This suggests that hydroclimatic conditions may be the causal mechanism of the contemporary change from net sink to net source.

Modeled net ecosystem CO_2 exchange response to climatic change scenarios indicate that warmer and wetter conditions would promote greater carbon acquisition at this fen site. Given that the local area is rising due to isostatic rebound (0.01 m y^{-1}), improved drainage could be impacting the surface water budget, thereby, influencing the long-term CO_2 balance. The contemporary trend of reduced carbon gain and perhaps switch to carbon loss suggests a progression toward drier conditions than in the past. Reduction in both summer and winter precipitation may be important for the recent trend in CO_2 exchange. Payette and Morneau (1993) and Gajewski *et al.*, (1993) using palaeo-climate reconstructions from the Eastern Arctic argue that climate in the region was warmer and more humid during the late Holocene with cooling and increased occurrence of fire during the last millennium. It may be that the Hudson Bay lowland peat complex stored the majority of its carbon during its early developmental phases.

Very little is known regarding climate change and its impact on nutrient cycling and the response of vegetation to long-term changes in soil moisture availability and

nutrients. There is some evidence that warmer conditions will promote nutrient turnover and nitrogen supply in arctic environments (Shaver *et al.*, 1998; Shaver *et al.*, 1986). Our equilibrium climate change scenario assumes that vascular vegetation will benefit from such conditions and increase its above ground biomass. Increasing the specific leaf area ratio (ratio of leaf area to plant mass) should increase gross ecosystem production of the fen. However, it is not clear how soil respiration rates will affect the NEE. Assuming a conservative response in soil respiration our model results support that, in most cases, increased above ground biomass will increase carbon sequestration at the this fen. Fens may, therefore, act to maintain their carbon sink potential in the long term. However, under extremely dry spring conditions as in 1994 it would appear that increased above ground biomass would be insufficient to offset the large soil carbon losses.

5.6. CONCLUSIONS

Model simulations and landscape-scale measurements of NEE substantiate the importance of spring hydroclimatic conditions on growing season Net ecosystem CO_2 exchange. Warm surface temperatures combined with wet soil conditions in the early growing season increase above ground biomass and carbon acquisition throughout the summer season. Sensitivity analysis supports that warmer and wetter conditions are optimal for carbon acquisition at this northern wetland. If climatic warming is characterized by greater winter and summer precipitation, northern wetlands should, therefore, become larger sinks for atmospheric CO_2.

5.7. Appendix A: Model Parameters and Initial Conditions

A1. Model variables and parameters

Variable	Parameter	Value	Units
QeP			$W\ m^{-2}$
	a_1	0.59	-
	a_2	1.08	-
Rs			
	b_1	0.80	-
	b_2	0.50	-
Wa			-
	wa_{max}	1.0	-
	c_1	1.0	-
	c_2	0.01	-
	c_3	0.07	-
ds			m
SY		0.36 to 0.06	-
WT			m
θs			$m^3\ m^{-3}$
	d_1	0.60	-
	d_2	0.28	-
	d_3	4.4	-
LAI			$m^2\ m^{-2}$
	G_1	0.002	$m^2\ g^{-1}\ C$
	LAI_{max}	0.60	$m^2\ m^{-2}$
AmQ			-
Pm			$g\ CO_2\ m^{-2}\ d^{-1}$
	Pm_{max}	13.0	$g\ CO_2\ m^{-2}\ d^{-1}$
	ϕ_m	0.044	$g\ CO_2\ m^{-2}\ d^{-2}\ \mu mol^{-1}\ PAR$
	k_m	0.9	-
Qmθ			-
	h_1	0.003	-
	h_2	0.025	-
	h_3	6.9	-
AvQ			-
Pv			$g\ CO_2\ m^{-2}\ d^{-1}$
	Pv_{max}	39.0	$g\ CO_2\ m^{-2}\ d^{-1}$
	ϕ_v	0.069	$g\ CO_2\ m^{-2}\ d^{-2}\ \mu mol^{-1}\ PAR$
	k_v	0.85	-
gs			-
	gs_{max}	1312.4	$mmol\ s^{-1}\ m^{-2}$
gs(Ts)			-
	m_1	-2399.2	-
	m_2	335.2	-
	m_3	-8.1	-
gs(vpd)			-
	n_1	1312.4	-
	n_2	-237.6	-
gs(Ψs)			-
	p_1	1285.2	-
	p_2	265.7	-
R_a			$g\ CO_2\ m^{-2}\ d^{-1}$
	R_{amax}	9.1	$g\ CO_2\ m^{-2}\ d^{-1}$
R_a(Ts)			-
	q_1	1.5	-
	q_2	0.25	-
R_a(θs)			-
	v_1	26.5	-
	v_2	-25.0	-
GEP			$g\ CO_2\ m^{-2}\ d^{-1}$
ER			$g\ CO_2\ m^{-2}\ d^{-1}$
NEE			$g\ CO_2\ m^{-2}\ d^{-1}$

A2. Initial conditions for each model simulation

Year	Date of Snowmelt	Initial Water Table Height	Fitness Condition
1994	May 10	-0.01 m	condition 2
1996	June 1	0.058 m	condition 1
1997	June 5	0.079 m	condition 1
1998	May 12	0.002 m	condition 3
1999	April 22	-0.005 m	condition 3

CHAPTER SIX

SUMMARY AND CONCLUSIONS

6.1. PURPOSE OF STUDY

This thesis investigated net ecosystem CO_2 exchange (NEE) at a subarctic fen located in the Hudson Bay lowland near Churchill, Manitoba, Canada. The study was conducted to improve the understanding of carbon cycling and biosphere feedback, and their relation to climatic change and the global carbon budget.

6.2. HISTORICAL CARBON BALANCE

The Hudson Bay lowland represents the second largest contiguous wetland in the world and has accumulated significant amounts of atmospheric carbon since the retreat of glacial ice and the isostatic emergence of the tundra wetlands from Hudson Bay. Examination of peat cores from the Churchill fen indicate that carbon has accumulated at an average rate of -7 g C m^{-2} y^{-1} over its 2200 year history. This rate of accumulation is directly related to the hydroclimatological and ecological conditions that have persisted over this period. On shorter time scales (days to years) the variability in NEE is related to changes in radiation, energy, water balance, and phenology.

6.3. CONTEMPORARY CARBON BALANCE

Micrometeorological measurements of landscape-scale NEE made during five growing seasons captured a wide range of climatological conditions and indicate that

there is a large amount of inter-annual and seasonal variation in NEE. These contemporary measurements represent extreme fluctuations relative to the historical average. It is evident from the five years of data that the fen can vary from a strong source to a moderate sink of atmospheric carbon dioxide.

The cause of inter-annual variation in NEE is extremely complex, driven by change in the photosynthetic rates of mosses and sedges and, by variation in heterotrophic and autotrophic respiration. Analysis of landscape and community-scale fluxes of carbon dioxide, combined with model simulations, provides strong evidence that gross ecosystem production (GEP) is more variable than ecosystem respiration (ER) on a diurnal, seasonal, and inter-annual time scale.

Growing season GEP is dependent on the timing of snowmelt, water table position, and phenology. These factors, in this subarctic environment, are intimately related and are especially sensitive to the length of growing season, spring and summer temperatures, and the seasonal water balance. Years with early snowmelt and strong water table recession experience lower rates of GEP and higher rates of soil respiration. Both 1994 and 1999 experienced early snowmelt, warm temperatures, and large water deficits. These conditions caused a marked reduction in moss and vascular gross photosynthesis and caused premature dormancy in the vascular plants. The large reduction in GEP relative to ER caused a growing season carbon loss of +76 g CO_2 m^{-2} in 1994 and a weak net sink of -30 g CO_2 m^{-2} in 1999.

During the 1996 season a normal snowmelt period combined with frequent precipitation events during the summer resulted in significant carbon acquisition. Large

photosynthetic rates were achieved early in the season due to the wet moss surface. GEP increased substantially after the emergence of the vascular species. The wet surface conditions sustained substantial carbon acquisition through to the end of the measurement period in late August. There was no evidence of a relaxation in carbon acquisition at the end of the measurement period and I hypothesize that dormancy was not initiated until the surface experienced freezing temperatures during mid October.

The importance of phenology is clearly illustrated from the comparison between the 1997 and 1998 growing seasons. Each of these years experienced similar temperature and precipitation over the measurement period. The difference in NEE between the years, however, was large. In 1997 and 1998, growing season carbon acquisition was -49 g CO_2 m^{-2} and -230 g CO_2 m^{-2} respectively. The disparity between these years is attributed to differences in the early spring hydroclimatic conditions resulting from unique patterns of large-scale atmospheric circulation. The difference in atmospheric circulation was caused by the 1997/1998 El Niño phenomenon.

The lack of NEE measurements during the early spring, fall, and winter seasons prevents a direct comparison with the historical rate of carbon exchange. Assuming a mean ER of 0.5 g CO_2 m^{-2} d^{-1} over the non-growing season (~240 days) suggests that the Churchill fen has been losing carbon at nearly three times the historical accumulation rate over the five-year measurement period. This estimate does not include the carbon losses resulting from methane exchange or the transport of DIC and DOC due to wetland runoff. Contemporary NEE flux measurements, therefore, indicate that the fen has changed from a historical net sink to a net source of atmospheric carbon. Nearly all studies examining

NEE in northern wetlands agree that these ecosystems are now contributors to the atmospheric greenhouse effect. Furthermore, if the large seasonal and inter-annual variability in NEE exists in other ecosystems then the so-called "missing carbon sink" may be partly explained by the low temporal resolution in terrestrial carbon flux measurements.

6.4. FUTURE CARBON BALANCE

The recent decline and perhaps switch from carbon sink to source may only represent a transient change in the long-term carbon budget of the fen. Examination of community-scale NEE, GEP, and ER show that small hummocks (sedge-moss communities) account for the majority of carbon exchange at the fen. Moss dominated hollows and lichen-moss covered large hummocks exhibit small fluxes of carbon dioxide. The effective scaling factor (relating plant community spatial distribution to carbon exchange) indicates that sedge-moss communities account for over 70% of NEE at this fen. The spatial pattern of NEE and its covariance with plant community type and mean water table position support that long-term changes in hydroclimatic variables will cause significant changes in carbon cycling at the fen. Lower water table position resulting from increased climatic warming will cause changes in plant community composition and, as well, spatial pattern. Despite the drier surface conditions these changes may lead to greater carbon acquisition due to higher GEP. These systems, therefore, have the potential to display homeostatic adjustment by changing plant community distribution. Areal weighted flux measurements and model simulations assuming increased spatial

distribution of sedge–moss communities indicate greater carbon acquisition in a warmer and drier climate.

Model simulations indicate that climatic change will have a significant impact on NEE at the Churchill fen. Warm and wet conditions will undoubtedly increase carbon acquisition and provide a negative feedback to the greenhouse effect. Warm and dry conditions will act to increase carbon transfer to the atmosphere providing a positive feedback to the greenhouse effect. However, given equilibrium conditions, increased above ground biomass due to changes in spatial organization of plant communities or increased above ground biomass may offset soil respiration losses and increase carbon acquisition over the long-term.

6.5. SIGNIFICANT FINDINGS

This thesis has made significant contributions to the understanding of the global carbon budget and provides considerable insight into the response of carbon cycling in northern wetlands to climatic change. Significant contributions of this research indicate the following:

1. NEE exhibits extreme temporal variability. The Churchill fen can range from a sink to source of carbon diurnally, seasonally, and inter-annually;
2. GEP is the primary source of the inter-annual variation in NEE.
3. Phenology is intimately related to the hydroclimatological conditions;
4. Large scale atmospheric circulation can be linked to the inter-annual variability in GEP;

5. Northern wetlands are currently contributing to the greenhouse effect through a net loss of carbon dioxide to the atmosphere;
6. These ecosystems have the potential for homeostatic adjustment. Their self-regulating nature may favour greater carbon acquisition given future climatic warming.

6.6. FUTURE RESEARCH

Future research endeavors must extend micrometeorological measurements of NEE beyond the growing season. It is imperative to measure the amount of carbon losses occurring during the non-growing season to better estimate the changes in local and global carbon budgets. As well, annual measurements will be beneficial in assessing the impact of winter and spring hydroclimatic conditions on growing season NEE. Such measurements will allow new insights into the factors affecting phenology and their impact on GEP. Phenology is a critical factor affecting the NEE of northern wetlands. It represents an important biophysical feedback in the climate system as it links the energy, water, and carbon cycle at the earth's surface. Future research endeavors need to describe the relation between inter-annual climatic variability and phenological behaviour.

GLOSSARY OF TERMS

Acclimation, morphological and physiological adjustment by individual plants to compensate for the decline in performance following exposure to unfavourable levels of one or more environmental factor

Anticyclone, an area of surface high pressure associated with stable sinking air-extending 1000s of km in dimension. Winds blow clockwise (northern hemisphere) around the center of high pressure

Arctic, characterized by low mean annual temperature (below -10 °C), continuous permafrost and tundra

Atmospheric source, loss of carbon from ecosystem and net transfer to the atmosphere

Autotrophic respiration, carbon respired by plants; includes photorespiration and dark respiration

Biometeorology, the study of heat and mass transfer in the biosphere, ranging from the leaf to synoptic scale

Bryophyte, non-vascular vegetation lacking true roots and leaves, includes mosses, liverworts, and hornworts

Calorimetric heat flux, ground heat flux calculated from the change in temperature of the soil environment occurring over a given time interval

Community scale, subunits of the larger ecosystem scale showing statistical similarity and correlation between plant species composition and surface environmental conditions having dimensions up to a meter

Cyclone, an area of low pressure around which the winds blow counterclockwise (Northern Hemisphere)

Dormancy, state of seeds, buds, rhizomes, that fail to grow when exposed to a favourable environment

Ecosystem respiration, sum of plant and heterotrophic respiration in an ecosystem

Ecosystem sink, net transfer from the atmosphere to the ecosystem

Efflux, net transfer a property from an ecosystem to the atmosphere

El Niño, an extensive oceanic warming that begins along the coast of Peru and Ecuador

Equilibrium scenario, climate change scenario assuming stable conditions and adjustment in ecosystem response

Feedback mechanism, a process whereby an initial perturbation will tend to amplify (positive feedback) or dampen (negative feedback) the initial change

Fen, a major type of wetland that receives a significant input of water and dissolved solids from a mineral source, such as runoff from mineral soil or groundwater discharge

Fetch, distance of airflow to an object, measured in the upwind direction

Fitness, the transfer of genetic information from one generation to the next

Germination, process during which a seed absorbs water, followed by the emergence of the radicle through the seed coat

Greenhouse effect, warming of the troposphere due to the trapping of infrared radiation by greenhouse gases (H_2O, CO_2, CH_4, N_2O, O_3, CFCs)

Gross ecosystem production (GEP), total amount of carbon fixed by an ecosystem per unit ground area

Gross photosynthesis, total amount of carbon fixed by photosynthesis per unit ground area

Heterotrophic respiration, respiration by non-autotrophic organisms, mainly microorganisms and animals

Homeostasis, tendency to maintain constant internal conditions in the face of a varying external environment

Isostatic rebound, decompression of the earth's crust following the retreat of glacial ice

Jet stream, relatively strong winds concentrated within a narrow band in the atmosphere; located at a height of approximately 250 mb

Kyoto Protocol, a treaty signed by industrialized nations during the 1997 Kyoto summit meeting to reduce greenhouse gas emissions

Landscape scale, ecosystem scale having dimensions of 10s to 1000s of square meters.

Leaf area index (LAI), total leaf area per unit area of ground

Mesoscale, the scale of meteorological phenomenon that range in size from a few km to about 100 km; including local winds, thunderstorms, and tornadoes

Net ecosystem exchange (NEE), the difference between gross ecosystem production and ecosystem respiration

Net photosynthesis, the difference between gross photosynthesis and dark respiration

Peatland, landscapes containing a significant accumulation (>0.30 m depth) of organic material

Permafrost, any material at or below 0°C for two consecutive years

Petagram (Pg), 1 petagram is equivalent to 1×10^{15} grams

Phenology, time course of periodic events in an organism that are correlated with climate

Photoinhibition, decline in photosynthesis upon exposure to high irradiance, caused by adjustment in the photosynthetic apparatus

Photorespiration, light respiration; production of CO_2 due to the oxygenation reaction catalyzed by Rubsico

Photosynthesis, process in which light energy is used to reduce CO_2 to organic compounds

Photosynthetically active radiation (PAR), portion of the electromagnetic spectrum (0.4 to 0.7 micrometers) that drives photosynthesis

Power spectrum, the sum of individual frequencies decomposed from a time series

Q_{10}, change in rate of a reaction in response to a 10 °C change in temperature

Redox potential, the tendency of an environment to exchange electrons

Rubisco, ribulose-1,5-bisphosphate carboxylase/oxygenase; Clavin-cycle enzyme catalyzing the attachment of CO_2 to a CO_2-acceptor molecule

Senescence, programmed series of metabolic events that involve metabolic breakdown of cellular constituents and transport of the breakdown products out of the senescing organ
Soil water potential,

Specific yield, fraction of water released from a saturated soil sample due to gravitational drainage

Stomatal conductance, diffusive transfer of water and carbon dioxide through the leaf stomata

Subarctic, characterized by low mean annual temperature (at or below 0 °C), discontinuous permafrost, open subarctic and tundra vegetation

Synoptic Scale, the typical weather map scale that shows features such as high- and low-pressure areas and fronts over a distance spanning a region or continent

Transient scenario, climate change scenario assuming a lagged ecosystem response

Water table, saturated ground or surface water, where water is at atmospheric pressure

Wetland, landscapes where the water table is at or near the surface for extensive periods, promoting the development of hydrophytic vegetation and rich organic soils

REFERENCES

Atkin, O.K. Botman, B. and Lambers, H. (1996). The causes of inherently slow growth in alpine plants: an analysis based on the underlying carbon economies of alpine and lowland *Poa* species, *Functional Ecology*, **10**: 698-707.

Atmospheric Environment Service. (1994). "Monthly weather summaries at Churchill, 1943-1994." Environment Canada, Downsview, Ontario, Canada.

Barnola, J.M. Raynaud, D. Dorotkevitch, Y.S. and Lorius, C. (1987). Vostok ice core provides 160,000 year record of atmospheric CO_2, *Nature*, **329**: 83-90.

Bevington, P.R. (1969). Data reduction and error analysis for the physical sciences, McGraw-Hill Book Company, New York, pp.336.

Bhardwaj, A. Seasonal variability of net carbon dioxide exchange in a headwater bog, Kenora, Ontario. M.Sc. Thesis, McGill University, Montreal Canada.

Billings, W.D. (1987a). Carbon balance of Alaskan tundra and taiga ecosystems: Past present and future, *Quaternary Science Reviews*, **6**: 165-177.

Billings, W.D. (1987b). Constraints to plant growth, reproduction, and establishment in arctic environments, *Arctic and Alpine Research*, **19**: 357-365.

Billings, W.D. Luken J.O. Mortensen, D.A. Peterson, K.M. (1982). Arctic tundra: a source or sink for atmospheric carbon dioxide in a changing environment?, *Oecologia*, **53**: 7-11.

Billings, W.D. Luken, J.O. Mortensen, D.A. and Peterson, K.M. (1983). Increasing atmospheric carbon dioxide: Possible effects on arctic tundra, *Oecologia*, *58*: 286-289.

Black, T.A. Den Hartog, G. Neumann, H.H. Blanken, P.D. Yang, P.C. Russell, C. Nesic, Z. Lee, X. Chen, S.C. Staebler, R. and Novak, M.D. (1996). Annual cycles of water vapor and carbon dioxide fluxes in and above a boreal aspen forest, *Global Change Biology*, **2**: 219-229.

Blanken, P.D. and Rouse, W.R. (1995). Modelling evaporation from a high subarctic willow-birch forest, *International Journal of Climatology*, **15**: 97-106.

Blanken, P.D. and Rouse, W.R. (1996). Evidence of water conservation mechanisms in several subarctic wetland species, *Journal of Applied Ecology*, **33**: 842-850.

Bradley, R.S. and England, J. (1979). Synoptic climatology of the Canadian High Arctic. *Geografiska Annaler*, **61**: 187-201.

Brown, P. (1999). "Examining the effects of nitrogen fertilizer on the leaf area index of subarctic sedge tundra." unpublished manuscript, McMaster University, Hamilton Ontario, Canada.

Bubier, J.L. Crill, P.M. Moore, T.R. Savage, K. and Varner, R.K. (1998). Seasonal patterns and controls on net ecosystem CO_2 exchange in a boreal peatland complex, *Global Biogeochemical* Cycles, **12**: 703-714.

Bubier, J.L. Moore, T.R. Bellisario, L. and Comer, N.T. (1995). Ecological controls on methane emissions from a northern peatland complex in the zone of discontinuous permafrost, Manitoba Canada, *Global Biogeochemical Cycles*, **9**: 455-470.

Burton, K.L. Rouse, W.R. and Boudreau, L.D. (1996). Factors affecting the summer carbon dioxide budget of subarctic wetland tundra, *Climate Research*, **6**: 203-213.

Ciais, P. Tans, P.P. Trolier, M. White, J.W.C. and Francey, R.J. (1995). A large northern hemisphere terrestrial CO_2 sink indicated by the $^{13}C/^{12}C$ ratio of atmospheric CO_2, *Science*, **269**: 1098-1102.

Cess, *et al.*, (1993). Uncertainties in carbon dioxide radiative forcing in atmospheric general circulation models, *Science*, **262**: 1252-1255.

Coristine, L.E. (1998). "A qualitative analysis of vegetation succession in relation to carbon balance for a Churchill, Manitoba sedge fen", unpublished manuscript, Department of Biology, Queen's University, Kingston, Ontario, Canada.

Coyne, P.I. and Kelley, J.J. (1975). CO_2 exchange over the Alaskan arctic tundra: Meteorological assessments by an aerodynamic method, *Journal of Applied Ecology*, **12**: 587-611.

D'Arrigo, R. Jacoby, G.C. and Fung, I.Y. (1987). Boreal forests and atmosphere-biosphere exchange of carbon dioxide, *Nature*, **329**: 321-323.

Dewar, R.C. (1993). A root-shoot partitioning model based on carbon-nitrogen-water-interactions and Münch phloem flow, *Fuctional Ecology*, **7**: 356-368.

Dudley, S.A. (1996). Differing selection on plant physiological traits in response to environmental water availability: A test of adaptive hypotheses, *Evolution*, **50**: 92-102.

Dugas, W.A. (1993). Micrometeorological and chamber measurements of CO_2 flux from bare soil, *Agricultural and Forest Meteorology*, **67**: 115-128.

Fahnestock, J.T. Jones, M.H. and Welker, J.M. (1999). Wintertime CO_2 efflux from arctic soils: Implications for annual carbon budgets, *Global Biogeochemical Cycles*, **13**: 775-780.

Fan, S.M. Wolfsy, S.C. Bakwin, P.S. and Jacob, D.J. (1992). Micrometeorological measurements of CH_4 and CO_2 exchange between the atmosphere and subarctic tundra, *Journal of Geophysical Research*, **97**: 16627-16643.

Frakes, B. and Yarnal, B. (1997). A procedure for blending manual and correlation-based synoptic classifications, *International Journal of Climatology*, **17**: 1381-1396.

Frolking, S.E. *et al.*, (1997). The relationship between ecosystem productivity and photosynthetically active radiation for northern peatlands, *Global Biogeochemical Cycles*, **12**: 115-126.

Frolking, S. (1997). Sensitivity of spruce/moss boreal forest net ecosystem productivity to seasonal anomalies in weather, *Journal of Geophysical Research*, **102**: 29053-29064.

Gajewski, K.S. Payette, S. and Ritchie, J.C. (1993). Holocene vegetation history at the boreal-forest-shrub-tundra transition in northwestern Quebec, *Journal of Ecology*, **81**: 433-443.

Gartner, B.L. Chapin, F.S. Shaver, G.R. (1986). Reproduction of *Eriophorum vaginatum* by seed in Alaskan tussock tundra, *Journal of Ecology*, **74**: 1-18.

Gerritsen, J. and Greening, H.S. (1989). Marsh seed banks of the Okefenokee Swamp: Effects of hydrologic regime and nutrients, *Ecology*, **70**: 750-763.

Gorham, E. (1991). Northern peatlands: role in the carbon cycle and probable responses to climatic warming, *Ecological Applications*, **1**: 182-195.

Green, T.G. and Lange, O.L. (1994). Photosynthesis in poikilohydric plants: A comparison of lichens and bryophytes. In: "*Ecophysiology of Photosynthesis*", (Eds Shulze, E.D. and Caldwell, M.M.), pp. 219-241. Springer-Verlag, New York.

Griffis, T.J. Rouse, W.R. and Waddington, J.M. (2000). Inter-annual variability of net ecosystem CO_2 exchange at a subarctic sedge fen, *Global Biogeochemical Cycles*, (in press).

Griffis T.J. Rouse, W.R. and Waddington, J.M. (2000). Scaling net ecosystem CO_2 exchange from the community to landscape-level at a subarctic fen, *Global Change Biology*, **6**: 459-473.

Griffis, T.J. Petrone, R. and Rouse, W.R. (2000). A synoptic climatological analysis of net ecosystem CO_2 exchange at a subarctic fen, *Arctic, Antarctic and Alpine Research* (submitted).

Griffis, T.J. and Rouse, W.R. (2000). Modelling the inter-annual variability of net ecosystem CO_2 exchange at a subarctic fen, *Global Change Biology*, (in press).

Goulden, M.L. Daube, B.C., Fan, S-M., Sutton, D.J., Bazzaz, A., Munger J.W., and Wofsy, S.C. (1997). Physiological responses of a black spruce forest to weather, Journal of Geophysical Research, **102**, 28987-28996.

Halliwell, D.H. and Rouse, W.R. (1987). Ground heat flux in permafrost terrain: Characteristics and accuracy of measurement, *Journal of Climatology*, **7**: 571-584.

Halliwell, D.H. and Rouse, W.R. (1989). A comparison of sensible and latent heat flux calculations using the Bowen ratio and aerodynamic methods, *Atmospheric and Oceanic Technology*, **6**: 563-574.

Heide, O.M. Bush, M.G. and Evans, L.T. (1985). Interaction of photoperiod and gibberellin on growth and photosynthesis of high-latitude *Poa pratensis*, *Physiologica Plantarum*, **65**: 135-145.

Hidore, J.J. and Oliver, J.E. (1993). "*Climatology: An Atmospheric Science*." Maxwell MacMillan Canada, Toronto, 423 pp.

Johanson U., Gehrke C., Bjorn L.O., Callaghan T.V., Sonesson M. (1995). The effects of UV-B radiation on a sub-arctic heath ecosystem, Ambio, **24**: 106-112.

Jano, A.P. Jefferies, R.L. and Rockwell, R.F. (1998). The detection of vegetational change by multi-temporal analysis of LANDSAT data: the effects of goose foraging, *Journal of Ecology*, **86**: 93-99.

Johnson, L.C. Shaver, G.R. Cades, D.H. Rastetter, E. Nadelhoffer, K. Giblin, A. Laundre, J. and Stanley, A. (2000). Plant carbon-nutrient interactions control CO_2 exchange in Alaskan wet sedge tundra ecosystems, *Ecology*, **81**: 453-469.

Joiner, D.W. Lafleur, P.M. McCaughey, J.H. and Bartlett, P.A. (1999). Interannual variability in carbon dioxide exchanges at a boreal wetland in the BOREAS northern study area, *Journal of Geophysical Research*, **104**: 27663-27672.

Kalisz, S. (1986). Variable selection on the timing of germination in *Collinsia verna* (Scrophulariaceae), *Evolution*, **40**: 479-491.

Kattenberg, A. Giorgi, F. Grassl, H. Meehl, G.A. Mitchell, J.F.B. Stouffer, R.J. Stouffer, Tokioka, T. Weaver, A.J. and Wigley, T.M.L. Climate models- Projections of future climate. In: "*Climate Change 1995: The Science of Climate Change, contribution of working group 1 to the second assessment report of the intergovernmental panel on climate change.*" (Eds), Houghton, J.T. Meira, L.G. Filho, B. Callander, A. Harris, N. Kattenberg, A. and Maskell, K., Cambridge University Press, Cambridge, pp. 285-357.

Keeling, C.D. (1986). "Atmospheric CO_2 concentrations-Mauna Loa Observatory, Hawaii 1958-1986." NEP-001/R1 Carbon Dioxide Information Centre, Oak Ridge National Laboratory, Oak Ridge Tennessee.

Keeling, C.D. Bacastow, R.B. Carter, A.F. Piper, S.C. Whorf, T.P. Heimann, M. Mook, W.G. and Roeloffzen, H. (1989). A three-dimensional model of atmospheric CO_2 transport based on observed winds, 1, Analysis of observational data, In: "*Aspects of Climate Variability in the Pacific and the Western Americas*", Geophysical Monography Series, 55, Editor: Peterson, D.H., AGU, Washington, D.C.

Keeling, C.D. Whorf, T.P. Wahlen, M. Van der Plicht, J. (1995). Inter-annual extremes in the rate of rise of atmospheric carbon dioxide since 1980, *Nature*, **375**: 666-670.

Kim, J. and Verma, S.B. (1992). Soil surface CO_2 flux in a Minnesota peatland, *Biogeochemistry*, **18**: 37-51.

Kindermann, J. Würth, G. Kohlmaier, G.H. and Badeck, F.W. (1996). Interannual variation of carbon exchange fluxes in terrestrial ecosystems, *Global Biogeochemical Cycles*, **10**: 737-755.

Kirchhofer, W. (1973). Classification of 500 mb patterns. *Arbeitsbericht Schwiz. Meteorology Zentralanstalt*, **43**: 16 pp.

Knapp, A.K. and Yavitt, J.B. (1992). Evaluation of a closed-chamber method for estimating methane emissions from aquatic plants, *Tellus*, **44B**: 63-71.

Lafleur, P.M. Griffis, T.J. and Rouse, W.R. (2000). Net ecosystem CO_2 exchange at the arctic treeline, *Climatic Change*, (submitted to Arctic, Antarctic, and Alpine Research).

Lafleur, P.M. McCaughey, J.H. Joiner, D.W. Bartlett, P.A. and Jelinski, D.E. (1997). Seasonal trends in energy, water, and carbon dioxide fluxes at a northern boreal wetland, *Journal of Geophysical Research*, **102**: 29009-29020.

Lafleur, P.M. (1999) Growing season energy and CO_2 exchange at a subarctic boreal woodland, *Journal of Geophysical Research*, **104**: 9571-9580.

Lafleur, P.M. McCaughey, J.H. Joiner, D.W. Bartlett, P.A. and Jelinski, D.E. (1997). Seasonal trends in energy, water, and carbon dioxide fluxes at a northern boreal wetland, *Journal of Geophysical Research*, **102**: 29009-29020.

Lambers, H. Chapin, F.S. Pons, T.L. (1998). "*Plant physiological ecology*." Springer, New York, 540 pp.

Matthias, A.D. Yarger, D.N. and Weinbeck, R.S. (1978). A numerical evaluation of chamber methods for determining gas fluxes, *Geophysical Research Letters*, **5**: 765-768.

Maxwell, B. (1992). Arctic climate: Potential for change under global warming. In: "*Arctic Ecosystems in a Changing Climate: An Ecophysiological Perspective.*" (Eds. Chapin, F.S. Jefferies, R.L. Reynolds, J.F. Shaver, G.R. Svoboda, J.) London: Academic Press Inc., pp.11-32.

McFadden, J.P. Chapin, F.S. and Hollinger, D.Y. (1998) Subgrid-scale variability in the surface energy balance of arctic tundra, *Journal of Geophysical Research*, **103**: 28947-28961.

Mitchell, J.F.B. Manabe, S. Meleshko, V. and Tolioka, T. (1990). Equilibrium climate change and its implications for the future, In: "*Climate Change: The IPCC Scientific Assessment.*", (Eds. Houghton, J. T. Jenkins, G. J. and Ephraums, J.J.) Cambridge Press, New York., pp. 135-164.

Moore, T.R. and Roulet, N.T. (1991). A comparison of dynamic and static chambers for methane emission measurements from subarctic fens, *Atmosphere-Ocean*, **29**: 102-109.

Moore, T.R. Roulet, N.T. Waddington, J.M. (1998). Uncertainty in predicting the effect of climatic change on the carbon cycling of Canadian peatlands, *Climatic Change*, **40**: 229-245.

Murry, K.J. Tenhunen, J.D. Nowak, R.S. (1993). Photoinhibition as a control on photosynthesis and production of *Sphagnum* mosses, *Oecologia*, **96**: 200-207.

Myneni, R.B. Keeling, C.D. Tucker, C.J. Asrar, G. Nemani, R.R. (1997). Increased plant growth in the northern high latitudes from 1981 to 1991, *Nature*, **386**: 698-702.

Nadelhoffer, K.J. Emmett, B.A. Gundersen, P. Kjonaas, O.J. Koopmans, C.J. Schleppi, P. Tietema, A. and Wright, R.F. (1999). Nitrogen deposition makes a minor contribution to carbon sequestration in temperate forests, *Nature*, **398**: 145-148.

National Oceanic and Atmospheric Administration (NOAA) and Cooperative Institute for Research in Environmental Sciences (CIRES), Climate Diagnostics Center. (1999). "*Global Atmospheric Data sets.*" website, http://www. Cdc.NOAA.gov/.

Neumann, H.H. den Hartog, G. King, K.M. and Chiapanshi, A.C. (1994). Carbon dioxide fluxes over a raised open bog at Kinosheo Lake tower site during the Northern Wetlands Study (NOWES), *Journal of Geophysical Research*, **99**: 1529-1538.

Norman, J.M. Kucharik, C.J. Gower, S.T. et al. (1997). A comparison of six methods for measuring soil-surface carbon dioxide fluxes, *Journal of Geophysical Research*, **102**: 28771-28777.

Oberbauer, S.F. Tenhunen, J.D. and Reynolds, J.F. (1992). Environmental effects on CO_2 efflux from water rack and tussock tundra in arctic Alaska, U.S.A. *Arctic and Alpine Research*, **23**: 162-169.

Oechel, W.C. and Billings, W.D. (1992). Effects of global change on the carbon balance of arctic plants and ecosystems, In: "*Arctic Ecosystems in a Changing Climate: An Ecophysiological Perspective.*" (Eds. Chapin, F.S. Jefferies, R.L. Reynolds, J.F. Shaver, G.R. and Svobada, J.). London: Academic Press. Press Inc. pp. 139-167.

Oechel, W.C. Hastings, S.J. Vourlitis, G.L. Jenkins, M.A. Riechers, G. and Grulke, N. (1993). Recent changes of arctic tundra ecosystems from a net carbon sink to a source, *Nature*, **361**: 520-523.

Oechel, W.C. and Billings, W.D. (1992). Effects of global change on the carbon balance of arctic plants and ecosystems. In: "*Arctic Ecosystems in a Changing Climate: An Ecophysiological Perspective.*" (Eds. Chapin, F.S. Jefferies, R.L. Reynolds, J.F. Shaver, G.R. Svoboda, J.). London: Academic Press Inc, pp.139-167.

Oechel, W.C. Vourlitis, G.L. Hastings, S.J. and Bochkarev, S.A. (1995). Change in arctic CO_2 flux over two decades: Effects of climate change at Barrow, Alaska, *Ecological Applications*, **5**: 846-855.

Oechel, W.C. Vourlitis, G. and Hastings, S.J. (1997). Cold season CO_2 emission from arctic soils, *Global Biogeochemical Cycles*, **11**: 163-172.

Olson, J.S. Garrels, R.M. Berner, R.A. Armentano, T.V. Dyer, M.I. and Yaalon, D.H. (1985). "The natural carbon cycle." In: *Atmospheric carbon dioxide and the global carbon cylce* (Ed. Trabalka, J.R.) U.S. Department of Energy, Washington, D.C. pp. 175-213.

Payette, S. and Morneau, C. (1993). Holocene relict woodlands at the Eastern Canadian Treeline, *Quaternary Science* **39**: 84-89.

Penning de Vries, F.W.T. (1975). The cost of maintenance processes in plants cells, *Annals of Botany*, **39**: 77-92.

Petrone, R. (1996). "A report on the effects of a nitrogen fertilizer on the productivity of a sedge fen", unpublished manuscript, McMaster University, Hamilton Ontario, Canada.

Petrone, R.M. and Rouse, W.R. (2000). Synoptic controls on the surface energy and water budgets in subarctic regions of Canada, *International Journal of Climatology,* (in press).

Petrone, R.M., Griffis, T.J., and Rouse W.R. (2000). Synoptic and Surface Climatology Interactions in the Central Canadian Arctic: Normal and El Niño Seasons, Physical Geography (in press).

Poorter, H.C. Remkes, C. and Lambers, H. (1990). Carbon and nitrogen economy of 24 wild species differing in relative growth rate, *Plant Physiology,* **94**: 621-627.

Prioul, J.L. Chartier, P. (1977). Partitioning of transfer and carboxylation components of intracellular resistance to photosynthetic CO_2 fixation: A critical analysis of the methods used, *Annals of Botany,* **41**: 789-800.

Purrington, C.B. and Schmitt, J. (1998). Consequences of sexually dimorphic timing of emergence and flowering in *Silene latifolia*, *Journal of Ecology,* **86**: 397-404.

Rolph, S.G. (1999). "The effects of nitrogen fertilizer addition to a subarctic sedge fen and its applicability as a simulation of climatic change", B.Sc. Thesis, McMaster University, Hamilton Ontario, Canada.

Roulet, N.T. Crill, P.M. Comer, N.T. Dove, A. Boubonniere, R.A. (1997). CO_2 and CH_4 flux between a boreal beaver pond and the atmosphere, *Journal of Geophysical Research,* **102**: 29313-29320.

Rouse, W.R. and Bello, R.L. (1985). Impact of Hudson Bay on the energy balance in the Hudson Bay lowlands and the potential for climatic modification. *Atmosphere-Ocean*, **23**: 375-392.

Rouse, W.R. (1991). Impacts of Hudson Bay on the terrestrial climate of the Hudson Bay lowlands, *Arctic and Alpine Research*, **23**: 24-30.

Rouse, W.R. Douglas, M.V. Hecky, R.E. Hershey, A.E. Kling, G.W. Lesack, L. Marsh, P. McDonald, M. Nicholson, B.J. Roulet, N.T. Smol, J.P. (1997). Effects of climate change on the freshwaters of arctic and subarctic North America, *Hydrological Processes*, **11**: 873-902.

Rouse, W.R. (1998). A water balance model for a subarctic sedge fen and its application to climatic change, *Climatic Chang,e* **38**: 207-234.

Rouse, W.R. (1991). Impacts of Hudson Bay on the terrestrial climate of the Hudson Bay Lowlands, *Arctic and Alpine Research*, **23**: 24-30.

Schlesinger, W.H. (1991). "*Biogeochemistry: An analysis of global change.*" Academic Press: New York., pp.443.

Schreader, C.P. Rouse, W.R. Griffis, T.J. Boudreau, L.D. and Blanken, P.D. (1998). Carbon dioxide fluxes in a northern fen during a hot, dry summer. *Global Biogeochemical Cycles*, **12**: 729-740.

Scott, P.A. Lavoie, C. MacDonald, G.M. Sveinbjörnsson, B. Wein, R.W. (1997). Controls on current and future position of northern treeline. In: "*Global Change and Arctic Terrestrial Ecosystems*" (Eds Oechel, W.C. Callaghan, T. Gilmanov,

T. Holten, J.I. Maxwell, B. Molau, U. Sveinbjörnsson, B.). Springer-Verlag, New York, pp. 245-266.

Semikhatova O.A. Gerasimenko, T.V. Ivanova, T.I. (1992). Photosynthesis, Respiration, and Growth of Plants in the Soviet Arctic. In: "*Arctic Ecosystems in a Changing Climate.*" (Eds. Chapin, F.S. Jefferies, R.L. Reynolds, J.F. Shaver, G.R. Svoboda, J. and Chu, E.W.). London: Academic Press, pp. 169-192.

Shaver, G.R. and Chapin, F.S. (1991). Production/biomass relationships and element cycling in contrasting arctic vegetation types, *Ecological Monographs*, **61**: 1-31.

Shaver, G.R. and Chapin, F.S. (1995). Long-term responses to factorial NPK fertilizer treatment by Alaskan wet and moist tundra sedge species, *Ecography*, **18**: 259-275.

Shaver, G.R. Chapin, F.S. and Gartner, B.L. (1986). Factors limiting seasonal growth and peak biomass accumulation in *Eriophorum Vaginatum* in Alaskan tussock tundra, *Journal of Ecology*, **74**: 257-258.

Shaver, G.R. Johnson, L.C. Cades, D.H. et al. (1998). Biomass and CO_2 flux in wet sedge tundras: responses to nutrients, temperature and light, *Ecological Monographs*, **68**: 75-97.

Shurpali, N.J. Verma, S.B. and Kim, J. (1995). Carbon dioxide exchange in a peatland ecosystem, *Journal of Geophysical Research*, **100**: 14319-14326.

Silvola, J.J. Alm, U. Ahlholm, H. Nykanen, and Martikainen, P.J. (1996). The contribution of plant roots to CO_2 fluxes from organic soils, *Biology of Ferlized. Soils*, **23**: 126-131.

Srivastava, D.S. and Jefferies, R.L. (1996). A positive feedback: herbivory, plant growth, salinity, and the desertification of an Arctic salt-marsh, *Journal of Ecology*, **84**: 31-42.

Sundquist, E.T. (1993). The global carbon dioxide budget, *Science* **259**: 934-941.

Suyker, A.E. Verma S.B. and Arkebauer, T.J. (1997). Season-long measurment of carbon dioxide exchange in a boreal fen, *Journal of Geophysical Research*, **102**: 29021-29028.

Taiz, L. and Zeiger, E. (1991). *Photosynthesis: Physiological and ecological considerations. Plant Physiology*. New York: The Benjamin/Cummings Publishing Company, Inc., pp. 249-264.

Tans, P.P. Fung I.Y. and Takahashi, T. (1990). Observational constraints on the global atmospheric CO_2 budget, *Science*, **247**: 1431-1438.

Tenhunen, J.D. Lange, O.L. Hahn, S. Siegwolf, R.T.W. and Oberbauer, S.F. (1992). The ecosystem role of poikilohydric tundra plants. In: "*Arctic Ecosystems in a Changing Climate: An Ecophysiological Perspective.*" (Eds. Chapin, F.S. Jefferies, R.L. Reynolds, J.F. Shaver, G.R. and Svoboda, J.). London: Academic Press Inc., pp.213-237.

Tieszen, L.L. (1973). Photosynthesis and respiration in arctic tundra grasses: field light intensity and temperature response. *Arctic and Alpine Research*, **5**: 239-251.

Townsend, A.R. Braswell, B.H. Holland, E.A. and Penner J.E. (1996). Spatial and temporal patterns in terrestrial carbon storage due to deposition of fossil fuel nitrongen, *Ecological Applications*, **6**: 806-814.

Van der Werf, A. Kooijman, A. Welschen, R. and Lambers, H. (1988). Respiratory energy costs for the maintenance of biomass, for growth and for ion uptake in roots of *Carex diandra* and *Carex acutiformis*, *Physiologia Plantarum*,**72**: 483-491.

Vleeshouwers, L.M. Bouwmeester, H.J. Karssen, C.M. (1995). Redefining seed dormancy: an attempt to integrate physiology and ecology, *Journal of Ecology*, **83**: 1031-1037.

Vourlitis, G.L. and Oechel, W.C. (1997). Landscape-scale CO_2, H_2O vapour and energy flux of moist-wet coastal tundra ecosystems over two growing seasons. *Journal of Ecology*, **85**: 575-590.

Vourlitis, G.L. Oechel, W.C. Hope, A. Stow, D. Boynton, B. Verfaillie, J. Jr. Zulueta, R. and Hastings, S.J. (2000). Physiological models for scaling plot measurements of CO_2 flux across an arctic tundra landscape, *Ecological Applications*, **10**: 60-72.

Waddington, J.M. and Roulet, N.T. (1999). Relationship between carbon biogeochemistry and peatland development in a northern peatland, *Global Change Biology*, **5**: 1-11.

Waddington, J.M. Griffis, T.J. and Rouse, W.R. (1998). Northern Canadian wetlands: Net ecosystem CO_2 exchange and climatic change, *Climatic Change*, **40**: 267-275.

Webb E.K. Pearman, G.I. and Leuning, R. (1980) Corrections of flux measurements for density effects due to heat and water vapour transfer, *Quarterly Journal of the Royal Meteorological Society*, **106**: 85-100.

Whiting, G.J. (1994). Seasonal CO_2 exchange in communities of the Hudson Bay lowlands, *Journal of Geophysical Research*, **99**: 1519-1528.

Yarnal, B. and Frakes, B. (1997). Using synoptic climatology to define representative discharge events. *International Journal of Climatology*, **17**: 323-341.

Yarnal, B. (1984). A procedure for the classification of synoptic weather maps from gridded atmospheric pressure surface data. *Computers and Geosciences*, **10**: 397-410.

Yarnal, B. (1993). "*Synoptic climatology in environmental analysis: A primer.*" Belhaven Press, UK, 195 pp.

Zalensky, O.V. (1977), "Ecophysiological aspects of photosynthesis investigations." In: Russian, 37th Timiryasev lecture, Nauka, Leningrad.

Zimov, S.A. Zimova, G.M. Daviodov, S. P. Daviodova, Y.V. Voropaev, Z.V. Voropaeva, S.F. Prosiannikov, O.V. Prosiannikova, I.V. Semiletova, I.V. and Semiletov, I.P. (1993). Winter biotic activity and production of CO_2 in Siberian soil: A factor in the greenhouse effect, *Journal of Geophysical Research*, **98**: 5017-5023.